# DESIGN OF ANTIOXIDANT NANOTHERAPEUTICS FOR ATTENUATION OF ATHEROGENESIS AND NEUROINFLAMMATION

By

REBECCA ANN CHMIELOWSKI

A dissertation submitted to the

School of Graduate Studies

Rutgers, The State University of New Jersey

In partial fulfillment of the requirements

For the degree of

Doctor of Philosophy

Graduate Program in Chemical and Biochemical Engineering

Written under the direction of Prabhas V. Moghe

and approved by

_____

_____

_____

_____

_____

_____

_____

New Brunswick, New Jersey

January 2018

**ABSTRACT OF THE DISSERTATION**

DESIGN OF ANTIOXIDANT NANOTHERAPEUTICS FOR ATTENUATION OF ATHEROGENESIS AND NEUROINFLAMMATION

By

REBECCA ANN CHMIELOWSKI

Dissertation Director:

Prabhas V. Moghe

Atherosclerosis and Parkinson's disease are both characterized by the uncontrolled uptake of modified proteins in chronic inflammatory cells, macrophages/microglia. The initial stages of atherosclerosis are characterized by oxidation of low density lipoprotein and its uptake by macrophages, which can lead to plaque progression in the arterial wall and possibly heart attack or stroke. Formation and increase of misfolded aggregates of proteins such as alpha synuclein (α-synuclein) are a key factor in several neurodegenerative diseases including Parkinson's disease. Both classes of diseases are exacerbated in macrophages/microglia due to a strong inflammatory component, which has been challenging to treat. The anti-atheroprotective and anti-inflammatory properties of antioxidants create an attractive target for treatment of atherosclerosis and Parkinson's disease. We propose a library of antioxidant nanoparticles that have the potential to address critical needs for both atherosclerosis and Parkinson's disease. For atherosclerosis applications, we advanced the delivery and formulation of antioxidants through the development of ferulic acid-based polymer nanoparticles, which are completely biodegradable and can achieve a sustained and tunable release of ferulic acid to limit

macrophage foam cell formation. The ferulic acid-based polymer nanoparticles attenuated macrophage lipogenesis and reactive oxygen species generation. The cellular mechanism of the nanoparticle efficacy involved the down regulation of the expression of three scavenger receptors, which are critical for modulation of lipid uptake in macrophages. For neuroinflammatory applications, we developed a dual antioxidant nanoparticle consisting of ferulic acid and tannic acid, which significantly reduced the generation of α-synuclein fibrils. This result suggests that the combination of antioxidants and the configuration of nanoparticle vehicles could be important factors for inhibiting α-synuclein fibril formation. Overall, antioxidant nanotherapeutics may be promising technologies for inhibition of early stages of both atherosclerosis and Parkinson's disease.

**PREFACE**

“Stay afraid, but do it anyway. What’s important is the action. You don’t have to wait to be confident. Just do it and eventually the confidence will follow.” – Carrie Fisher

“Go find your joy. It’s what you’re going to remember in the end.” – Sandra Bullock

“Everyone's dream can come true if you just stick to it and work hard.” – Serena Williams

“Research is what I'm doing when I don't know what I'm doing.” – Wernher von Braun

## DEDICATION

This thesis is dedicated to my family and friends, especially my parents, brother, husband Tim, and son Hunter who have supported my part time journey through this PhD program. Special thanks to my husband for watching Hunter and doing everything possible around the house so I could finish my graduate studies. This thesis is also dedicated to both of my grandmothers who passed away this year but I know they would be proud of my accomplishments during my graduate school tenure.

**ACKNOWLEDGEMENTS**

I am grateful and blessed to have the opportunity to perform part time research at Rutgers University in hopes of attaining a PhD degree. I would like to express my gratitude to Dr. Prabhas Moghe who gave me this opportunity that altered my life in one of the best ways and for being a great mentor. I would also like to thank my committee members, Dr. Uhrich, Dr. Joseph, Dr. Tugcu, Dr. Baum, and Dr. Roth for being great mentors who guided and supported me through this journey. Special thanks to Dr. Joseph who taught me the essence of biology and became a great friend in the process. Special thanks to Dr. Uhrich for encouraging us to publish a paper from the initial ferulic acid nanoparticle results.

Special thanks to the Moghe lab whom taught me how to conduct cell culture work, associated assays, and for being awesome people and friends. A few of the lab members deserve a special thanks for their contributions towards my degree: Adam York, Latrisha Petersen, Aaron Carlson, Vidya, Nicola Francis, Harini, Margot Zevon, Adrianna Martin, Katrina, and undergrads Sonali, Nick, Janice, and Hassan. Thanks to John Faig and Xue Yang for their assistance with our publications.

Special thanks to the flow cytometry and confocal core lab in EOHSI, especially Carol Gardner, Theresa Choi, and Jessica Cervelli.

Thanks to all of my friends for their support during my PhD studies. Also, for anyone that I forgot to mention, please know that I am writing this thesis in a very tired and pregnant mode and that my appreciation is no less than for those listed here.

Finally, thanks to God who makes all things possible and for my past relatives who were lifting me up on days when my energy or spirit was low.

Sections of this thesis have been reproduced from the following publication:

R.A. Chmielowski, D.S. Abdelhamid, J.J Faig, L.K. Petersen, C.R. Gardner, K.E. Uhrich, L.B. Joseph, P.V. Moghe. Athero-inflammatory nanotherapeutics: Ferulic acid-based poly(anhydride-ester) nanoparticles attenuate foam cell formation by regulating macrophage lipogenesis and reactive oxygen species generation. Acta Biomaterialia. 2017, 57, 85-94.

## Table of Contents

**List of Figures**

# CHAPTER 1 - Introduction to the design of antioxidant therapeutics, scavenger receptor biology, and macrophage/microglia dynamics in atherosclerosis and Parkinson's disease

## INTRODUCTION

Atherosclerosis and Parkinson's disease are both characterized by the uncontrolled uptake of modified proteins in chronic inflammatory cells, macrophages/microglia. The initial stages of atherosclerosis are characterized by oxidation of low density lipoprotein and its uptake by macrophages, which can lead to plaque progression in the arterial wall and possibly heart attack or stroke. Formation and increase of misfolded protein aggregates are a key factor in several neurodegenerative diseases [1]. Alpha synuclein aggregates cause neuroinflammation, neurodegeneration, and cell death and are the primary mechanism of neurodegenerative disorders called α-synucleinopathies [2]. Parkinson's disease is characterized as an α-synucleinopathy. Limited treatment options exist for both atherosclerosis and Parkinson's disease. Furthermore, both diseases can be difficult to diagnose in early stages. The following thesis focuses on development of scavenger receptor targeted nanotherapeutics with aims of 1) attenuating foam cell formation to impede the early stages of atherosclerosis and 2) inhibiting α-synuclein aggregation to alter the progression of Parkinson's disease.

## ATHEROSCLEROSIS OVERVIEW

Cardiovascular disease is the leading cause of death amongst adults in the United States with medical costs estimated at about $320 billion annually and rising [3]. A major trigger for cardiovascular disease is atherosclerosis, which is a highly complex and chronic inflammatory etiology. An overview of atherosclerosis is summarized in **Figure 1**.

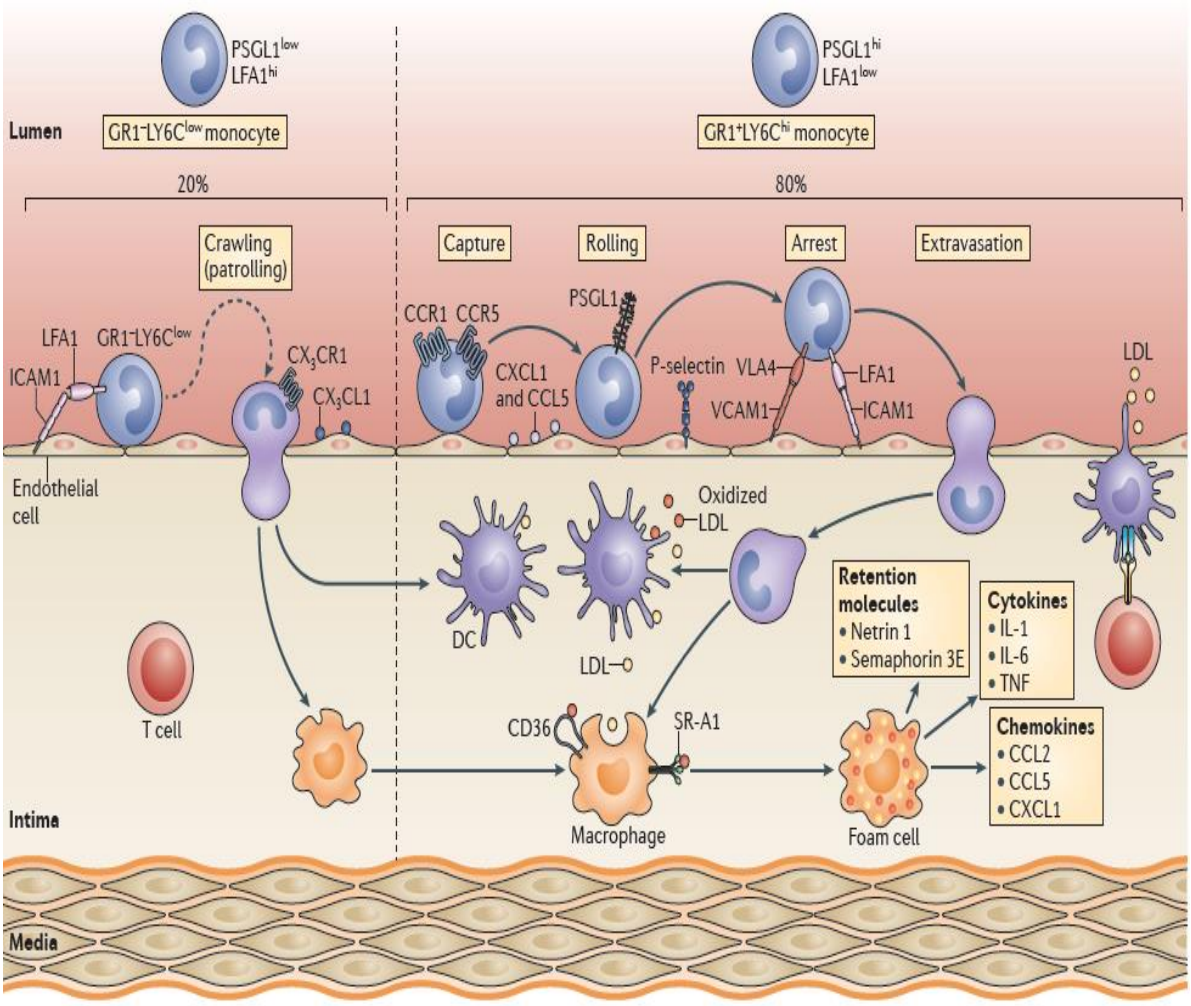


**Figure 1.** ***Mechanism of monocyte differentiation and accumulation into plaques.*** Adapted from Moore KJ, Sheedy FJ, Fisher EA. Nature Reviews Immunology, 2013, 13(10), 709-721.

Atherosclerosis is a product of an inflammatory response in the arterial vascular wall, which is initiated by the accumulation of low density lipoprotein (LDL) [4,5]. LDL is susceptible to various modifications including oxidation, enzymatic and non-enzymatic cleavage, and aggregation [6]. Oxidative stress, induced by reactive oxidative and nitrated species, can promote the oxidation of lipids and lead to the formation of oxidized LDL (oxLDL) [7]. OxLDL can activate endothelial cells and lead to inflammatory responses within the arterial wall. This event leads to recruitment of monocytes and other leukocytes

into the subendothelial space. Monocytes that enter the subendothelial space will differentiate into macrophages in response to either macrophage colony-stimulating factor (MCSF) or granulocyte-macrophage colony stimulating factor (GMCSF) [8]. Macrophages will ingest the modified lipoprotein complexes mainly through pattern recognition receptors, which includes a cluster of differentiation (CD-36), lectin-like oxidized low density lipoprotein receptor (LOX-1), and scavenger receptor A1 (MSR-1) [9,10]. Uncontrolled macrophage uptake of oxLDL leads to foam cell formation and is a critical trigger for atherosclerosis. Foam cells have minimal migratory capacity and become apoptotic, which leads to plaque that consists of apoptotic cells along with cholesterol and other extracellular material [8]. Plaque ruptures account for about 70% of coronary thrombosis events [8].

*Scavenger Receptors and Their Role in Atherosclerosis*

Pattern recognition receptors or scavenger receptors play key roles for uptake of modified lipids and progression of macrophages to foam cells. In 1979, Brown and Goldstein were the first to describe a scavenger receptor function on macrophages that can process modified LDL differently compared to the processing of native LDL [11]. Modified LDL is not cleared in circulation by the endocytic LDL receptor and must bind to scavenger receptors instead leading to foam cell formation [12]. The first scavenger receptors were identified using labeled acetylated LDL (acLDL) and classified as a family of structurally unrelated molecules [13-15]. In 1997, Krieger and colleagues suggested eight classifications of scavenger receptors labeled A to H [16] (**Figure 2**). Recently, the scavenger receptor classes have expanded to ten classes [17]. Additions to the class include CD163 receptor (Class I) and SR-J1 receptor or membrane-bound form of RAGE (Class

J) [17]. However, both of these receptors have been mainly linked to anti-inflammatory responses in macrophages [17].

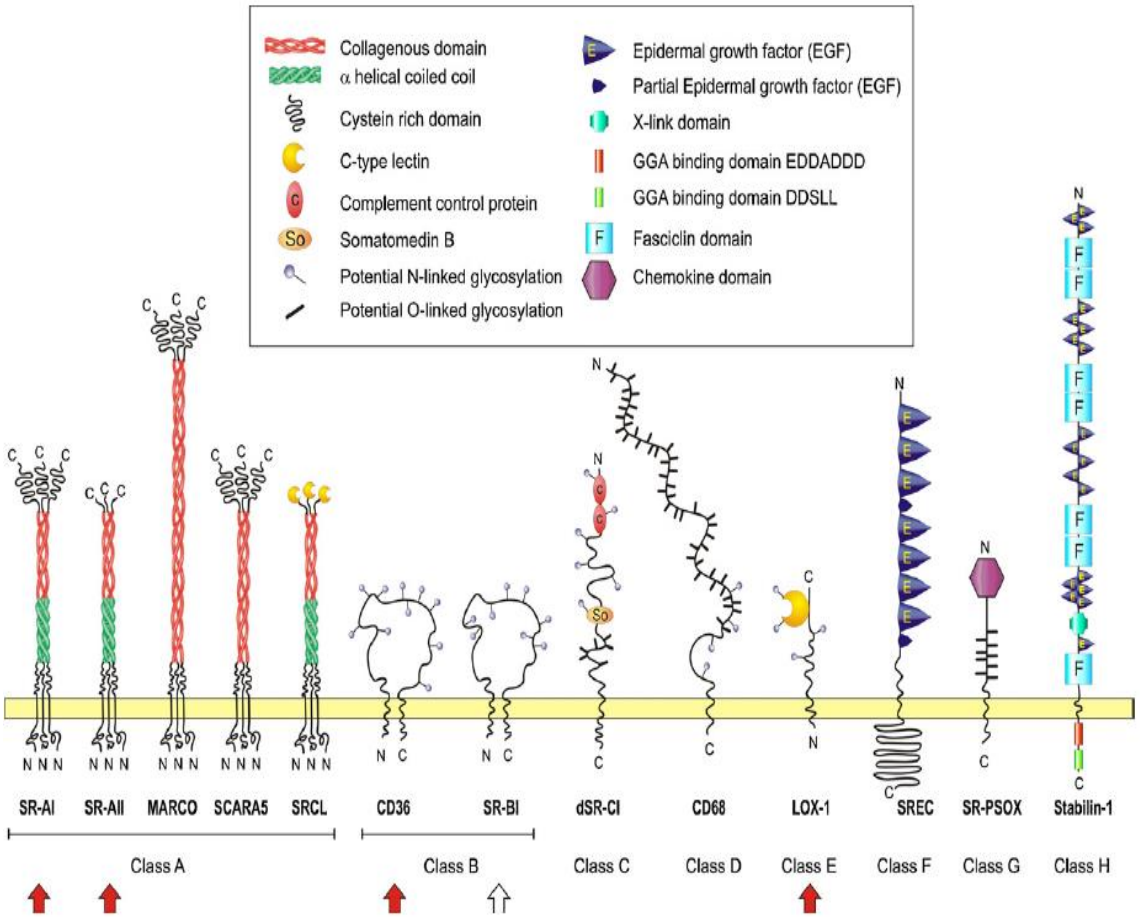


**Figure 2.** ***Macrophage scavenger receptors listed per classification.*** Adapted from J. Kzhyshkowska, C. Neyen, S. Gordon. Role of macrophage scavenger receptors in atherosclerosis. Immunobiology. 2012, 217, 492-502.

Even though the identification of these scavenger receptors was driven by labeled acLDL, all of these receptors displayed in **Figure 2** have contributed to the development of atherosclerosis. Clearance of modified LDL, such as oxLDL, is regulated through either scavenger receptor mediated endocytosis or phagocytosis [12]. For the endocytosis pathway, oxLDL and scavenger receptor form a complex, which is delivered to the

endosomal compartment and then transfers to acidic endosomes where the scavenger receptor can either dissociate from oxLDL and recycle back to the cell surface or degrade in the lysosome [12]. For the phagocytosis pathway, oxLDL promotes accumulation of intracellular cholesterol ester in lipid droplets [12].

All of the scavenger receptors shown in **Figure 2** have been reported in the literature to recognize oxLDL except for the Class H, Stabilin 1 receptor. In particular, both CD36 and MSR1 (or SRA1) have been reported to be associated with oxLDL internalization and linked to foam cell formation [12]. CD36 was linked to several signaling pathways including Lyn and MEKK2 pathways, JNK2, and STAT1 which correlated to uptake of oxLDL and foam cell formation [18-19]. Literature from *in vivo* experimentation with peritoneal macrophages suggested both CD36 and MSR1 accounted for about 75-90% of degradation of oxLDL or acLDL [20]. In addition, deficient mice for CD36 and MSR1 showed no macrophage accumulation of oxLDL [20]. Since scavenger receptors play critical roles in promotion of atherogenesis, these receptors provide an attractive target for development of novel therapeutic approaches for management of atherosclerosis. Based on this hypothesis, previous work in our lab has shown a correlation between reduced oxLDL uptake by macrophages with a reduction in scavenger receptor expression of CD36 and MSR1 using an amphiphilic macromolecule (AM) functionalized with an anionic group (i.e. 1cM) for mimicking the negative charge of scavenger receptor ligands such as MSR1 [21-22]. This thesis will expand upon this work by investigating nanoparticle formulations including 1cM in combination with antioxidants as a novel nanoscale therapy.

*Current Treatments for Atherosclerosis*

Interestingly, there are no current pharmaceutical interventions to modulate expression of macrophage scavenger receptors to directly disrupt foam cell formation. Pharmaceutical agents for treating atherosclerosis involve decreasing the serum low density lipoprotein cholesterol (LDL-C) levels, which are believed to predispose patients to atherosclerosis. These agents can also raise high density lipoprotein cholesterol (HDL-C) and lower triglyceride levels both of which are thought to protect against atherosclerosis [23]. The most effective cholesterol lowering class of drugs that have demonstrated a reduced rate of mortality from coronary artery disease are called statins [24]. Statins inhibit HMG-CoA reductase, which reduces the hepatic synthesis of cholesterol and lowers circulating levels of low density lipoprotein cholesterol (LDL-C) [25]. The main drawback of statins is their inability to address inflammation and localized oxidative damage that accompanies atherosclerosis [26]. Alternative clinical approaches using small molecules or proteins for treating atherosclerosis have been ineffective or contained an off-target effect [27-31].

Recently, proprotein convertase subtilisin/kexin type 9 (PCSK9) antibodies have shown effective for lowering LDL-C levels and have been linked to reduce the risk of cardiovascular events [32]. The main mechanism of action of PCSK9 antibodies relate to a direct interaction and degradation of the hepatic LDL receptor (LDLR), which leads to reductions in plasma LDL-C levels [33]. These PCSK9 antibodies will only inhibit plasma PCSK9 but not production of PCSK9 and therefore could miss the importance of determining the impact of intracellular PCSK9 on inflammation and atherosclerosis [33]. Furthermore, the cost of PCSK9 antibodies over five years is expected to increase by an

estimated $592 billion compared to the reduction in cardiovascular care costs of about $29 billion [34]. Therefore, the cost benefit of PCSK9 antibodies at the current price does not seem favorable for patients. Development of novel, cost effective treatments for atherosclerosis may be paramount for prevention of coronary artery disease. Antioxidants formulated into nanoparticles were investigated in this thesis as an alternative therapy for attenuating foam cell formation and reducing early stages of atherosclerosis. The choice of both antioxidants and amphiphilic macromolecule (AM) for these nanoscale formulations are critical in order to achieve maximum efficacy and binding to macrophage scavenger receptors. The next two sections describe the choice of amphiphilic macromolecule utilized in the targeting shell of the nanoparticles along with the potential of antioxidants in relation to atherosclerosis and explained our choice of antioxidant for the core of the nanoparticles.

### *Amphiphilic Macromolecule Nanoparticle Formulations as a Novel Therapy for Atherosclerosis*

The initial development of amphiphilic macromolecules focused on polymer charge and the biological application to atherosclerosis [35]. Previous research from Dr. Moghe's lab in conjunction with Dr. Uhrich's lab discovered the importance of polymer charge and stereochemistry in relation to uptake of oxLDL in macrophages [36-40]. An amphiphilic polymer containing a carboxylic acid group, 1cM, significantly decreased the uptake of oxidized low density lipoprotein (oxLDL) in human monocyte derived macrophages (HMDMs) compared to an amphiphilic polymer without charge, 0cM [36, 40].

1cM is an amphiphilic macromolecule that contains both hydrophobic (four carbon side chains with twelve carbons in each chain as shown in green) and hydrophilic (a 5,000 Dalton polyethylene glycol chain shown in blue) properties (**Figure 3**) [36,37,40]. The corresponding hydrophobic analog to 1cM is called M12, which is the hydrophobic component is 1cM without the polyethylene glycol group (**Figure 3**) [41]. The amphiphilic properties of 1cM promote self-assembling into a micelle above the critical concentration and give the multimer complex an increased anionic negative charge [42]. This increase in anionic charge allows the 1cM to preferentially interact and bind competitively over oxLDL to the scavenger receptor SRA-1 on HMDMs [43-45].

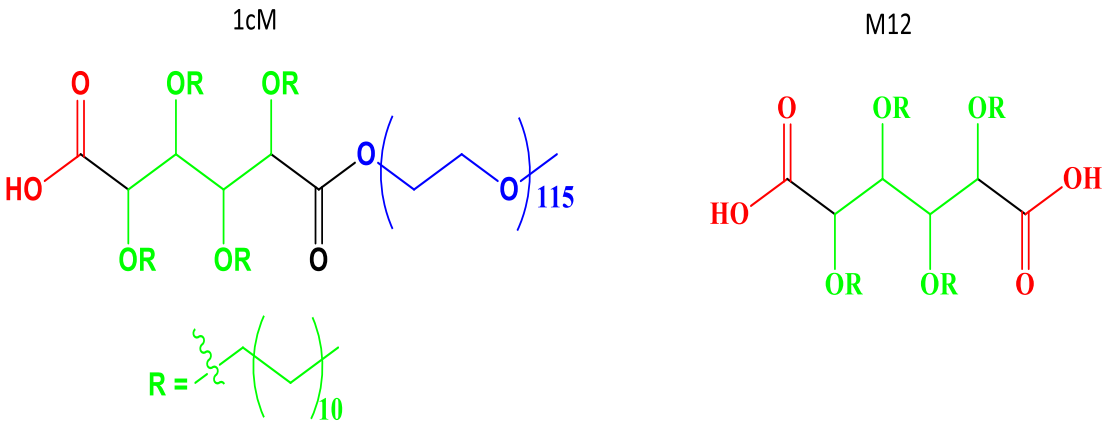


**Figure 3.** ***Chemical structures of 1cM and M12.*** The carboxylic acid group is shown in red while the hydrophobic group is shown in green. 1cM is recognized as a shell in the nanoparticles while M12 is a core. 1cM has a molecular weight of 5931 g/mol and CMC of 3.2 x $10^{-7}$ M. M12 has a molecular weight of 931 g/mol and log P of ~12. Adapted from York AW, Zablocki KR, Lewis DR, Gu L, Uhrich KE, Prud'homme RK, Moghe PV. Advanced Materials, 2012, 24(6): 733-739.

The 1cM micelle structure can be prone to instability when introduced into a physiological environment due to the equilibrium that exists between micelle and unimeric chains [41, 46]. In order to enhance the stability of 1cM micelles, previous research by Adam York proposed to formulate 1cM into a nanoparticle [41]. Some advantages of nanoparticles as a delivery vehicle compared to micelles include the following: narrow and consistent particle size distribution, enhanced stability in a physiological environment, high encapsulation efficiency, and tunable loading of the core [41, 42, 47].

The nanoparticle formulation developed by Adam York consisted of using a technique called flash nanoprecipitation [48-50]. Flash nanoprecipitation is based on both thermodynamics and transport phenomena principles. The rapid mixing, within nanoseconds, of a water-miscible organic stream composed of a soluble hydrophobic solute and amphiphilic macromolecule with an aqueous stream enables the formation of a nanoparticle assembly (**Figure 4**) [41]. Nanoparticles are produced due to the supersaturation of the hydrophobic solute in the aqueous medium, which induces spontaneous precipitation and nanoparticle nucleation and growth. The amphiphilic macromolecule self-assembles around the hydrophobic solute core and forms the shell of the nanoparticle, which stabilizes the nanoparticle assembly.

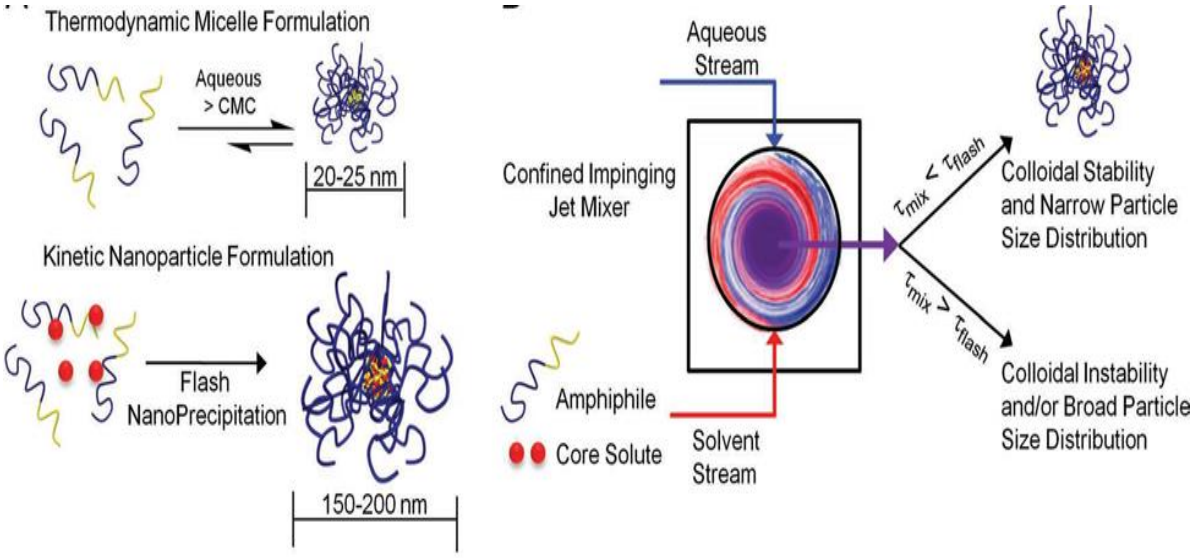


**Figure 4.** ***The fabrication of kinetically assembled AM nanoparticles using the flash nanoprecipitation technique compared to the thermodynamic equilibrium between a micelle and unimers.*** Adapted from York AW, Zablocki KR, Lewis DR, Gu L, Uhrich KE, Prud'homme RK, Moghe PV. Advanced Materials, 2012, 24(6): 733-739.

The amphiphilic macromolecule, 1cM, formed the shell of the nanoparticle while the more hydrophobic analog, M12, formed the core of the nanoparticle. This nanoparticle was called 1cM-M12 (shell-core). Previous research by Adam York demonstrated the stability of the 1cM-M12 nanoparticle in media containing fetal bovine serum (FBS) [41]. In addition to stability in FBS, 1cM-M12 also demonstrated a higher bioactivity than 1cM micelles for reduction of oxLDL uptake in HMDMs [41]. Nano flashprecipitation will form the basis of nanoparticle formulation with various antioxidants for achieving each thesis aim since highly stable and bioactive nanomaterials can be generated using this technique.

*Antioxidants and Their Potential as a Therapy for Atherosclerosis*

Oxidative stress can initiate atherosclerosis through various mechanisms, which include endothelial dysfunction, activate immune responses to inflammation, and thrombus formation [51]. In particular, oxidation of LDL has been correlated to the beginning stages of atherosclerosis [51]. LDL can be oxidized by various methods including using transition metal ions, radical generators, and oxidizing enzymes [52]. Each method could result in the formation of different oxLDL complexes based on the content of oxidized lipid and extent of apolipoprotein B modification [53]. Antioxidants have been effective for limiting the early stages of atherosclerosis by the following two mechanisms: 1) Inhibition of oxLDL after pre-incubation with anti-oxidants and 2) Inhibition of LDL oxidation [54]. The efficacy of an anti-oxidant can be variable for either mechanism since the type of antioxidant and method of oxidation or inhibition of oxLDL is critical to its success [54].

Phenolic, polyphenolic, hydrophilic antioxidants, vitamin C, and tocopherols have been shown to inhibit LDL oxidation [54]. In particular, vitamin E has been studied extensively for its ability to inhibit lipid peroxidation and as an epidemiological marker for heart disease since it is the major anti-oxidant present in human LDL. On average, five to nine vitamin E molecules are present on each LDL particle and have been shown to prevent lipid peroxidation and modification of proteins in LDL by reactive oxygen species (ROS) *in vitro* [55 – 56]. Initial clinical trials involving vitamin E intake lowered the risk of cardiovascular disease by about 34% and cardiac death by about 58% [57 – 58]. Based on these initial results, additional and larger scale clinical trials were conducted involving vitamin E and beta-carotene [59 - 60]. These trials showed neither oxidant could decrease cardiovascular disease [59 - 60].

Additional research has shown the type and dose of anti-oxidant used to assess the progression of atherosclerosis are important factors to consider. For example, higher concentrations of vitamin E acted as a pro-oxidant and accelerated the oxidation of LDL [61]. For applications in atherosclerosis, the antioxidant dose is critical since higher concentrations of anti-oxidants can result in establishing localized concentration of pro-oxidants within the arterial wall, which can inadvertently exacerbate foam cell formation [62]. Therefore, it is essential to design a formulation that can deliver the most efficacious therapeutic dose of the desired anti-oxidant at a gradual, controlled rate while avoiding a burst release.

Ferulic acid (4-hydroxy-3-methoxy cinnamic acid) is a potent, natural anti-oxidant that can scavenge free radicals and has also been approved as a food additive to prevent lipid peroxidation (**Figure 5**) [63]. Ferulic acid possesses a few distinctive chemical groups that could contribute to the compound's ability to scavenge free radicals. The electron donating groups on the benzene ring allow for stopping of free radical chain reactions [63]. The carboxylic acid group can provide additional sites for free radicals and also protect against lipid peroxidation [63].

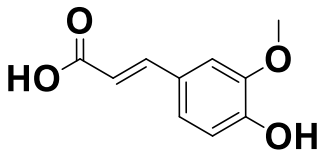


**Ferulic acid**

**Figure 5.** ***Chemical structure of ferulic acid.***

Ferulic acid has the potential to scavenge free radicals through its ability to form a resonance stabilized phenoxy radical, which accounts for its antioxidant potential [64 – 65]. Any reactive radical will remove a hydrogen atom from ferulic acid to form the phenoxy radical [63]. In addition, this phenoxy radical will not initiate a radical chain reaction and will most likely begin a condensation reaction with another ferulate radical to yield the dimer curcumin [63]. Since curcumin will contain two phenolic hydroxyl groups, then the radical scavenging activity will be substantially enhanced compared to ferulic acid. This property of ferulic acid also makes it attractive for atherosclerosis applications, since its free radical will not cause lipid peroxidation as in the case of vitamin E.

Ferulic acid has shown potential in modulating lipid transport from macrophages by two mechanisms. The first mechanism involved a reduction of oxLDL uptake in macrophages through a decrease in CD36 expression [66]. However, multiple antioxidant compounds were combined with ferulic acid in this study. Therefore, it is difficult to discern the impact of ferulic acid on lipid uptake and also the dose required to limit lipid uptake in macrophages. The second mechanism involved an increase in a cholesterol efflux regulatory protein named ATP-binding cassette transporter A1 (ABCA1) [66 - 67]. ABCA1 is responsible for reverse cholesterol transport from macrophages to lipid depleted apolipoproteins [68]. Altering the lipid content of a macrophage foam cell could potentially reverse the atherosclerosis cascade. Expression of ABCA1 has been shown to be regulated by the nuclear receptor, Liver X receptor (LXR) [55]. However, previous LXR agonists have been shown to increase liver triglycerides in an *in vivo* mouse model [69].

Since ferulic acid has shown potential to reduce macrophage lipogenesis, it was further studied in this dissertation as a potential therapy to combat early stages of atherosclerosis. The first focus of this thesis involved the investigation of ferulic acid analogs to address two major components of atherosclerosis: foam cell formation and macrophage inflammation. The second focus of this thesis involved the investigation of antioxidants to alter the aggregation rate of α-synuclein, which is a major factor for initiation and progression of Parkinson's disease. The next sections will provide an overview of Parkinson's disease and history of antioxidants for treatment of Parkinson's disease.

## PARKINSON'S OVERVIEW

Parkinson's disease is estimated to affect up to 1 million people or 0.3% of the population in the United States and this result is estimated to double by 2050 [70]. Parkinson's disease mostly affects people aged at least 50 years but can also affect younger people and has a tendency to affect males more than females [71]. Total costs, which include direct and indirect costs, for Parkinson's disease are approximately $15.5 billion per year [71]. Parkinson's disease is characterized by severe motor symptoms including muscular rigidity and uncontrollable resting tremor along with additional symptoms such as cognitive dysfunction, mood disorders, and sleep abnormalities [72 - 73].

The pathophysiology of Parkinson's disease results from the loss of neuromelanin-containing dopaminergic neurons in the substantia nigra pars compacta (SN) and the presence of Lewy bodies [1]. Alpha synuclein (α-synuclein) is a 14kDa protein consisting of 140 amino acids and is an unfolded protein in solution but can form oligomers or fibril structures under certain conditions, such as oxidative stress and post-translational

modifications [1]. Alpha synuclein β-sheet-rich fibrils are one of the major protein components of Lewy bodies [1]. The mechanism of alpha synuclein toxicity is currently under investigation but possibly linked to the aggregation and fibrillization of α-synuclein at higher concentrations [72]. Both oligomers and fibrils have been shown to display neuronal toxicity and apoptosis [74 - 77]. In addition, neuronal dysfunction can lead to α-synuclein aggregation and release (**Figure 6**) [78]. The α-synuclein aggregates and fibrils could interact with glia cells, such as microglia and astrocytes, to initiate cellular activation and initial stages of Parkinson's disease (**Figure 6**) [78].

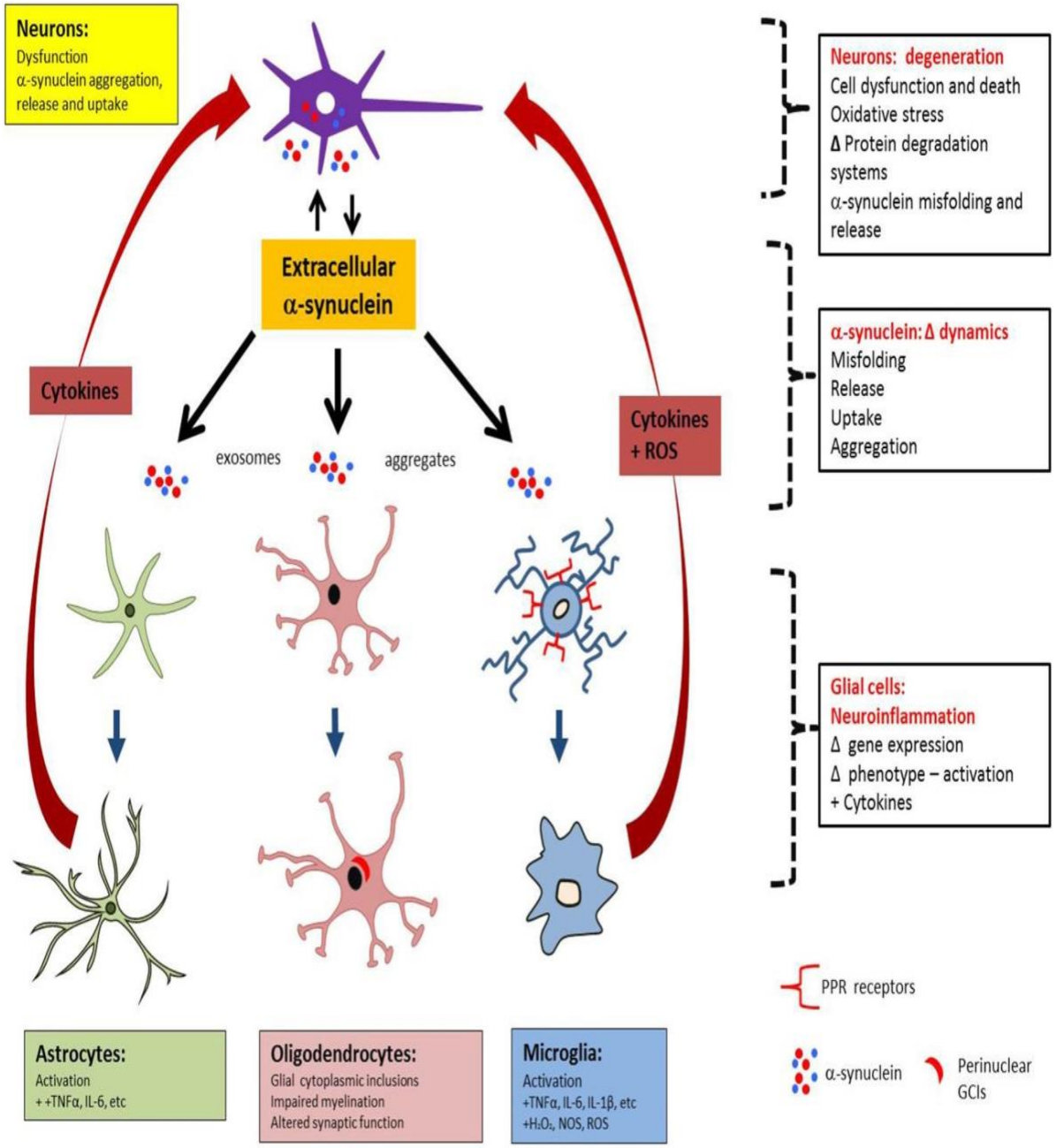


**Figure 6.** ***Alpha synuclein aggregates release from damaged neurons and activate glial cells such as astrocytes and microglia.*** Adapted from B. Di Marco Vieira, R.A. Radford, R.S. Chung, G.J. Guillemin, D.L. Pountney. Neuroinflammation in multiple system atrophy: response to and cause of α-synuclein aggregation. Front. Cell. Neurosci. 2015, 9. 437.

*Microglia and Their Role in Parkinson's*

Microglia cells are brain resident macrophage-like cells that are critical in maintaining a homeostasis in the central nervous system [79]. Microglia account for about 10-15% of brain cell population and contain different morphologies across regions of the brain [80]. Microglia are involved in maintenance of the neuronal environment and purge pathogens and apoptotic cells [80]. In a healthy brain, astrocytes and neurons keep microglia in a resting state [79]. However, when microglia respond to an immune stimuli, microglia become activated and can upregulate several surface receptors, such as pattern-recognition receptors and receptors for cytokines and neurotransmitters [81 - 83]. Microglia can also produce pro-inflammatory cytokines, such as TNF-α and IL-6, which can produce reactive oxygen species [79]. In addition, microglia can activate into a M1 phenotype if exposed to cytokines, such as IFN-γ or TNF-α (**Figure 7**) [80]. If microglia are exposed to cytokines, such as IL-4 or IL-13, microglia can transform into a M2 phenotype (**Figure 7**) [80]. In addition, microglia can uptake α-synuclein in an activated state and lead to progression of early stages of Parkinson's disease [84].

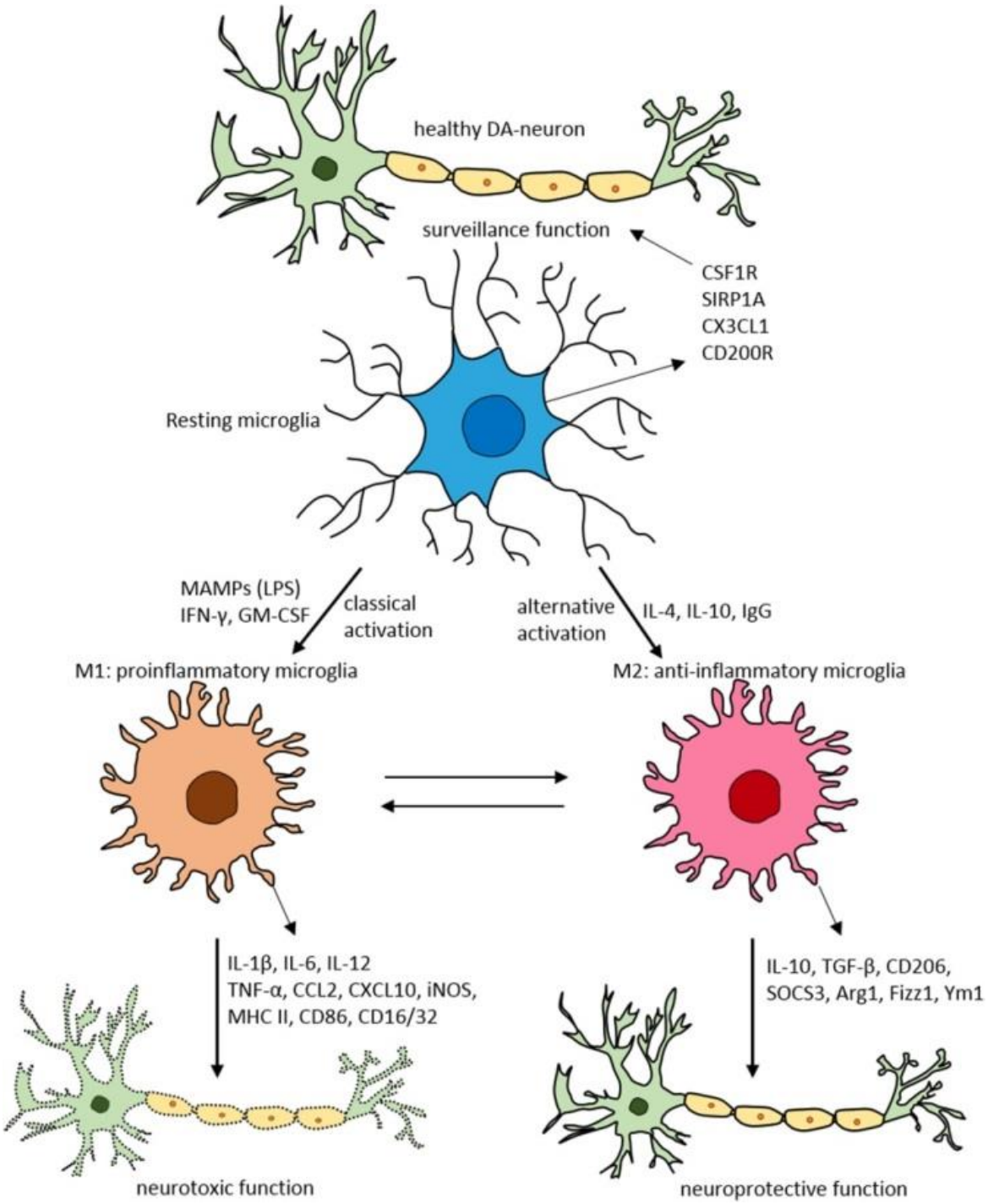


**Figure 7.** ***Microglia polarization states and function.*** Adapted from S.R. Subramaniam, H.J. Federoff. Targeting microglial activation states as a therapeutic avenue in Parkinson's disease. Frontiers in Aging Neuroscience. 2017, 9, 176.

Alpha synuclein has been shown to interact with microglia, monocytes, and macrophages through a variety of amino acid sequence motifs. The N-terminal region (1-60 amino acids) consists of multiple amphipathic α-helices, which is similar to the lipid binding domain of apolipoproteins, and can allow for penetration and transportation into microglia and macrophages [85]. The C-terminal region (96-140 amino acids) is mainly composed of acidic amino acids and can activate microglia and macrophages [85 - 86]. The central region (61-95 amino acids) consists of a very hydrophobic peptide that can initiate α-synuclein aggregation [87 - 88].

Limited evidence exists for the cellular mechanisms of α-synuclein uptake by microglia. The uptake of α-synuclein by microglia initiated the activation of mitogen-activated protein (MAP) kinase pathways, which suggested the activation of MAP could be a receptor-mediated event [89]. Some studies have indicated that scavenger receptors might play a role in microglia activation and possibly recognize α-synuclein. The first study showed a knockout of the CD36 receptor decreased microglia activation and pro-inflammatory response to α-synuclein [90]. Another study concluded that toll-like receptor 4 (TLR4) regulated the uptake of α-synuclein monomers by microglia, suppressed pro-inflammatory cytokine release, and lowered ROS production [86]. Furthermore, TLR2 was shown to interact with α-synuclein aggregates and also activate microglia [91].

Microglia scavenger receptors such as CD36, TLR2, and TLR4, can interact and uptake α-synuclein. These results coupled with previous literature showing the involvement of scavenger receptors, such as CD36, MSR1, TLR2, and TLR4, for modulation of amyloid beta clearance lead our group to investigate the role of microglia scavenger receptors for uptake of α-synuclein [92]. Our lab's initial findings showed that

α-synuclein uptake can be regulated by microglia scavenger receptors CD36 and MSR1 [93]. The addition of antioxidant nanoparticles containing ferulic acid (i.e. 1cM-PFAA) reduced both the inflammation and activation state of the microglia and also reduced intracellular aggregation [93]. The final aim of this thesis will focus on development of additional antioxidant formulations and their impact on the rate of α-synuclein aggregation and fibrillization. The next section will describe the current treatments for Parkinson's disease and describe why antioxidants could serve as a novel treatment approach along with the choice of antioxidants utilized in our nanoparticle formulations.

*Current Treatments for Parkinson's Disease*

The current treatments for Parkinson's disease only slow down the disease progression. Treatment options include medication, surgery, lifestyle modifications, and physical and speech therapy [94]. Most drugs aim to increase or mimic the dopamine levels in the brain and are named dopaminergic drugs [94]. The most common drugs include Levodopa, dopamine agonists, monoamine oxidase-B inhibitors and catechol O-methyltransferase inhibitors [94]. Exercise and physical therapy can help improve mobility, muscle tone, and relieve muscle stiffness. Speech therapy can improve swallowing difficulties along with use of language and speech. The most common type of surgery performed is deep brain stimulation where an electrode is implanted inside the brain and electrical impulses are sent to block the electrical signals that cause symptoms [94]. This procedure has a high risk of hemorrhage and infection and is only utilized for advanced stages of Parkinson's disease.

The treatment options and diagnosis for Parkinson's disease are limited since there are no reliable biomarkers for early disease detection. Therefore, after the clinical

diagnosis of Parkinson's disease has been established, the disease has matured in the patient over years of progression. Since α-synuclein has been shown to play an important role in the pathogenesis of Parkinson's disease, recent studies have been conducted to search for biomarkers related to α-synuclein protein modification. For example, one study focused on the level of α-synuclein in red blood cells since it has been reported that more than 99% of the α-synuclein in human blood resides in the red blood cells [95]. This study concluded that the ratio of α-synuclein/oligomer to total red blood cell protein was higher in Parkinson's disease patients than controls and could potentially become a diagnostic biomarker for Parkinson's disease [96]. Another study discovered that T cells from Parkinson's disease patients responded to two peptide fragments derived from α-synuclein leading to a possible autoimmune response in Parkinson's disease [97].

Our lab's approach to finding new treatment options for Parkinson's disease also centered around α-synuclein. Since Parkinson's disease initiation has been linked to microglia activation and aggregation of α-synuclein, our lab has started to investigate the potential of antioxidants for treatment of Parkinson's disease. Our lab's initial results focused on ferulic acid polymers and their potential to reduce intracellular α-synuclein aggregation and microglia activation [93]. The history of antioxidants for treatment of Parkinson's disease will be explained in the next section followed by the choice of antioxidants for investigation to reduce α-synuclein aggregation and fibrillation.

*Antioxidants and Their Potential as a Therapy for Parkinson's*

Alpha synuclein fibrillization involves an increase in prefibrillar oligomers that is stimulated by post-translational modifications, such as tyrosine nitration and methionine oxidation, which occur under conditions of oxidative stress [98]. One pathway for reactive

oxygen species (ROS) generation is a decrease in activity of mitochondrial complex I found in Parkinson's patients [98]. Furthermore, dopaminergic neurons in the SN also contain high levels of ROS due to metabolism and auto-oxidation of dopamine [98]. Antioxidants can prevent ROS generation and could represent one strategy for treatment of Parkinson's disease and other synucleinopathy disorders.

The following antioxidant compounds have been shown to decrease α-synuclein fibrillization with approximately a half-maximal effective concentration ($EC_{50}$) in the low micromolar range: 1) polyphenolics (i.e. baicalein, curcumin, epigallocatechin gallate (EGCG), ferulic acid, myricetin, nordihydroguaiaretic acid (NDGA), rosmarinic acid, and tannic acid and 2) non-polyphenolics (ie. amphotericin B, perphenazine, and rifampicin [98 - 102]. Some antioxidants such as curcumin and dieckol have also shown the ability to reduce α-synuclein aggregation in neuronal cells [102 - 103]. Recently studies have shown curcumin inhibited α-synuclein aggregation in an *in vivo* Parkinson's disease rat model [104]. Furthermore, antioxidants such as curcumin, myricetin, NDGA, rosmarinic acid, and tannic acid, have shown potential for disruption of preformed α-synuclein fibrils with $EC_{50}$ values in the low micromolar range [100].

The one challenge for using antioxidants to inhibit α-synuclein fibrillization is the potential of the antioxidant to generate α-synuclein oligomers. For example, α-synuclein oligomers generated in the presence of EGCG did not contain β-sheet structure and were conformationally distinct from the β-sheet-rich, toxic fibrils shown to permeabilize cellular membranes [101]. Therefore, it is critical to determine if inhibition of α-synuclein fibrillation by an antioxidant forms any conformationally distinct α-synuclein oligomers and if these oligomers are toxic to neuronal cells.

In the last aspect of this thesis, we aimed to expand upon previous work and investigate the effect of various antioxidant nanoparticles on fibrillation and aggregation of α-synuclein. Tannic acid and retinoic acid were chosen as the core for the nanoparticle formulations. Tannic acid was demonstrated to both inhibit α-synuclein aggregation and also disrupt preformed α-synuclein fibrils. Retinol was demonstrated to increase α-synuclein content in a neural cell line [105]. Retinoic acid was utilized as a positive control nanoparticle formulation. The ferulic acid polymer, PFAA, was also chosen as a core based on its previous ability to decrease α-synuclein intracellular aggregation [93].

## THESIS OVERVIEW AND HYPOTHESIS

The objective of this thesis is to examine novel therapeutic approaches focusing on nanotechnology combined with antioxidants for addressing the attenuation of foam cell formation in atherosclerosis and inhibition of synucleinopathy in Parkinson's disease. Regulation of oxidized low density lipoprotein (oxLDL) interactions with macrophages can possibly attenuate foam cell formation and decrease macrophage inflammation formed the first hypothesis of this work. The composition of the nanoparticle formulation will strongly impact the ability of the nanoparticle to inhibit α-synuclein fibrillization formed the second hypothesis of this work. To test these hypotheses, the following three aims were created:

1) To develop novel, antioxidant nanoparticle formulations to modulate the uptake of oxLDL by human monocyte derived macrophages (HMDMs)
2) To elucidate the cellular mechanisms of oxLDL uptake and impact of antioxidant nanoparticles to regulate macrophage inflammation

3) To develop novel, antioxidant nanoparticle formulations to inhibit or decrease the aggregation and fibrillization of α-synuclein

Chapter 2 describes studies developing ferulic acid nanoparticles and their impact on modulating the impact of oxLDL at various concentrations. Ferulic acid polymers as the core coupled with an amphiphilic macromolecule as the shell resulted in the most stable and size appropriate nanoparticles for further *in vitro* experimentation. In addition, the ferulic acid polymer linked by diglycolic acid (ie. PFAG) was the most efficacious for limiting oxLDL uptake by HMDMs at all oxLDL concentrations studied. In Chapter 3, the impact on ferulic acid nanoparticles on the expression level of scavenger receptors was investigated. Three scavenger receptors, CD36, MSR1, and LOX1, were downregulated by the PFAG nanoparticle, which correlated to its ability to limit oxLDL uptake by HMDMs. Furthermore, the levels of ROS were significantly reduced for all of the ferulic acid nanoparticle formulations indicating the impact of ferulic acid in the core of the nanoparticle for reducing cellular ROS and inflammation. Chapter 4 describes the development of tannic acid and retinoic acid nanoparticles and their effect on inhibiting α-synuclein aggregation and fibril formation. Tannic acid nanoparticles significantly reduced α-synuclein fibrillization. Chapter 5 illustrates future studies building on our findings from the three aims listed above. Overall, these studies provide a template for designing novel antioxidant nanoparticle formulations to counteract foam cell formation and synucleinopathy.

# CHAPTER 2 – DESIGN OF FERULIC ACID NANOPARTICLES FOR REGULATION OF MACROPHAGE LIPOGENESIS


## ABSTRACT

Enhanced bioactive anti-oxidant formulations are critical for treatment of inflammatory diseases, such as atherosclerosis. A hallmark of early atherosclerosis is the uptake of oxidized low density lipoprotein (oxLDL) by macrophages, which results in foam cell and plaque formation in the arterial wall. The hypolipidemic, anti-inflammatory, and antioxidative properties of polyphenol compounds make them attractive targets for treatment of atherosclerosis. However, high concentrations of antioxidants can reverse their anti-atheroprotective properties and cause oxidative stress within the artery. Here, we designed a new class of nanoparticles with anti-oxidant polymer cores and shells comprised of scavenger receptor targeting amphiphilic macromolecules (AMs). Specifically, we designed ferulic acid-based poly(anhydride-ester) nanoparticles to counteract the uptake of high levels of oxLDL in human monocyte derived macrophages (HMDMs). Compared to all compositions examined, nanoparticles with core ferulic acid-based polymers linked by diglycolic acid (PFAG) showed the greatest inhibition of oxLDL uptake. At high oxLDL concentrations, the ferulic acid diacids and polymer nanoparticles displayed similar oxLDL uptake. Based on these results, we propose that ferulic acid-based poly(anhydride ester) nanoparticles may offer an opportunity to regulate macrophage lipogenesis and foam cell formation.

INTRODUCTION

A major trigger for cardiovascular disease is atherosclerosis, which has a highly complex and chronic inflammatory etiology. A common focal point for the initiation of atherosclerosis is believed to be localized damage to the endothelial lining of the artery, ultimately leading to plaque formation [4-5, 106]. Damage of the endothelium initiates an immune response recruiting monocytes into the subendothelial space where they may differentiate into macrophages [4-5, 106]. As phagocytic cells, macrophages ultimately transform into foam cells after ingestion of oxidized lipids and cholesterol [106]. The subintimal accumulation of foam cells may rupture leading to a cerebrovascular episode [107].

Oxidized low density lipoprotein (oxLDL), a component of foam cells, is a major contributing factor to the escalation of atherosclerosis [6]. Oxidative stress, induced by reactive oxidative and nitrated species, promotes the oxidation of lipids in the blood stream [7]. Oxidized LDL binds to pattern recognition receptors expressed on macrophages, which includes a cluster of differentiation (CD-36), lectin-like oxidized low density lipoprotein receptor (LOX-1), and scavenger receptor A1 (MSR-1) [12]. Uncontrolled macrophage uptake of oxLDL leads to foam cell formation and is a critical trigger for atherosclerosis. Interestingly, there are no current pharmaceutical intervention to directly disrupt foam cell formation. Therefore, there exists a need to develop bioactive formulations to attenuate foam cell formation.

Our laboratories have developed a series of amphiphilic macromolecules (AMs) focused on polymer properties such as charge, stereochemistry, and hydrophobicity, for limiting macrophage uptake of oxLDL [37, 109 - 110]. Polymer charge is critical for

bioactivity since the amphiphilic polymer (denoted as 1cM) containing a carboxylic acid group significantly decreased the uptake of oxLDL in HMDMs compared to an amphiphilic polymer without charge, 0cM [40]. This increase in anionic charge allows 1cM to preferentially interact with macrophage scavenger receptors and competitively bind vis-a-vis oxLDL, which enables further downregulation of the key scavenger receptors, MSR1 and CD36 [36]. To enable long-term stability and activity of the polymers in physiologic microenvironments, the AMs were formulated via flash nanoprecipitation using hydrophobic cores, which result in stable nanoparticles (NPs) [41]. It has also been observed that the 1cM-M12 nanoparticle (comprising 1cM shell and M12 hydrophobic core) is highly efficacious *in vivo* by reducing plaque blockage in the arterial wall [111]. However, the high anionic charge of 1cM and its corresponding hydrophobic analog, M12, can have collateral effects, for example, on the gene expression of inflammatory markers in HMDMs and also modulate the inherent phagocytic activity of macrophages toward bacteria and other foreign substances, such as modified low density lipoprotein [112]. Therefore, we investigated alternative core molecules that could lower the inflammatory state of the macrophages while exhibiting the ability to reduce the macrophage uptake of oxLDL, especially following high levels of atherogenic challenge.

Polyphenol compounds, including vitamin E, have been marketed as atherosclerosis therapeutics due to their hypolipidemic, anti-inflammatory, and antioxidative properties [113 - 116]. These results have been inconsistent, especially for vitamin E, due to conflicting clinical trial results [117, 118]. The type and dose of anti-oxidant used to assess the progression of atherosclerosis are important factors to consider. Some anti-oxidants will only control the oxidization state of low density lipoprotein while

others have been found to contain pro-atherogenic properties, depending on the administered dose [119, 120]. In fact, the delivery of the anti-oxidant is critical since higher concentrations of anti-oxidants can result in establishing localized concentrations of pro-oxidants within the arterial wall, which can inadvertently exacerbate foam cell formation [121]. Therefore, it is essential to design a formulation that can deliver the most efficacious therapeutic dose of the desired anti-oxidant at a gradual, controlled rate while avoiding a burst release.

Ferulic acid is known as a potent natural anti-oxidant, which has been approved as a food additive to prevent lipid peroxidation [63]. Ferulic acid appears to have potential in mitigating atherosclerosis by prevention of smooth muscle cell migration, modulating lipid transport from macrophages, and reducing pro-inflammatory cytokines [66 - 67, 122]. Pre-treatment with ferulic acid reduced oxLDL uptake by macrophages, which correlated to a reduction in scavenger receptor CD-36 expression while scavenger receptor MSR-1 expression remained unchanged from the control [66]. In addition, pre-treatment with ferulic acid increased expression of ATP-binding cassette transporter A1 (ABCA1), which can facilitate cholesterol efflux and reduce its accumulation in macrophages [66 - 67].

Ferulic acid is an attractive target for atherosclerosis based on its ability to reduce macrophage lipogenesis. However, the efficacy of ferulic acid may be limited due to stability, dosing, and delivery to the intended site of action. Our approach for creation of novel ferulic acid nanoparticle formulations contained two main aspects. First, ferulic acid was chemically conjugated within a poly(anhydride-ester) using either an adipic acid or diglycolic acid linker [123]. This approach allowed for protection of the carboxylic acid from decarboxylation, enhanced the total mass of ferulic acid incorporated into the

polymer, and allowed for a controlled release of ferulic acid avoiding transient pro-oxidant localized concentrations. The choice of adipic versus diglycolic linker results in different ferulic acid release rates, which allows for fine tuning of formulations for specific atherosclerosis applications. The second aspect involved utilization of the bioactive amphiphilic macromolecule, 1cM. The 1cM is a stabilizing shell for the nanoparticle formulation due to its scavenger receptor targeting and hydrophobic and hydrophilic properties. The hydrophobic carbon arms will allow encapsulation of the ferulic acid-based polymers, while the poly(ethylene glycol) reduces nanoparticle aggregation and subsequent uptake by the reticuloendothelial system (RES) [124]. 1cM has been shown to limit oxLDL uptake in HMDMs by lowering scavenger receptor expression, the strategic role of 1cM as the shell of the nanoparticle will allow enhanced macrophage targeting for delivery of the ferulate-based polymers and diacids [22]. In this chapter, we demonstrate the formulation of ferulic acid-based polymers and the diacid intermediates into nanoparticles, which are efficacious as atheroprotection agents against various concentrations of oxidized low density protein (oxLDL) in macrophages.

## MATERIALS AND METHODS

### *Reagents, chemicals, and raw materials*

All chemicals/materials were purchased from Sigma-Aldrich (Milwaukee, WI) or Fisher Scientific (Pittsburgh, PA) and used as received unless otherwise noted. 18 MΩ·cm resistivity deionized (DI) water was obtained using PicoPure 2 UV Plus (Hydro Service and Supplies - Durham, NC). The following items were purchased from the indicated vendors: Ficoll-Paque Premium and Percoll from GE Healthcare (Pittsburgh, PA), RPMI 1640 from ATCC (Manassas, VA), macrophage colony stimulating factor (M-CSF) from

PeproTech (Rocky Hill, NJ), fetal bovine serum (FBS) from Life Technologies (Grand Island, NY), unlabeled oxLDL from Biomedical Technologies Inc. (Stoughton, MA), 3,3'-dioctadecyloxacarbocyanine (DiO) labeled oxLDL from Kalen Biomedical (Montgomery Village, MD), and human buffy coats from either the Blood Center of New Jersey (East Orange, NJ) or New York (New York, NY) blood centers. Flow cytometry (FACS) wash buffer was prepared from phosphate buffered saline (PBS), 0.5 w/v% bovine serum albumin, 0.1 w/v% sodium azide, and 1 v% normal goat serum.

*Amphiphilic macromolecule (AM) and antioxidant molecule synthesis*

Macromolecules 1cM and M12 were synthesized as previously detailed and characterized using established techniques including $^{1}$H NMR-spectroscopy, gel permeation chromatography, differential scanning calorimetry, and dynamic light scattering [125 - 127]. The critical micelle concentration, size, and charge data has been published in the literature [127]. Anti-oxidant molecules were synthesized and characterized as reported previously in the Uhrich laboratory [128].

*Preparation and characterization of nanoparticle formulations*

Nanoparticles were fabricated using the flash nanoprecipitation technique as shown in **Figure 8** as described previously [41, 129]. Briefly, each shell and core component were dissolved separately in the appropriate solvent and mixed together. The chemical structure of each core component is shown in **Figure 9**. Flash nanoprecipitation was performed by mixing the solvent stream with an aqueous stream containing phosphate buffered solution (PBS) at pH 7.4. The nanoparticles were either dialyzed against PBS using a 6000 MW cutoff ultrafiltration membrane or the solvent was displaced from the solution using vacuum. Nanoparticles were characterized by dynamic light scattering

(DLS) using a Malvern-Zetasizer Nano Series DLS detector with a 22 mW He−Ne laser operating at λ 632.8 nm using general purpose resolution mode as previously described [41]. To prepare the sample for zeta potential measurement, each nanoparticle formulation was dialyzed against deionized water using a 3500 Dalton molecular weight cutoff ultrafiltration membrane for approximately 24 hours. Approximately 1mL of sample was added into a zeta potential cell and measured using dynamic light scattering. **Figure 8** shows the size, polydispersity index (PDI), and zeta potential of each nanoparticle formulation.

*Cell culture of human monocyte derived macrophages (HMDMs)*

Peripheral blood derived monocytes (PBMCs) were isolated from human buffy coats by a Ficoll-Paque (1.077 g/cm$^3$) density gradient followed by a Percoll (1.131 g/cm$^3$) density gradient as previously described [130]. After both gradient separations, PBMCs were collected and washed with PBS containing 1mM EDTA. PBMCs were plated into FEP teflon-coated cell culture bags at a density of $\geq$ 8.0 x $10^7$ monocytes per bag. Monocytes were differentiated into macrophages by addition of about 5 to 10 ng/mL recombinant human MCSF and incubated at 37°C in 5% carbon dioxide with media RPMI-1640 supplemented with 2% human serum and 1% P/S for 7 days. After seven days, cell culture bags containing differentiated macrophages were placed on ice for at least 1 hour. The cell suspension was transferred into 50 mL Falcon tubes and centrifuged at 1000 rpm for 10 minutes. Media was removed and cells were resuspended in 20 mL of RPMI-1640, 10% FBS, and 1% P/S. Cells were counted using trypan blue and a hemocytometer. Cells were replated at a density of 150,000 cells/mL and let to rest for at least 1 hour prior to treatment.

*OxLDL uptake by HMDMs*

HMDMs were co-incubated with a mixture of labeled and unlabeled DiO oxLDL for a final concentration of either 5 µg/mL or 50 µg/mL and 1 x $10^{-5}$ M of nanoparticles in RPMI-1640 with 10% FBS and 1% P/S for 24 hours at 37°C in 5% carbon dioxide. Experimental controls included macrophages treated with either medium (basal) or 5 µg/mL or 50 µg/mL of oxLDL. After 24 hours, cells were washed to remove the treatments and 1mL of 10 mM EDTA in PBS pH 7.4 was added to each well. Cells were collected by incubating the plate on ice for up to 15 minutes and removed from the surface of the plate by pipetting and transferred to a flow tube. Each well was washed with 1 mL of FACS buffer, which was also added to the flow tube. Cells were centrifuged at 1000 rpm for 10 minutes at 4°C, supernatant was decanted and cells were resuspended. FACS wash buffer was added to the cells, centrifuged and supernatant decanted. Cells were fixed with 1 v% paraformaldehyde in PBS. Cell fluorescence was measured using a Gallios flow cytometer. OxLDL uptake was quantified using the geometric mean fluorescence intensity (MFI) of the intact HMDMs and analyzed using FlowJo software (Treestar). Results are the average of at least three independent experiments with two replicates per experiment. The percentage of oxLDL uptake was calculated using the following formula [22]:

$$\frac{DiO\ oxLDL\ MFI\ of\ treatment\ sample}{DiO\ oxLDL\ MFI\ of\ oxLDL\ only\ control\ sample}\ x\ 100 = Percentage\ of\ oxLDL\ uptake$$

*Confocal microscopy*

Uptake of oxLDL was visualized using a SP5 confocal microscope (Leica) with a 40x oil immersion objective. HMDMs were plated in an eight well labtek at a density of 150,000 cells/mL. HMDMs were co-incubated with oxLDL and nanoparticles as described

previously. HMDMs were washed with PBS pH 7.4 three times and fixed with 4 v% PFA for 20 minutes room temperature. Cells were washed once with PBS pH 7.4 and Hoescht (0.1 μg/mL) was added for 15 minutes. Cells were washed with PBS pH 7.4, covered in foil, and stored at 4°C until imaging.

*Quantification of ferulic acid by reverse phase high performance liquid chromatography (RP-HPLC)*

Ferulic acid released from the medium in each nanoparticle treatment with HMDMs was analyzed and quantified using RP-HPLC as described previously [123]. Briefly, an XTerra® RP18 column with a 5 μm pore size and dimensions of 4.6 x 150 mm (Waters, Milford, MA) on a Waters 2695 Separations Module equipped with a Waters 2487 Dual λ Absorbance Detector was utilized for chromatographic separation and detection of ferulic acid. The mobile phase was comprised of 70% of 50 mM $KH_2PO_4$ with 1 % formic acid at pH 2.5 (Buffer A) and 30% of acetonitrile (Buffer B) run at 1 mL/min at a column temperature of 25°C. Absorbance was monitored at a wavelength of 335 nm and the concentration of ferulic acid in each sample was calculated from a standard curve.

*Anti-oxidant potential by measurement of DPPH*

Anti-oxidant potential of released ferulic acid was determined using a 2,2-diphenyl-1-picrylhydrazyl (DPPH) radical scavenging assay following previous published methods [131]. In brief, anti-oxidant potential of released ferulic acid was determined by incubating about 100 microliters of the media after a 24 hour treatment of ferulic acid nanoparticles and oxLDL as described above in a DPPH solution (0.024 mg/mL in 3.9 mL methanol). After incubating for 1 hour, the DPPH absorbance change at 517 nm was monitored and compared to a reference (0.1 mL blank – oxLDL solution – in 3.9 mL methanol). DPPH reduction percentage was determined by the equation $[Abs_{t0} - Abs_t]/Abs_{t0} * 100\%$ where

$Abs_{to}$ and $Abs_t$ are the reference and sample solution respectively. All studies were conducted in triplicate.

*Statistical analysis*

Data presented are from at least three independent experiments ($n \geq 3$) and values are represented as mean ± SEM unless otherwise indicated. Statistical analysis was performed considering $p < 0.05$ to be statistically significant. Statistical significance was determined using a one-way ANOVA with Tukey's posthoc test for comparisons between multiple treatment groups.

RESULTS

*Formulation, Stability, and Release Profile of Ferulic Acid Nanoparticles*

All nanoparticles with polymer cores ranged from about 160 – 300 nm with a polydispersity index (PDI) of ≤ 0.3, indicating stable and non-aggregated nanoparticles (**Figure 8**). The 1cM-PFAG and 1cM-PFAA nanoparticles were stable for up to 3 months at 4°C (**Figures 10A & B**). The size of the 1cM-FAA acid nanoparticles is starting to decline at 3 months at 4°C (**Figure 10C)**. The size of the 1cM-FAG acid nanoparticles is within 30nm after storage up to 3 months at 4°C (**Figure 10D**). The ferulate-based polymer based nanoparticles (i.e., 1cM-PFAG and 1cM-PFAA) will release ferulic acid at a slower rate than their corresponding ferulic diacid nanoparticles (1cM-FAA acid and 1cM-FAG acid) (**Figure 11A**). Therefore, the ferulic diacid nanoparticles will be used to assess the impact of a faster release formulation. The maximum concentration of ferulic acid released into the medium was about 100 µM and occurred with the 1cM-FAG acid nanoparticles (**Figure 11A**). Zeta potential values were uniformly highly negative for all compositions (-24.0 to -27.4 mV), except for 1cM-FAA acid nanoparticles, which were slightly less

negative in charge, -18.2mV. The PDI of the nanoparticles with non-polymeric cores, namely ferulic acid diacids (i.e., 1cM-FAG and 1cM-FAA) was 0.3 - 0.4, which indicates these nanoparticles may aggregate over time due to increases in both size and polydispersity. It might be possible to lower the nanoparticle PDI and size by incorporating a lower amount of the ferulic diacids into the nanoparticle assembly. However, for this study, the amount of ferulic acid-based polymer and diacid was held constant between formulations. This reduction in zeta potential for 1cM-FAA acid nanoparticles may also explain the tendency for aggregation of the nanoparticles since the surface charge is reduced.

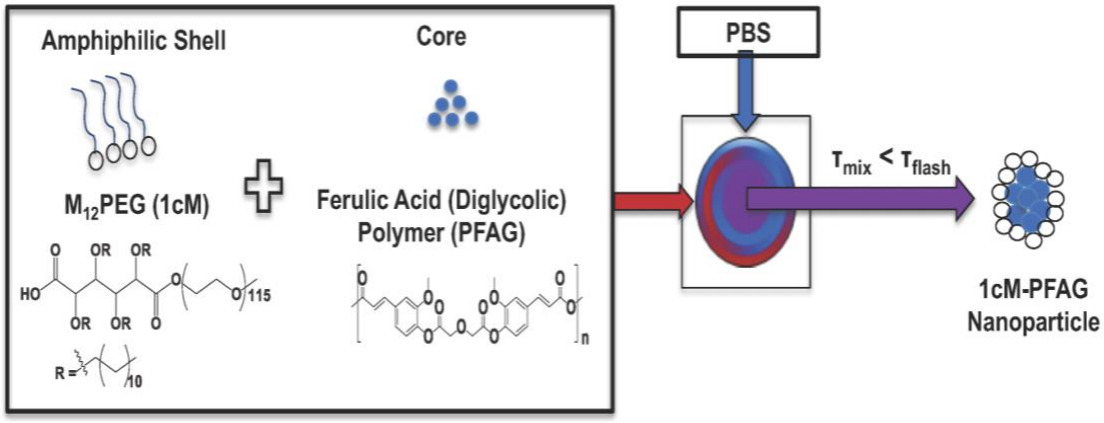


| Shell Material | Core Material | Nanoparticle | $Z_{average}$ (nm) | Polydispersity Index (PDI) | Zeta Potential (mV) |
|---|---|---|---|---|---|
| 1cM (M12P5) | M12 | | 168 ± 9 | 0.233 ± 0.055 | -24.0 |
| | Polystyrene (PS) | | 264 ± 34 | 0.151 ± 0.006 | -26.4 |
| | PFAG | | 215 ± 31 | 0.252 ± 0.056 | -25.5 |
| | PFAA | | 236 ± 20 | 0.140 ± 0.009 | -27.4 |
| PS-PEG | PS | | 150 ± 17 | 0.212 ± 0.071 | N/A |
| | PFAG | | 180 ± 39 | 0.286 ± 0.072 | N/A |
| | PFAA | | 205 ± 21 | 0.242 ± 0.053 | N/A |

**Figure 8.** ***Nanoparticle Formulation & Results Summary***. Top: Description of the flash nanoprecipitation process for the formulation of 1cM-PFAG nanoNanparticles. Bottom: Table with size, PDI, and zeta potential results for each nanoparticle formulation.

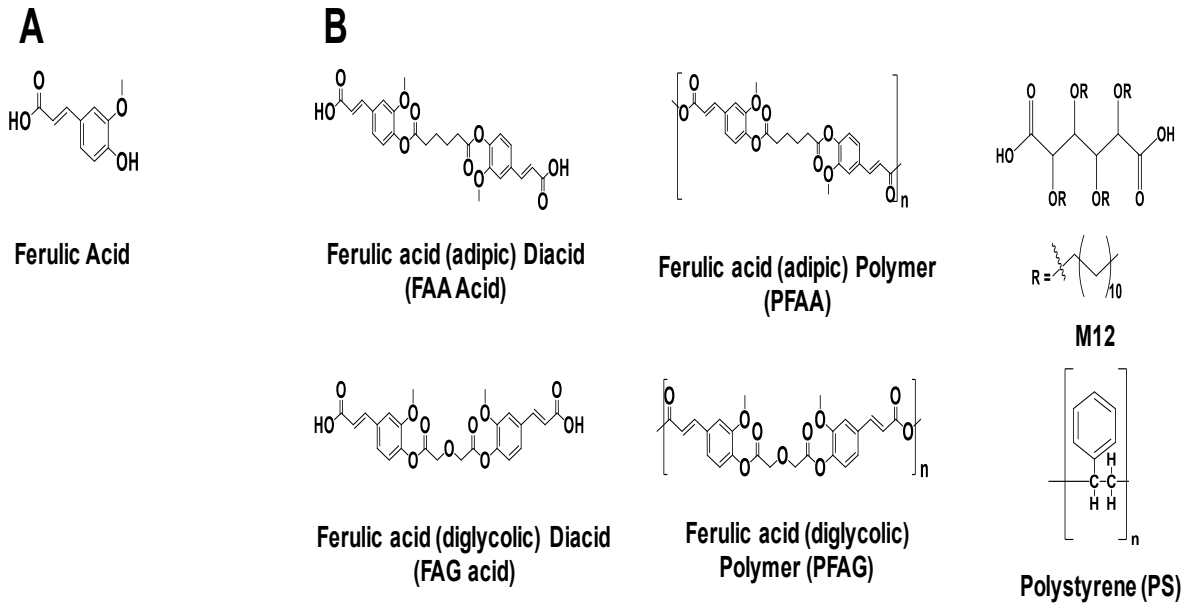


**Figure 9.** ***Overview of Antioxidant Structures.*** Chemical structure of ferulic acid **(A)** compared to the ferulic acid polymer and diacids, M12, and polysytrene **(B)**.

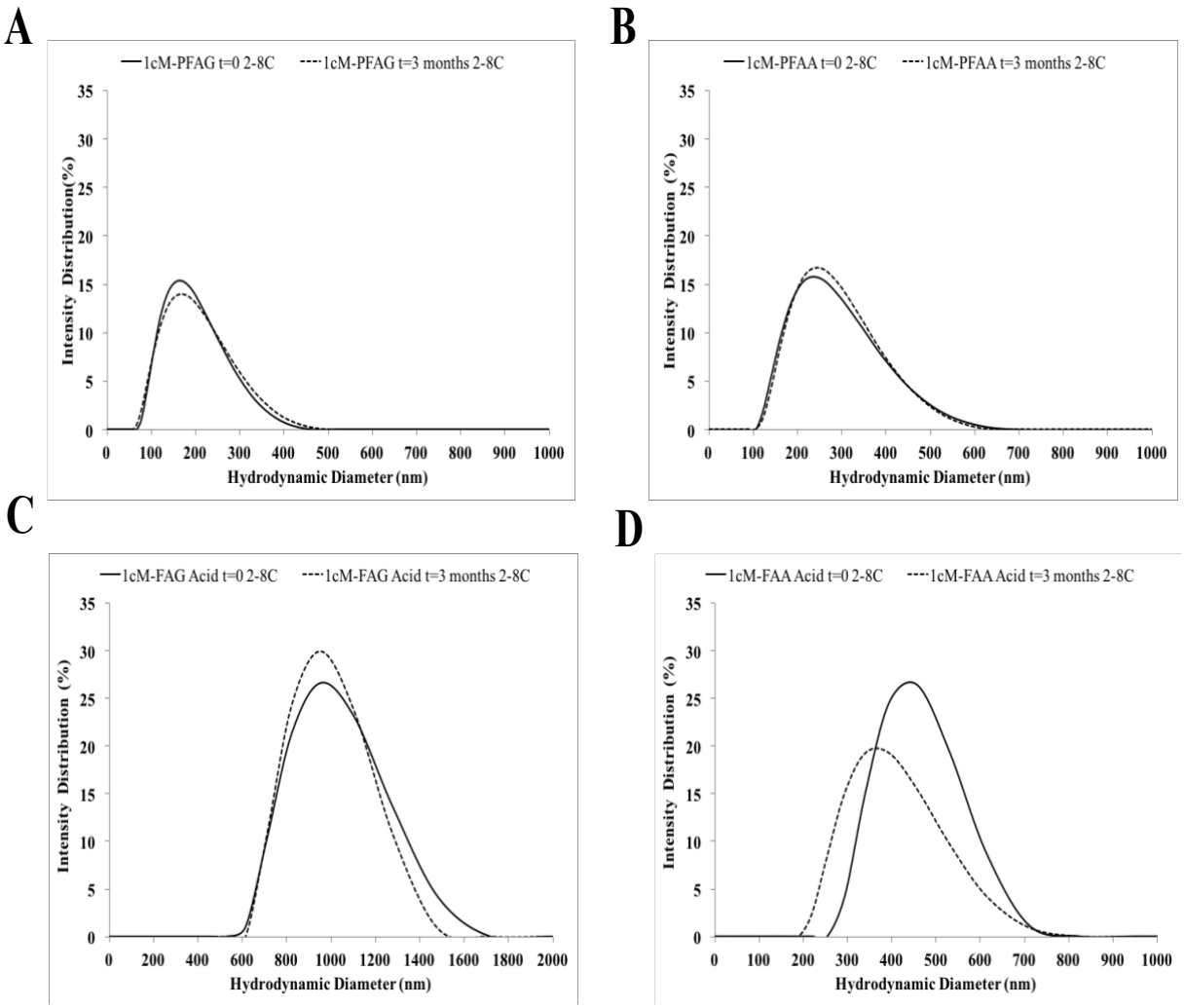


**Figure 10.** ***Stability Results for Antioxidant Nanoparticles.*** Stability measured by dynamic light scattering of 1cM-PFAG **(A),** 1cM-PFAA **(B)**, 1cM-FAG Acid **(C)**, and 1cM-FAA Acid **(D)** after storage for 3 months at 4°C.

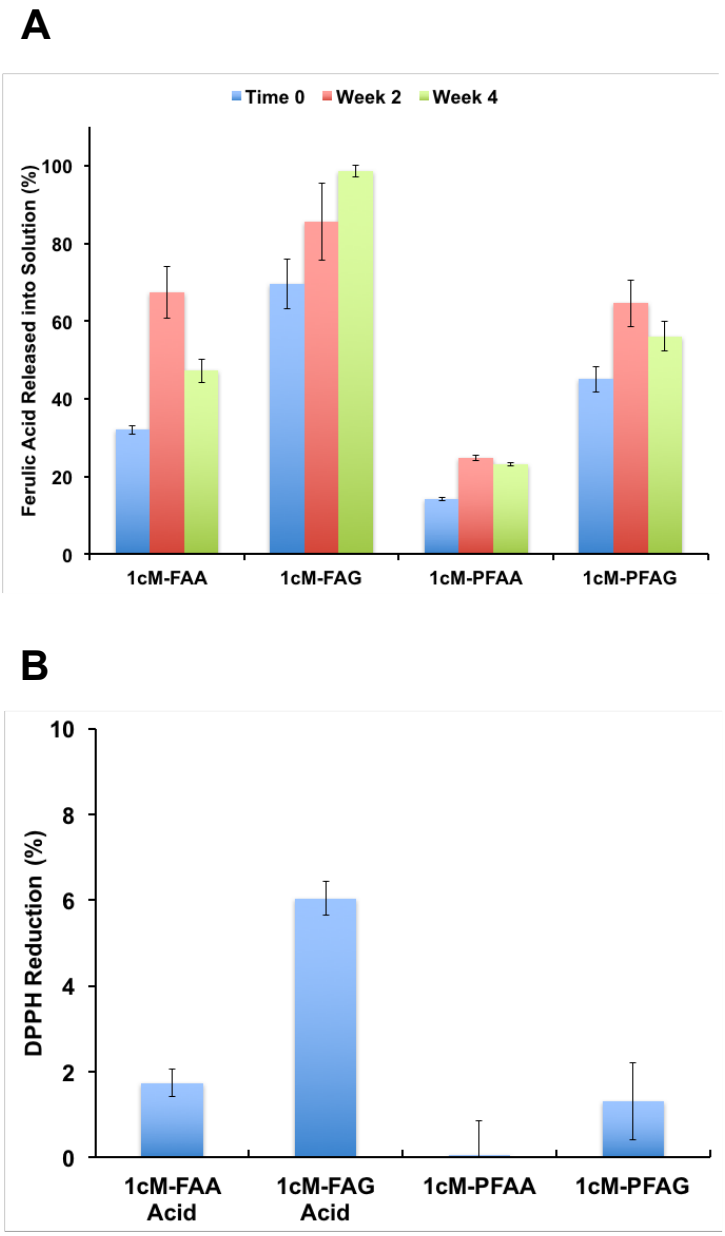


**Figure 11.** ***Ferulic acid release profile and DPPH reduction for diacid and polymer nanoparticles.*** Ferulic acid release profile and anti-oxidant activity of nanoparticle formulations after 24 hour incubation with macrophages and oxLDL (5 µg/mL) at 37ºC and 5% carbon dioxide. **A)** 1cM-PFAA released only about 10-30% of ferulic acid into the media while 1cM-FAG released about 70-100% of ferulic acid after storage of the nanoparticles up to 4 weeks at 2-8ºC ($n \geq 3$). At 2 weeks storage at 2-8ºC, each formulation except for 1cM-FAG, released the highest amount of

ferulic acid into the media during cell treatment. **B)** 1cM-FAG showed the highest DPPH reduction at 6% due to the highest amount of ferulic acid released into the media ($n \geq 3$).

*Effect of Ferulic Acid Nanoparticles on oxLDL Uptake in HMDMs*

All of the nanoparticle formulations were statistically significant ($p < 0.01$) for limiting oxLDL transport into HMDMs at an oxLDL concentration of 5 µg/mL (**Figure 12A**). After treatment with 1cM-PFAG, the oxLDL uptake was about 14% indicating that the 1cM-PFAG displayed the highest bioactivity in HMDMs (**Figures 12A & B**). In addition, the 1cM-PFAG formulation was statistically significant ($p < 0.05$) for inhibiting oxLDL uptake compared against the 1cM-M12 formulation (**Figure 12B**). An in-depth analysis of the flow cytometry data revealed the 1cM-PFAG and 1cM-PFAA formulations showed a large reduction of oxLDL uptake for about 25% of macrophages compared to either 1cM-M12 or 1cM-PS (**Figure 13)**. 1cM-PFAA, 1cM-FAA, 1cM-FAG, and 1cM-PS displayed similar oxLDL uptake levels ranging from about 20 to 25% (**Figure 12A**). Confocal images also show lower levels of oxLDL uptake for the ferulic acid nanoparticles compared to the oxLDL control (**Figure 12C)**. It is possible that a small portion of the bioactivity of both the ferulic acid-based polymer and diacid formulations originates from the release of ferulic acid since 100 µM of ferulic acid had an oxLDL uptake of about 70% (**Figures 12A & B**). The difference in the ferulate-based polymers, PFAA and PFAG, is the adipic versus diglycolic acid linker, which resulted in an additional 5 to 15% of oxLDL inhibition based on the error bars (**Figure 12B**). The ferulic acid release profiles and nanoparticle uptake rates of PFAA and PFAG formulations were also substantially different. 1cM-PFAG displayed a slightly higher uptake by HMDMs compared to 1cM-PFAA, which could account for some of the increase in bioactivity (**Figure 14**). In

addition, the release of ferulic acid into the media during cell treatment is about 50% for 1cM-PFAG and 20% for 1cM-PFAA (**Figure 11A**). These results suggest that the percentage of ferulic acid released over time is critical for regulating macrophage lipogenesis. The 1cM-PS nanoparticle (with inert core and active shell) showed an oxLDL uptake of about 25% indicating the 1cM shell has a larger contribution for lowering the oxLDL uptake in HMDMs. The oxLDL concentration was increased to 50 µg/mL to determine the effect of the nanoparticle core on oxLDL uptake and scavenger receptor expression.

At an oxLDL concentration of 50 µg/mL, the nanoparticle formulations were found to be statistically significant ($p < 0.01$) for oxLDL uptake compared to the oxLDL and ferulic acid treatments (**Figure 12D**). The oxLDL transport into macrophages increases by about 6–11% for every nanoparticle formulation (**Figure 12D**). The oxLDL levels ranged from 25-30% and were similar for the ferulic acid-based polymer and diacid nanoparticles (**Figure 12D**). Confocal images also show lower levels of oxLDL uptake for the ferulic acid nanoparticles compared to the oxLDL control (**Figure 12E)**. Treatment with either 1cM-PFAG and 1cM-PFAA maintained a subset of macrophages with slightly lower oxLDL uptake (**Figure 13)**. The size of this subset population of macrophages was also smaller as indicated by forward light scattering, which also indicates minimal uptake of oxLDL and lower chance of foam cell formation. The oxLDL uptake of 100µM of ferulic acid was minimal at about 90%.

A

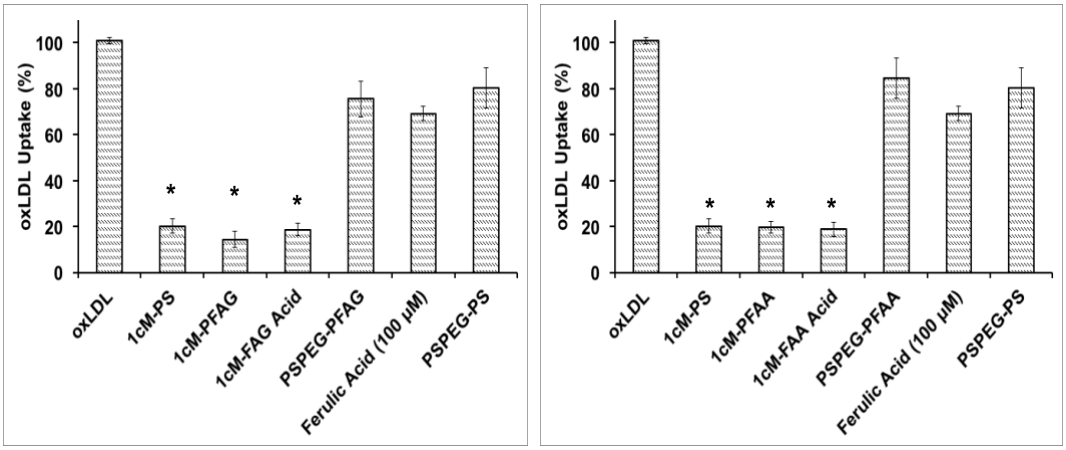
oxLDL Uptake (%)
100
80
60
40
20
0
*
*
*
oxLDL
1cM-PS
1cM-PFAG
1cM-FAG Acid
PSPEG-PFAG
Ferulic Acid (100 µM)
PSPEG-PS
oxLDL Uptake (%)
100
80
60
40
20
0
*
*
*
oxLDL
1cM-PS
1cM-PFAA
1cM-FAA Acid
PSPEG-PFAA
Ferulic Acid (100 µM)
PSPEG-PS

B

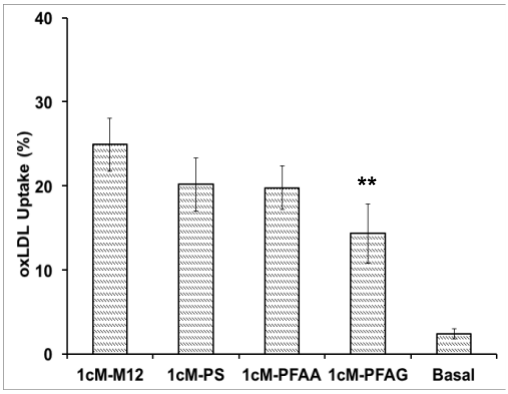
oxLDL Uptake (%)
40
30
20
10
0
**
1cM-M12
1cM-PS
1cM-PFAA
1cM-PFAG
Basal

D

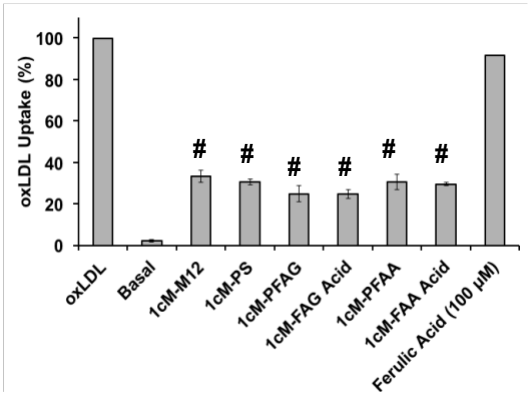
oxLDL Uptake (%)
100
80
60
40
20
0
#
#
#
#
#
#
oxLDL
Basal
1cM-M12
1cM-PS
1cM-PFAG
1cM-FAG Acid
1cM-PFAA
1cM-FAA Acid
Ferulic Acid (100 µM)

C

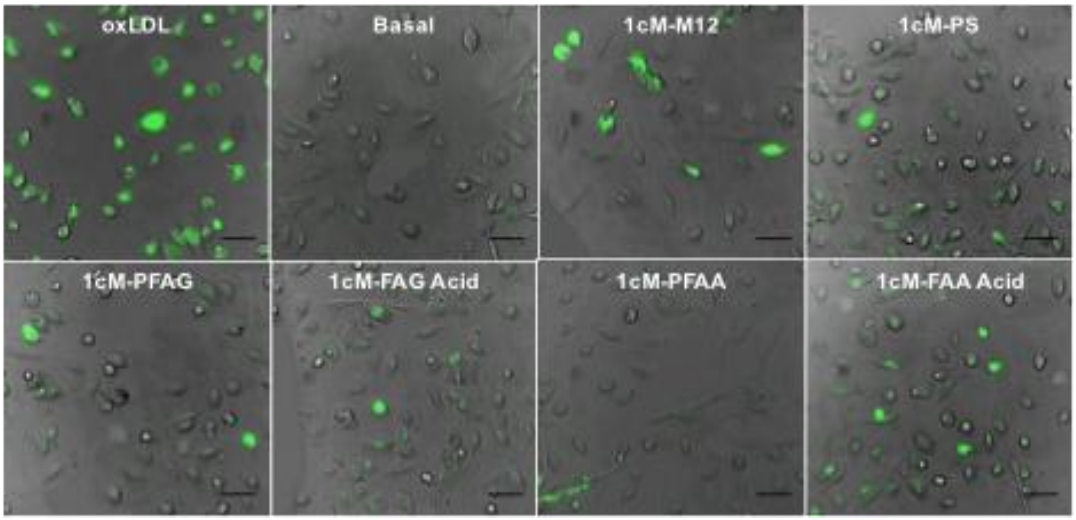
oxLDL
Basal
1cM-M12
1cM-PS
1cM-PFAG
1cM-FAG Acid
1cM-PFAA
1cM-FAA Acid

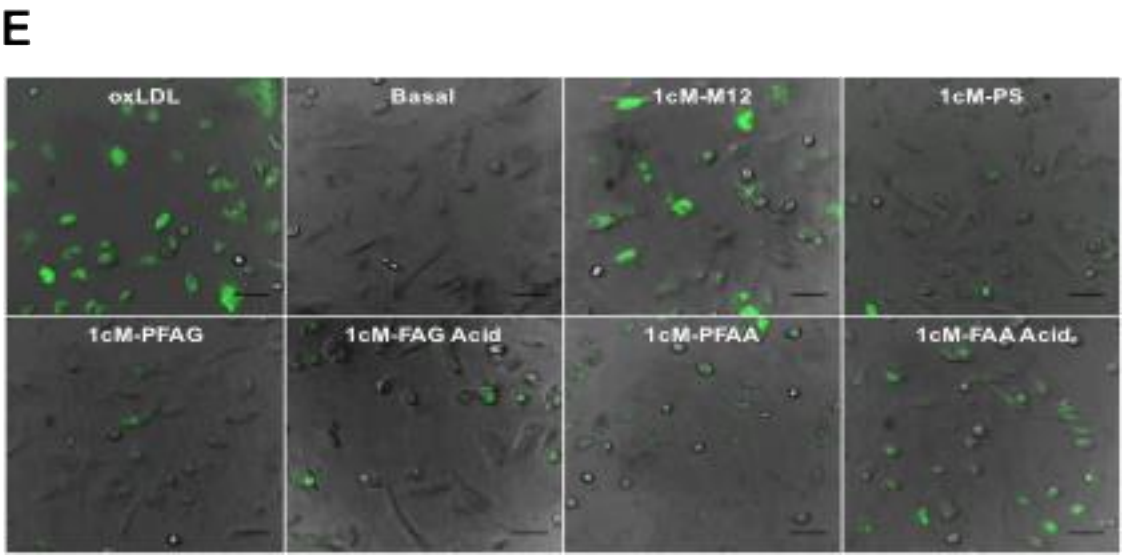


**Figure 12.** ***Effect of Ferulic Acid-based Poly(anhydride-ester) Nanoparticles on oxLDL uptake in HMDMs.*** **A & B)** 1cM-PFAG had the highest bioactivity for limiting oxLDL uptake at an oxLDL concentration of 5 µg/mL ($n \geq 5$, * $p < 0.01$ compared to the following controls: ferulic acid, PSPEG-PFAG, PSPEG-PS, and 5 µg/mL oxLDL, ** $p < 0.05$ compared to 1cM-M12 for 5 µg/mL oxLDL). **C)** Representative fluorescent images of oxLDL (green) at 5 µg/mL confirming flow cytometry results. Scale bar = 50 µm. **D)** Macrophages treated with 1cM-PFAG maintain the lowest uptake of oxLDL at a concentration of 50 µg/mL ($n \geq 5$, # $p < 0.01$ compared to ferulic acid and 50 µg/mL oxLDL). **E)** Representative fluorescent images of cells treated with 50 µg/mL oxLDL (green) confirming flow cytometry results. Scale bar = 50 µm.

# DISCUSSION

Long-term sustainable solutions to counteract atherosclerosis will require the chronic administration of pharmacologic molecules that can exhibit efficient bioavailability within the vascular intima where atherosclerotic lesions are concentrated and targeted inhibition of both atherogenesis and pro-oxidative inflammatory processes. To meet the challenge of harnessing the anti-atherogenic properties of antioxidant compounds, more targeted and robust delivery systems are needed to achieve an efficacious dose while limiting localized spikes in pro-oxidants. The emergence of controlled release mechanisms using polymer chemistry coupled with advances in nanotechnology could be one avenue for development of novel, bioactive antioxidant formulations for atherosclerosis applications [132 - 134]. In this study, we advanced the delivery and formulation of antioxidants through development of ferulic acid-based polymer nanoparticles, which are completely biodegradable and can achieve a sustained and tunable release of ferulic acid to obtain maximum bioactivity for limiting macrophage foam cell formation. By investigation of different ferulic acid intermediate and polymer formulations, we demonstrated the optimal release rate of ferulic acid correlated to a diglycolic linker within the poly(anhydride-ester) backbone for minimizing oxLDL uptake in HMDMs.

The design of ferulic acid nanoparticles was motivated by two factors: hydrophobicity of polymer backbone to control nanoparticle size and ferulic acid release, coupled with the choice of chemical linkers to achieve varying release rates of ferulic acid. Polyanhydrides were chosen for ferulic acid conjugation due to their high surface hydrophobicity, which restricts hydrolytic degradation to the polymer surface and enables

a zero order release of ferulic acid [135]. The ferulic acid-based polymers (i.e., PFAG and PFAA) formed stable nanoparticles due to the improved solubility as a polymer over the ferulic acid intermediates (ie. FAG acid and FAA acid). As previously demonstrated, the adipic acid linker releases a small percentage of ferulic acid per day compared to the diglycolic linker when ferulic acid is incorporated into a poly(anhydride-ester) backbone [128]. When ferulic acid is chemically linked using either an adipic or diglycolic acid forming a diacid compound, the release rate is faster than the corresponding polymer moiety (**Figure 11A**). Our findings indicated that when the ferulic acid release rate was increased by the inclusion of the more water-soluble diglycolic linker within the poly(anhydride-ester) (i.e., PFAG), the oxLDL uptake by HMDMs was minimal at 5μg/mL and increased slightly when the oxLDL level was increased to 50 μg/mL. This data suggests 1cM-PFAG may be crucial to prevent the subsequent formation of foam cells.

When macrophages internalize a large amount of oxidized lipoproteins, macrophages will transform into foam cells and become apoptotic [136]. Our results suggest that 1cM-PFAG may decrease plaque necrosis and thrombosis within the arterial wall and thereby preventing macrophage apoptosis and efferocytosis. By reducing oxLDL uptake, macrophages could be potentially preserved, which is critical for the roles that macrophages play in limiting the development and remodeling of plaque and controlling the disease stage of atherosclerosis [137 - 139]. Together, these results suggest that both the hydrophobicity of the ferulic acid conjugate along with the choice of chemical linker were critical factors in order to formulate bioactive nanoparticles for limiting oxLDL uptake in HMDMs.

## CONCLUSION

Antioxidants have potential as anti-atherogenic agents due to their hypolipidemic and anti- inflammatory properties. However, their bioactivity is limited by the lack of an appropriate delivery system to avoid localized pro-oxidant concentrations. In this study, we advanced the delivery and formulation of antioxidants through development of ferulic acid-based polymer nanoparticles, which are completely biodegradable and can achieve a sustained and tunable release of ferulic acid to obtain maximum bioactivity for limiting macrophage foam cell formation. To our knowledge, this study is the first report demonstrating the ability of ferulic acid polymer nanoparticles to reduce oxLDL uptake in HMDMs.

SUPPLEMENTARY FIGURES

**A**

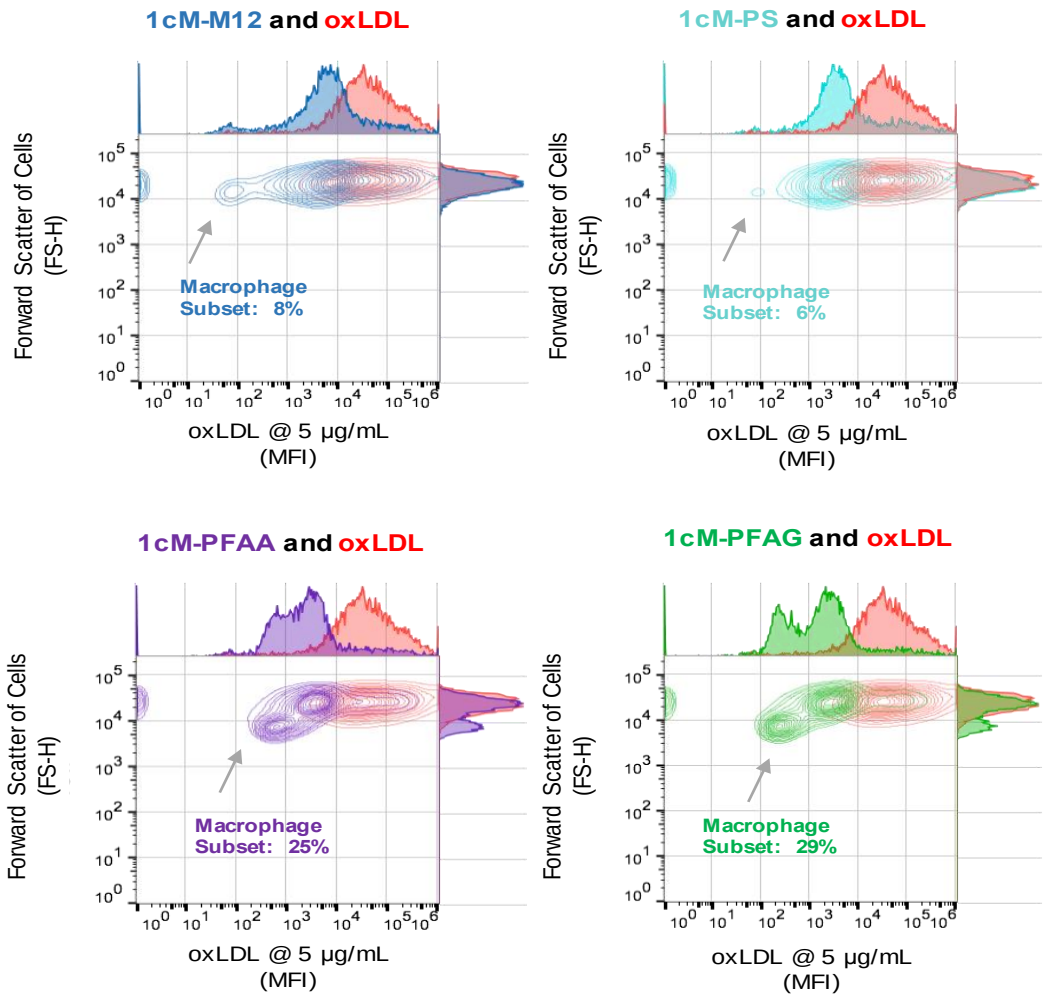

**B**

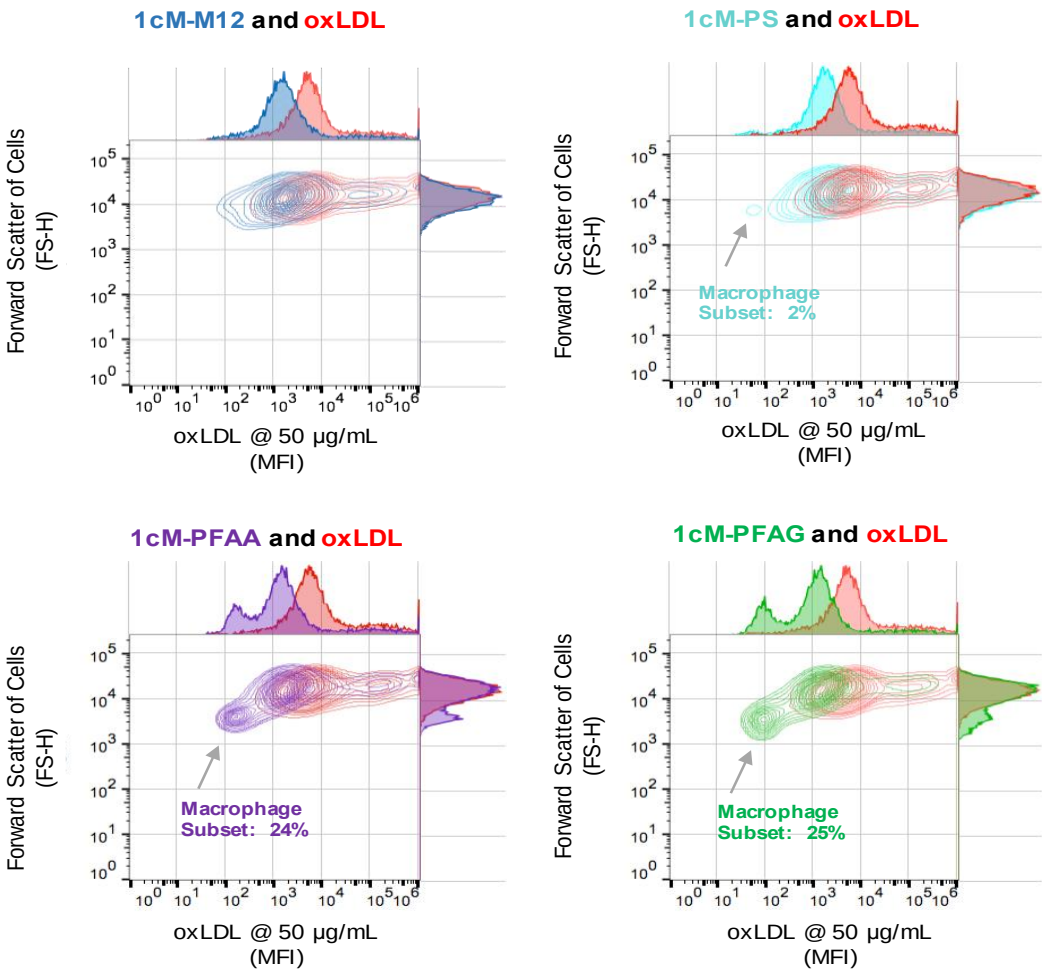


**Figure 13.** ***Effect of Ferulic Acid-based Poly(anhydride-ester) Nanoparticles on oxLDL uptake in HMDMs.*** **A)** Flow cytometry graphs are depicted as the forward scatter of cells (FS-H) versus oxLDL @ 5 µg/mL. A macrophage subset with lower oxLDL uptake was discovered when treated with 1cM-PFAG or 1cM-PFAA. In addition, these macrophage subsets have a lower cell size as indicated by the reduced forward scatter of the cells. **B)** Flow cytometry graphs are depicted as the forward scatter of cells (FS-H) versus oxLDL @ 50 µg/mL. The percentage of macrophages with low oxLDL levels did not change for the 1cM-PFAG and 1cM-PFAA formulations but decreased for 1cM-M12 and 1cM-PS when HMDMs were treated with 50 µg/mL of oxLDL. After treatment of either 1cM-PFAG or 1cM-PFAA, the macrophage subsets have a slightly lower size as depicted by the reduced FS-H.

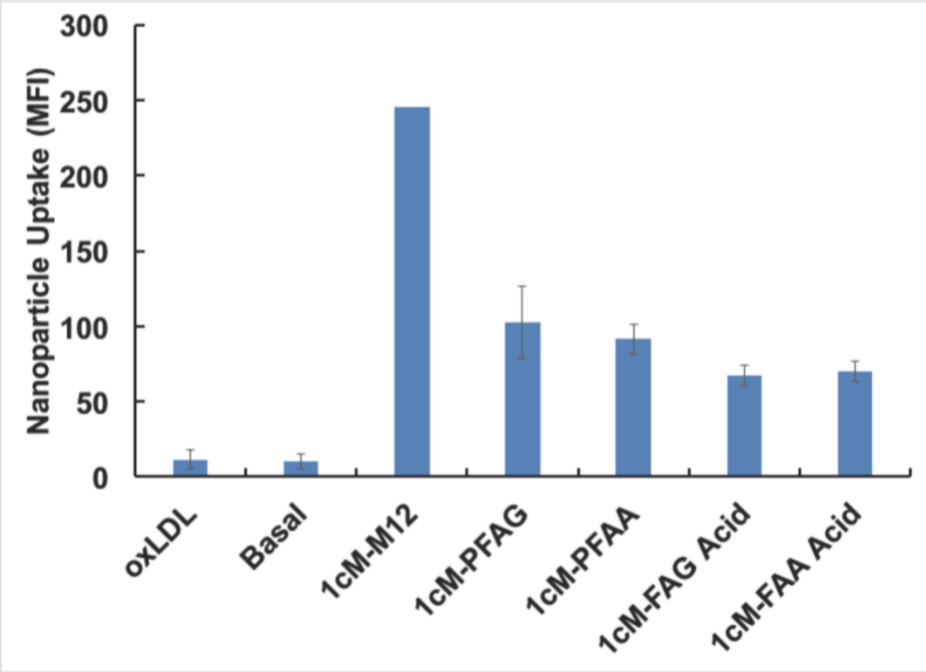


**Figure 14.** ***Impact of nanoparticle core on nanoparticle uptake by HMDMs.*** 1cM-M12 showed the highest nanoparticle uptake by HMDMs. The antioxidant formulation with the highest uptake by HMDMs was 1cM-PFAG. All nanoparticles were labeled with AlexaFluor 680. Nanoparticle uptake was measured by flow cytometry ($n = 2$ for 1cM-M12, $n \geq 3$ for remainder of formulations).

# CHAPTER 3 – FERULIC ACID NANOPARTICLES INFLUENCE MACROPHAGE SCAVENGER RECEPTOR EXPRESSION AND INFLAMMATORY STATE


## ABSTRACT

Macrophage scavenger receptors have been linked to foam cell formation through their ability to bind and internalize oxLDL and generate ROS. The ability of ferulic acid nanoparticles to decrease the expression of key macrophage scavenger receptors was assessed and compared to the current most efficacious nanoparticle, 1cM-M12. Treatment with the PFAG nanoparticles downregulated the expression of macrophage scavenger receptors, CD-36, MSR-1, and LOX-1 by about 20-50%, one of the causal factors for the decrease in oxLDL uptake. The PFAG nanoparticle lowered ROS production by HMDMs, which is important for maintaining macrophage growth and prevention of apoptosis. Based on these results coupled with the reduction in oxLDL uptake, we propose that ferulic acid-based poly(anhydride ester) nanoparticles may offer an integrative strategy for the localized passivation of the early stages of the atheroinflammatory cascade in cardiovascular disease.


## INTRODUCTION

Macrophage scavenger receptors or pattern recognition receptors were initially identified based on their ability to bind and internalize oxLDL, which led to foam cell formation and atherosclerosis. The following three scavenger receptors have been linked to oxLDL uptake through a variety of activation pathways: MSR1 (or SRA1), CD36, and LOX-1 [17]. In addition, MSR1 and CD36 also can influence macrophage apoptosis while LOX-1 has been related to smooth muscle cell apoptosis [140 – 143]. CD36 and LOX-1 have also been correlated with macrophage pro-inflammatory signaling in response to

oxLDL uptake [142, 144]. Previously, both 1cM and ferulic acid have shown the ability to reduce macrophage scavenger receptor expression and subsequently oxLDL uptake [22, 66]. Therefore, it is important to understand the impact of nanoparticle shell (1cM) and core composition (ferulic acid polymers, PFAG and PFAA, M12, and PS) on the expression of scavenger receptors and also link these results to oxLDL uptake.

In addition to macrophage uptake of oxLDL, macrophage generation of ROS has also been identified as one of the early events of atherosclerosis and constitutes one of the key pro-inflammatory signals in atherosclerosis. Recent literature has shown some correlation to scavenger receptor expression and ROS generation. MSR1 has been shown to uptake oxLDL but does not signal ROS production in macrophages [145]. On the other hand, CD36 has been recognized to inhibit ROS production by macrophages and also regulate oxLDL uptake [145]. Since the ferulic acid nanoparticles have the potential to modulate scavenger receptor expression, the ability of these nanoparticles to influence production of ROS in macrophages was also investigated.

In this chapter, we explore the cellular mechanism behind the reduction of oxLDL uptake in HMDMs along with the anti-inflammatory properties of the ferulic acid nanoparticles. The cellular mechanism of oxLDL inhibition was elucidated by evaluating expression of scavenger receptors, SRA-1, CD36, and LOX-1. In addition, we explore the second key attribute of such newly designed ferulic acid-based nanoparticles, namely their ability to regulate reactive oxygen species (ROS) generation in macrophages as anti-oxidative therapeutics.

# MATERIALS AND METHODS

## *Reagents, chemicals, and raw materials*

All chemicals/materials were purchased from Sigma-Aldrich (Milwaukee, WI) or Fisher Scientific (Pittsburgh, PA) and used as received unless otherwise noted. 18 MΩ·cm resistivity deionized (DI) water was obtained using PicoPure 2 UV Plus (Hydro Service and Supplies - Durham, NC). The following items were purchased from the indicated vendors: Ficoll-Paque Premium and Percoll from GE Healthcare (Pittsburgh, PA), RPMI 1640 from ATCC (Manassas, VA), macrophage colony stimulating factor (M-CSF) from PeproTech (Rocky Hill, NJ), fetal bovine serum (FBS) from Life Technologies (Grand Island, NY), unlabeled oxLDL from Biomedical Technologies Inc. (Stoughton, MA), 3,3'-dioctadecyloxacarbocyanine (DiO) labeled oxLDL from Kalen Biomedical (Montgomery Village, MD), and human buffy coats from either the Blood Center of New Jersey (East Orange, NJ) or New York (New York, NY) blood centers. Flow cytometry (FACS) wash buffer was prepared from phosphate buffered saline (PBS), 0.5 w/v% bovine serum albumin, 0.1 w/v% sodium azide, and 1 v% normal goat serum.

## *Preparation and characterization of nanoparticle formulations*

Nanoparticles were fabricated using the flash nanoprecipitation technique as described previously [41]. Briefly, each shell and core component were dissolved separately in the appropriate solvent and mixed together. Flash nanoprecipitation was performed by mixing the solvent stream with an aqueous stream containing phosphate buffered solution (PBS) at pH 7.4. The nanoparticles were either dialyzed against PBS using a 6000 MW cutoff ultrafiltration membrane or the solvent was displaced from the solution using vacuum. Nanoparticles were characterized by dynamic light scattering

(DLS) using a Malvern-Zetasizer Nano Series DLS detector with a 22 mW He−Ne laser operating at λ 632.8 nm using general purpose resolution mode as previously described [41]. To prepare the sample for zeta potential measurement, each nanoparticle formulation was dialyzed against deionized water using a 3500 Dalton molecular weight cutoff ultrafiltration membrane for approximately 24 hours. Approximately 1mL of sample was added into a zeta potential cell and measured using dynamic light scattering.

*Cell culture of human monocyte derived macrophages (HMDMs)*

Peripheral blood derived monocytes (PBMCs) were isolated from human buffy coats by a Ficoll-Paque (1.077 g/cm$^3$) density gradient followed by a Percoll (1.131 g/cm$^3$) density gradient as previously described [130]. After both gradient separations, PBMCs were collected and washed with PBS containing 1mM EDTA. PBMCs were plated into FEP teflon-coated cell culture bags at a density of $\geq$ 8.0 x $10^7$ monocytes per bag. Monocytes were differentiated into macrophages by addition of about 5 to 10 ng/mL recombinant human MCSF and incubated at 37°C in 5% carbon dioxide with media RPMI-1640 supplemented with 2% human serum and 1% P/S for 7 days. After seven days, cell culture bags containing differentiated macrophages were placed on ice for at least 1 hour. The cell suspension was transferred into 50 mL Falcon tubes and centrifuged at 1000 rpm for 10 minutes. Media was removed and cells were resuspended in 20 mL of RPMI-1640, 10% FBS, and 1% P/S. Cells were counted using trypan blue and a hemocytometer. Cells were replated at a density of 150,000 cells/mL and let to rest for at least 1 hour prior to treatment.

*Macrophage surface expression by HMDMs*

HMDMs were co-incubated with a mixture of labeled and unlabeled DiO oxLDL for a final concentration of either 5 µg/mL or 50 µg/mL and 1 x $10^{-5}$ M of nanoparticles in RPMI-1640 with 10% FBS and 1% P/S for 24 hours at 37°C in 5% carbon dioxide. For visualization of MSR-1, unlabeled oxLDL was used in the experiment. Experimental controls included macrophages treated with either medium (basal) or 5 µg/mL or 50 µg/mL of oxLDL. After 24 hours, cells were washed to remove the treatments and 1mL of 10 mM EDTA in PBS pH 7.4 was added to each well. Cells were collected by incubating the plate on ice for up to 15 minutes and removed from the surface of the plate by pipetting and transferred to a flow tube. Each well was washed with 1 mL of FACS buffer, which was also added to the flow tube. Cells were centrifuged at 1000 rpm for 10 minutes at 4°C, supernatant was decanted and cells were resuspended. FACS wash buffer was added to the cells, centrifuged, and supernatant decanted. Cells were incubated for 1 hour at 4°C with either PE anti-human MSR1 antibody (clone: U23-56, BD Biosciences), APC anti-human LOX-1 antibody (clone: 15C4, Biolegend) and APC anti-human CD36 antibody (clone: 5-271, Biolegend) or their corresponding isotype control APC mouse IgG2a,κ (clone: MOPC-173, Biolegend) and PE mouse IgG1,κ (clone: MOPC-21, BD Biosciences). Following antibody incubation, the cells were washed twice with FACS wash buffer and then fixed with 1 v% paraformaldehyde in PBS. Cell fluorescence was measured using a Gallios flow cytometer. Macrophage surface expression were quantified using the geometric mean fluorescence intensity (MFI) of the intact HMDMs and analyzed using FlowJo software (Treestar). Results are the average of at least three independent experiments with two

replicates per experiment. The percentage of macrophage scavenger receptor (SR) expression was calculated using the following formula [22]:

$$\frac{SR\ MFI\ of\ treatment\ sample}{SR\ MFI\ of\ oxLDL\ only\ control\ sample}\ x\ 100 = Percentage\ of\ SR\ expression$$

*Confocal microscopy*

Expression of CD-36 and MSR-1 were visualized using a SP5 confocal microscope (Leica) with a 40x oil immersion objective. HMDMs were plated in an eight well labtek at a density of 150,000 cells/mL. HMDMs were co-incubated with oxLDL and nanoparticles as described previously. HMDMs were washed with PBS pH 7.4 three times and fixed with 4 v% PFA for 20 minutes room temperature. The 4% PFA was removed and cells were incubated with blocking buffer (5 v% goat serum, 0.5 w/v% BSA in PBS pH 7.4) for 15 minutes at room temperature. For CD-36 and MSR-1 expression, HMDMs were treated with 1:50 dilution of the antibodies in blocking buffer overnight at 4°C. Cells were washed three times with PBS pH 7.4 and then incubated with 1:500 dilution of a goat anti-rabbit secondary IgG antibody tagged with either Alexa Fluor 633 or 647 in blocking buffer for about 30 minutes at room temperature in the dark. Cells were washed three times with PBS pH 7.4 and Hoescht (0.1 µg/mL) was added for 15 minutes. Cells were washed with PBS pH 7.4, covered in foil, and stored at 4°C until imaging.

*Measurement of cellular reactive oxygen species (ROS)*

HMDMs were co-incubated with HMDMs were co-incubated with oxLDL and nanoparticles as described in Chapter 2. After 24 hours, each treatment was removed and cells were washed once with PBS pH 7.4 at 37°C. Cells were incubated with 12.5 µM of CellRox Red (Fisher Scientific) at 37°C, 5% carbon dioxide for 30 minutes. The CellRox Red was removed and cells were washed three times with PBS pH 7.4. RPMI-1640, 10%

FBS, 1% P/S, 7 g/L HEPES was added to the cells for live imaging at 37°C. OxLDL and ROS fluorescence were visualized using a SP5 confocal microscope (Leica) with a 40x oil immersion objective. ROS levels were quantified by ImageJ and normalized to cell count.

*Statistical analysis*

Data presented are from at least three independent experiments ($n \geq 3$) and values are represented as mean ± SEM unless otherwise indicated. Statistical analysis was performed considering $p < 0.05$ to be statistically significant. Statistical significance was determined using a one-way ANOVA with Tukey's posthoc test for comparisons between multiple treatment groups.

RESULTS

*Effect of polymeric antioxidant structure on scavenger expression in HMDMs*

While 1cM-PFAG demonstrates clear efficacy at the reduction of oxLDL uptake by HMDMs, we sought to elucidate the underlying mechanism, by comparing its effects to other control formulations, 1cM-M12 and 1cM-PS nanoparticles. The expression of the following macrophage surface markers was tested by flow cytometry to determine the cellular pathway of oxLDL inhibition: CD-36, MSR-1, and LOX-1. It was notable that 1cM-PFAG displayed a statistically significant ability to down regulate all three of the macrophage receptors. After treatment with 1cM-PFAG and oxLDL at 5 μg/mL, the expression of CD-36 was reduced to about 55% (**Figure 15A**). The reduction in CD-36 expression directly correlated with a reduction in oxLDL uptake by HMDMs (**Figure 19**). As visualized by confocal, a subset of macrophages contained lower levels of oxLDL but also maintain some surface expression of CD-36 (**Figure 15C**). 1cM-M12 and 1cM-PFAA nanoparticles also reduce CD-36 expression but to a lesser extent at about 30% (**Figures**

**15A & B**). 1cM-M12 has been previously demonstrated to reduce CD-36 expression [40]. After treatment with either 1cM-PFAG or 1cM-PFAA, a subpopulation of macrophages (ie. 20-24% of the cells) displayed a further decrease in CD36 expression as compared to the entire population (**Figure 19**). The CD-36 expression levels of the control formulations, PSPEG-PFAA, PSPEG-PFAG and 1cM-PS, were about 90%, which suggests that the down regulation of CD-36 occurs mainly by macrophage uptake of the nanoparticle by HMDMs and resultant release of the core molecule. When the oxLDL levels are increased to 50 µg/mL, the CD-36 expression level is at least 90% for all the formulations with exception of 1cM-PFAG (**Figure 15D**). The CD-36 expression level was about 78% for the 1cM-PFAG nanoparticle, which indicates a 22% increase in CD-36 expression when the oxLDL concentration was increased from 5 to 50 µg/mL.

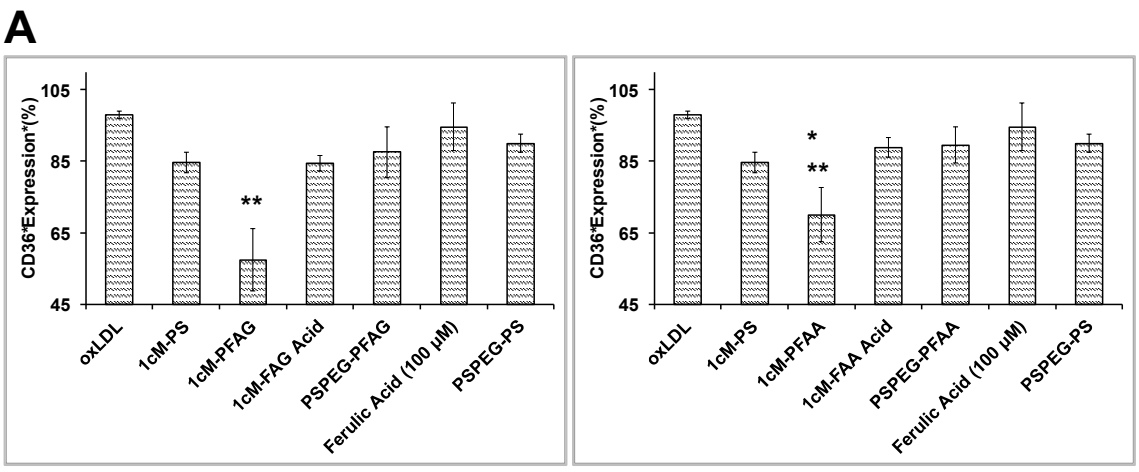

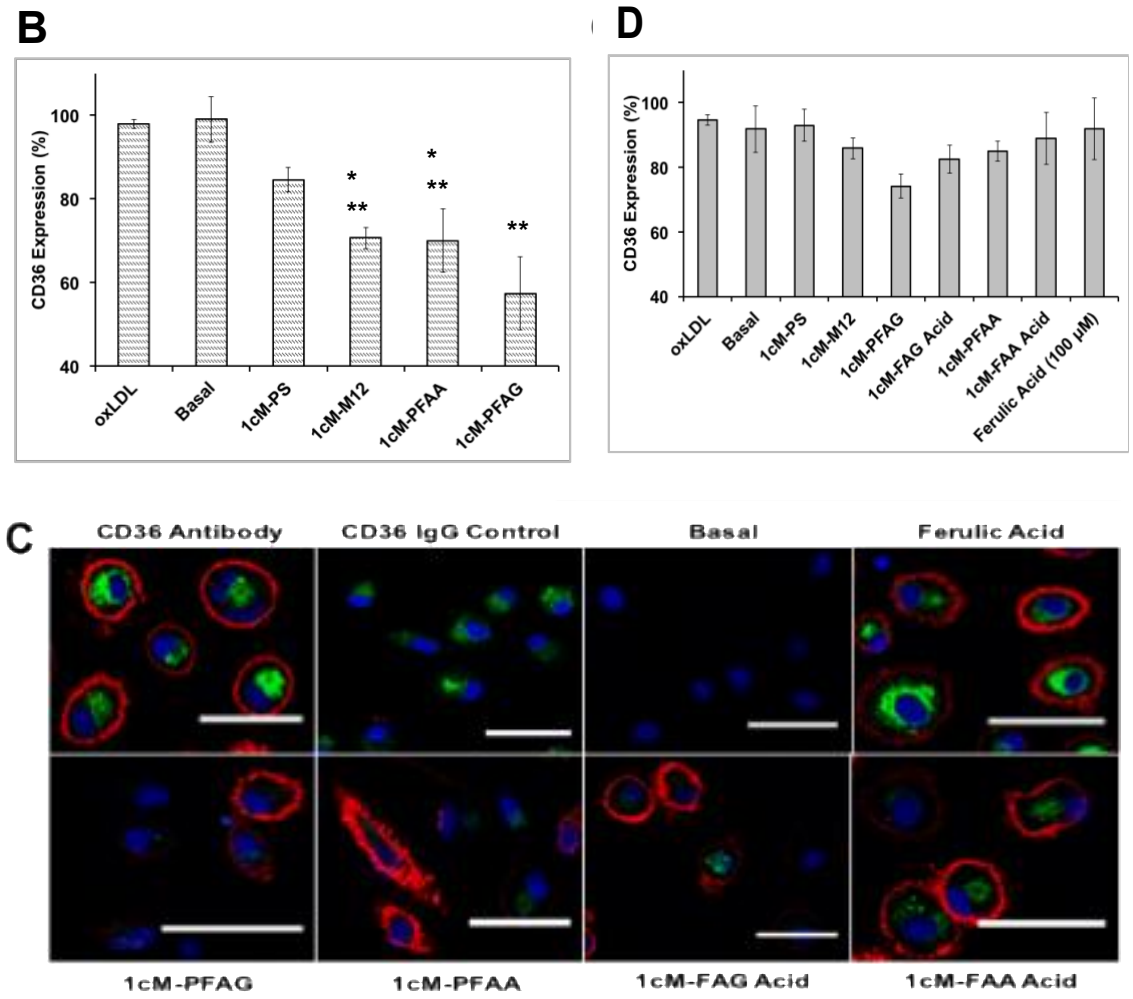


**Figure 15.** ***Composition of Ferulic Acid-based Poly(anhydride-ester) Nanoparticles differentially modulates CD36 expression in HMDMs***. **A-B)** 1cM-PFAG down regulated CD36 expression by about 40% (oxLDL 5 µg/mL) ($n \geq 3$, ** $p < 0.01$ compared to 1cM-PS, 1cM-PFAG Acid, 1cM-PFAA Acid, ferulic acid, and oxLDL). 1cM-M12 and 1cM-PFAA also down regulated CD36 expression by about 30% (oxLDL 5 µg/mL) ($n \geq 3$, * $p < 0.05$ compared to ferulic acid, ** $p < 0.01$ compared to oxLDL). **C)**. Representative fluorescent images of cells treated with 5 ug/ml oxLDL (green), Cell nuclei (blue), CD36 expression (red), which confirm flow cytometry results. Scale bar = 50 µm. **D)** CD36 expression increased for 1cM-M12, 1cM-PFAG, and 1cM-PFAA with increased oxLDL (50 µg/mL).

MSR-1 expression was significantly reduced by 30% after treatment with 1cM-PFAG and 5 µg/mL oxLDL (**Figure 16A**). An in-depth analysis by flow cytometry shows that the MSR-1 expression is substantially down-regulated in 17% of the macrophage population (**Figure 16B**). Confocal microscopy images confirm the ability of 1cM-PFAG to down regulate MSR-1 expression compared to the other formulations studied (**Figure 16C**). From the confocal images and flow cytometry graph, it appears that the majority of macrophages with reduced oxLDL levels after treatment with 1cM-PFAG also have very minimal MSR-1 expression, which contrasts with the trends compared to CD-36 expression. When the oxLDL levels were increased to 50 µg/mL, MSR-1 expression increased to the baseline level even after treatment with 1cM-PFAG (**Figure 20A**). This result indicates that the ability of 1cM-PFAG to down-regulate MSR-1 on HMDMs as a function of oxLDL concentration.

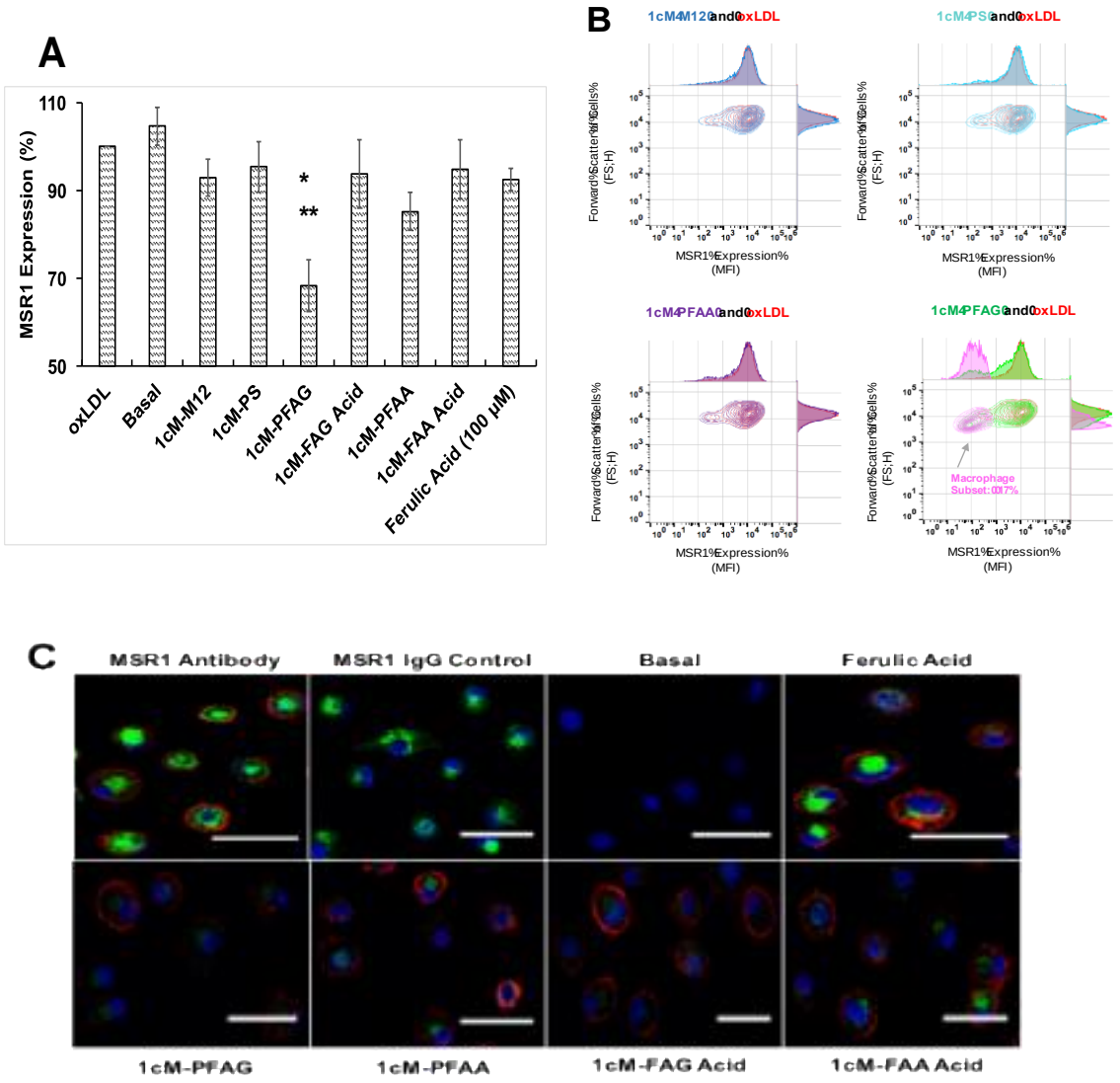


**Figure 16.** ***Composition of Ferulic Acid-based Poly(anhydride-ester) Nanoparticles differentially modulates MSR1 expression in HMDMs.*** **A)** 1cM-PFAG down regulated MSR1 expression by about 30% (oxLDL 5 µg/mL) (n = 3, * $p < 0.05$ compared to 1cM-PS, 1cM-PFAA Acid; ** $p < 0.01$ compared to oxLDL). **B)** Flow cytometry graphs are depicted as the forward scatter of cells (FS-H) versus 5 µg/mL oxLDL. A macrophage subset (5 ug/mL oxLDL) was observed with decreased MSR1 expression after treatment with 1cM-PFAG compared to 1cM-PFAA, 1cM-M12, and 1cM-PS. The size of this macrophage subset is slightly smaller than the entire population as evidenced by the small decrease in forward scatter of cells. expression in

HMDMs. **C)** Representative fluorescent images of cells treated with 5 ug/ml oxLDL (green), cell nuclei (blue) and MSR1 expression (red), which confirm flow cytometry results. Scale bar = 50 µm.

LOX-1 scavenger receptor expression exhibited about a 20% reduction after treatment with 1cM-PFAG and 5 µg/mL of oxLDL (**Figure 17A**). In contrast, 1cM-M12 and 1cM-PS both displayed a small increase LOX-1 expression. 1cM-PFAG nanoparticles showed a significant reduction of LOX-1 expression compared to 1cM-M12 and 1cM-PS (**Figure 17A**). About 8% of the macrophage population showed a further reduction of LOX-1 expression after treatment with 1cM-PFAG and 5 µg/mL of oxLDL (**Figure 17B**). LOX-1 expression ranged from about 90-100% for all formulations when HMDMs were treated with 50 µg/mL of oxLDL (**Figure 20B**). The difference in chemical linker used for the ferulic acid-based polymer (i.e., glycolic versus adipic acid) had a significant effect on the down-regulation of CD-36, MSR-1, and LOX-1 receptors on HMDMs and directly correlated with the ability to reduce oxLDL uptake.

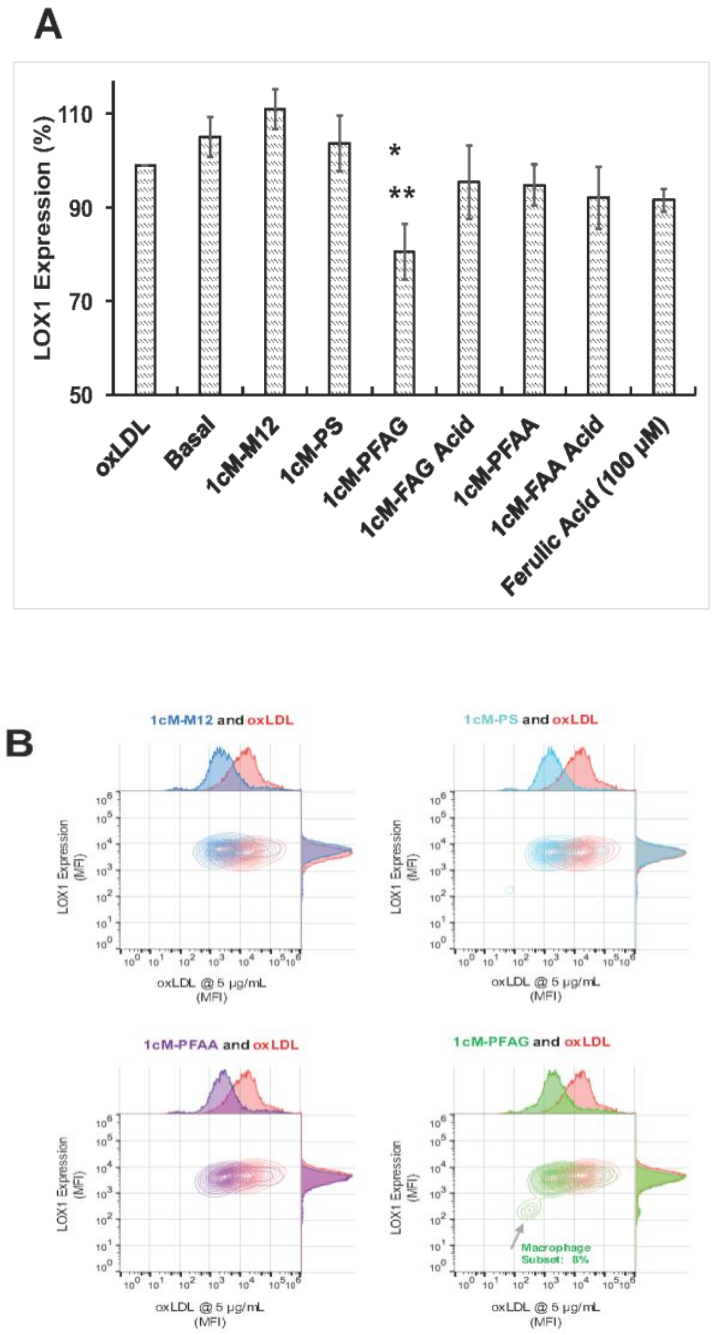


**Figure 17.** ***Composition of Ferulic Acid-based Poly(anhydride-ester) Nanoparticles differentially modulates LOX1 expression in HMDMs.*** **A)** 1cM-PFAG down regulated LOX1 expression by about 20% (oxLDL 5 µg/mL) ($n \geq 3$, * $p < 0.05$ compared to 1cM-PS; ** $p < 0.01$ compared to 1cM-M12). **B)** Flow cytometry graphs are depicted as LOX-1 expression versus 5

μg/mL oxLDL. A macrophage subset (5 ug/mL oxLDL) was observed by with decreased LOX-1 expression after treatment with 1cM-PFAG compared to 1cM-PFAA, 1cM-M12, and 1cM-PS.

*Effect of polymeric antioxidant structure on regulation of ROS levels in HMDMs*

Since oxLDL can activate macrophages and produce high levels of reactive oxygen species (ROS), the effect of each nanoparticle formulation on regulation of ROS was investigated using HMDMs. The ferulic acid polymer and diacid nanoparticles showed the lowest levels of ROS (30-40%) compared to the other formulations with the exception of 1cM-PS (**Figure 18A**). These results indicate the diglycolic linker did not have a significant impact on the decrease in macrophage ROS levels compared to the polymer with an adipic acid linker. The 1cM-PS nanoparticle also showed lower levels of macrophage ROS at about 37%, which indicated the 1cM shell did not likely elicit substantial increase in macrophage ROS (**Figure 18A**). However, when the PS core was switched to M12, the ROS levels increased by about 2-fold indicating the M12 core is highly inflammatory (**Figure 18A**). Furthermore, the nanoparticle core appears to modulate macrophage ROS levels with the ferulic acid polymer and diacid nanoparticles as the most promising formulations for regulating macrophage ROS levels (**Figure 18B**).

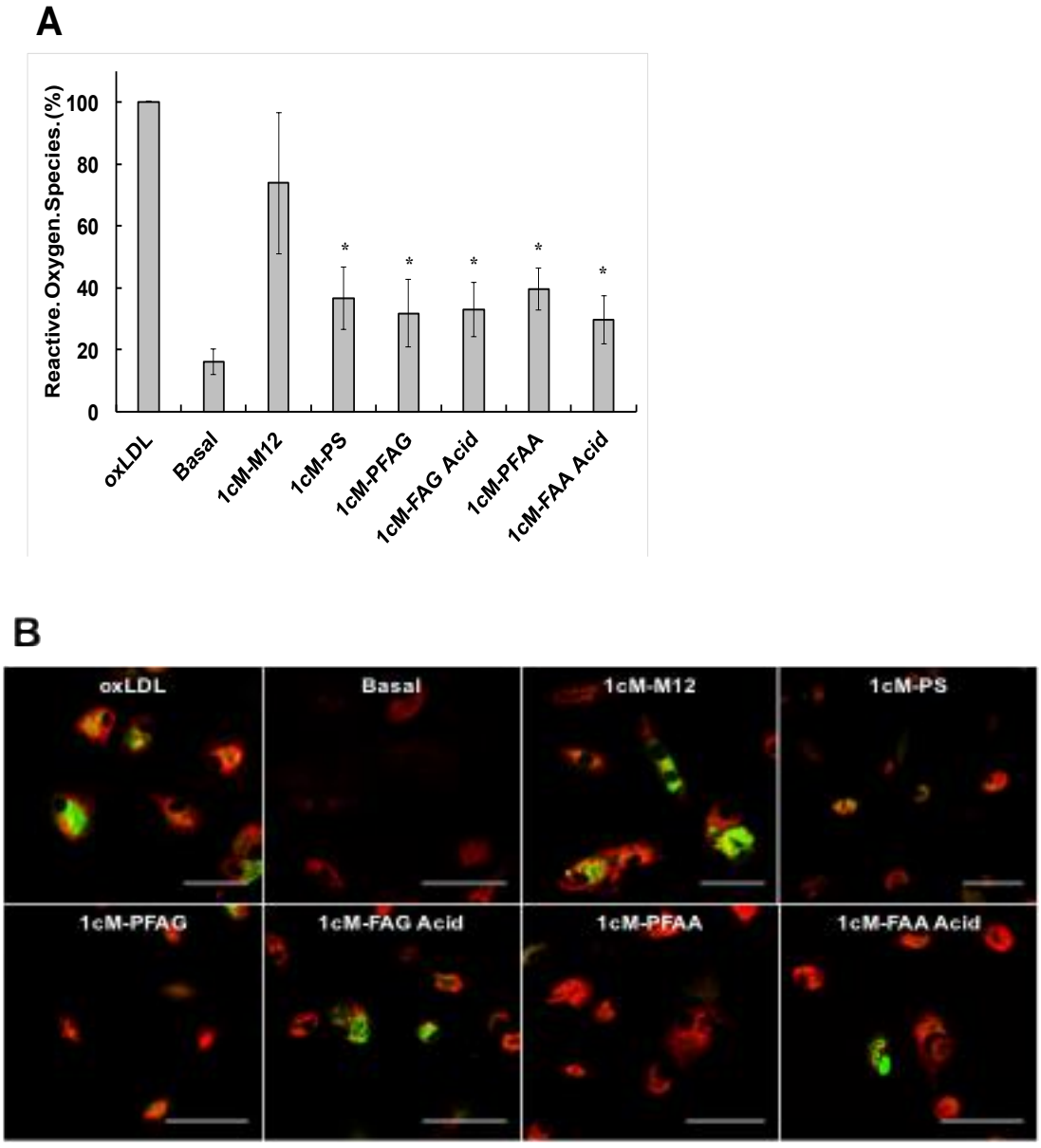


**Figure 18.** ***Effect of composition of Ferulic Acid-based Poly(anhydride-ester) Nanoparticles on reactive oxygen species (ROS) generation in HMDMs.*** **A)** Macrophages treated with 1cM-PFAG show the lowest levels of ROS generation compared to the oxLDL control at 50 µg/mL (n = 4, * $p < 0.05$ compared to oxLDL). **B)** Representative fluorescent images of oxLDL (green) at 50 µg/mL and ROS (red) show 1cM-PFAG has the highest potential to limit ROS generation. All scale bars represent 50 µm.

DISCUSSION

We sought to elucidate the nature of cellular mechanisms by which the ferulic acid-based polymer and intermediate nanoparticles modulate oxLDL uptake. We limited our focus on the expression of extracellular scavenger receptors, CD36, MSR1, and LOX1, which predominantly account for uptake of oxLDL by HMDMs [146]. Our results indicated only the 1cM-PFAG nanoparticle was able to significantly downregulate all three HMDM surface scavenger receptors, CD36, MSR1, and LOX-1, at an oxLDL concentration of 5 μg/mL. We hypothesized the downregulation of the above scavenger receptors occurs intracellularly by the release of ferulic acid from the 1cM-PFAG nanoparticle after phagocytosis by HMDMs. When we employed the 1cM-PS formulation, which contains a bioactive shell and non-bioactive polystyrene core, we did not observe any significant downregulation of any of the three scavenger receptors, which validated this hypothesis. When the oxLDL concentration was increased to 50 μg/mL, the ability of 1cM-PFAG to downregulate each cellular receptor was significantly reduced, as expected, which indicated expression of these scavenger receptors is strongly correlated to oxLDL concentration. In addition, since the oxLDL uptake remained low at 30-40%, it is possible that additional scavenger receptors, such as CD163 and SR-B1, could be downregulated by the ferulic acid-based nanoparticles but this mechanism would need further investigation [146]. Furthermore, the ability of ferulic acid nanoparticles to inhibit low density lipoprotein (LDL) oxidation could also be investigated based on previous literature [147].

Recent studies demonstrated a direct correlation of oxLDL uptake in mouse macrophages with an increase in reactive oxygen species (ROS) levels [148 - 149]. We

hypothesized the primary effect of the ferulic acid nanoparticles is the inhibition of oxLDL receptor expression, which could result in the inhibition of ROS production. Ferulic acid has the potential to scavenge free radicals through its ability to form a resonance stabilized phenoxy radical, which accounts for its antioxidant potential [64, 65]. Our results indicated the ferulic acid-based nanoparticles had a pronounced and statistically significant effect on reducing ROS levels compared to the oxLDL control. Future work could include the investigation of iNOS expression coupled with nitrate/nitrate levels to further understand the inhibition of ROS production. The ability to regulate macrophage ROS has significant implications for atherosclerosis. Reactive oxygen species can play key roles in macrophage polarization along with cell death, proliferation, motility, and phagocytic ability [150]. Taken together this data suggests that 1cM-PFAG reduces the oxLDL uptake and subsequently regulates the generation of ROS by HMDMs, which are two critical aspects for prevention of foam cell formation and apoptosis.

## CONCLUSION

To our knowledge, this study is the first report demonstrating the ability of ferulic acid polymer nanoparticles to regulate both scavenger receptor expression and ROS in HMDMs. The 1cM-PFAG nanoparticle downregulated the expression of all three scavenger receptors, CD-36, MSR-1, and LOX-1, which correlated with the reduction in oxLDL uptake by HMDMs. In addition, the ferulic acid nanoparticles lowered the generation of ROS in HMDMs compared to the oxLDL control and 1cM-M12 nanoparticle. Overall, the formulation of a variety of ferulic acid polymer and intermediate diacid nanoparticles for prevention of macrophage foam cell formation is a major step

forward for development of novel, antioxidant formulations for treatment of atherosclerosis.

SUPPLEMENTARY FIGURES

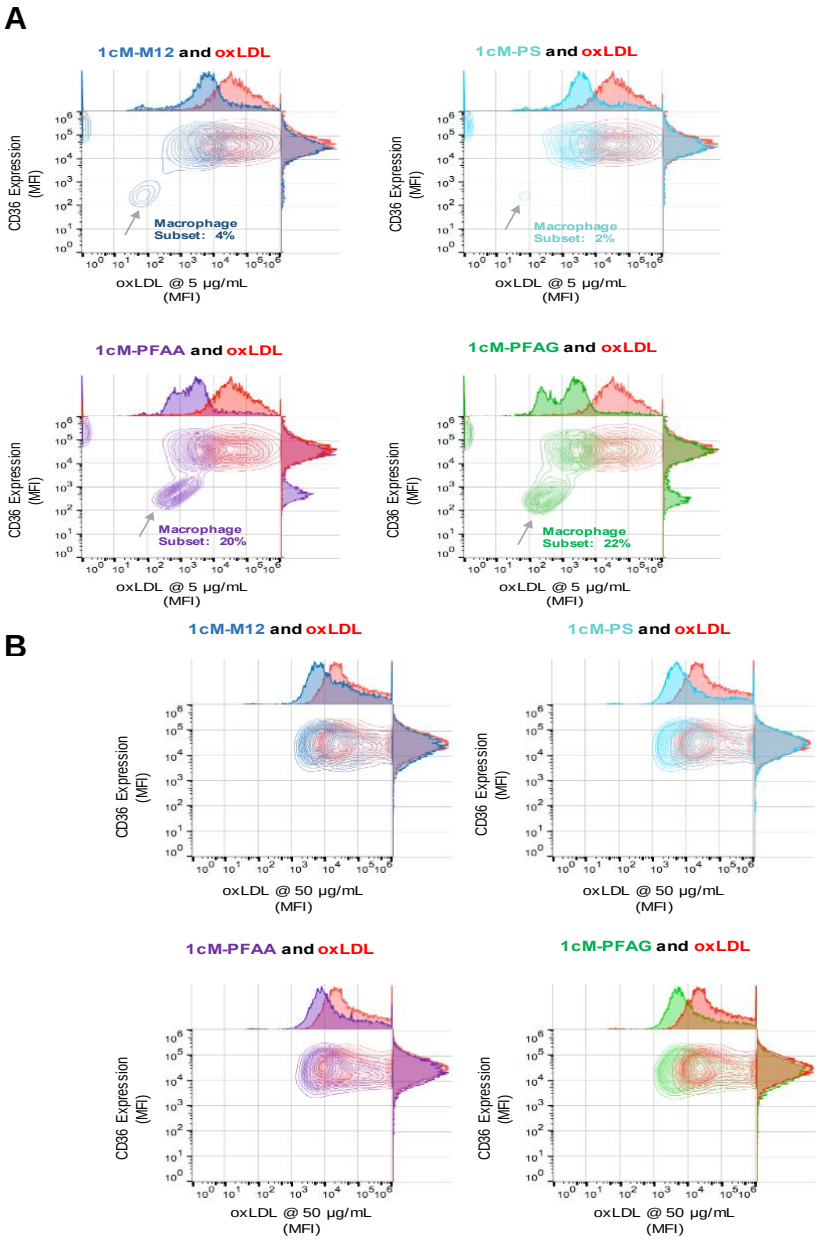


**Figure 19.** ***Composition of Ferulic Acid-based Poly(anhydride-ester) Nanoparticles differentially modulates CD36 expression in HMDMs.*** **A)** Flow cytometry graphs are depicted as CD36 expression versus 5 µg/mL oxLDL. A macrophage subset (oxLDL 5 µg/mL) with reduced CD36 expression was discovered after treatment with 1cM-PFAG or 1cM-PFAA. **B)** Flow cytometry graphs are depicted as CD36 expression versus 50 µg/mL oxLDL. Flow

cytometry graphs showed an increase for both oxLDL fluorescence and CD36 expression with no subset populations.

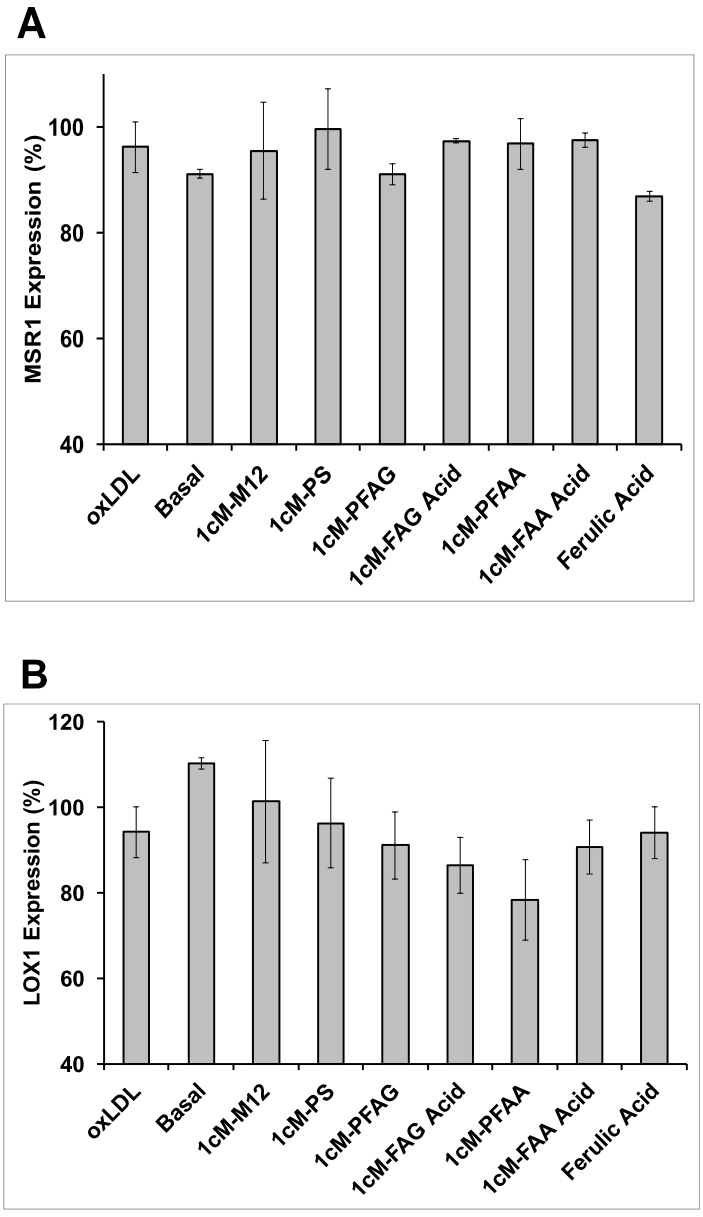


**Figure 20.** ***Effect of 50 µg/mL oxLDL on MSR1 and LOX1 expression in HMDMs.*** MSR1 expression **(A)** and LOX1 expression **(B)** increased for 1cM-PFAG with increased oxLDL (50 µg/mL) compared to oxLDL levels at 5 µg/mL (n = 3 for LOX1 and MSR1).

# CHAPTER 4 – ANTIOXIDANT NANOPARTICLES MODULATE ALPHA SYNUCLEIN FIBRIL FORMATION


## ABSTRACT

The pathophysiology of Parkinson's disease results from the loss of neuromelanin-containing dopaminergic neurons in the substantia nigra pars compacta (SN) and the presence of Lewy bodies. Alpha synuclein fibrils cause neuroinflammation, neurodegeneration, and cell death and are located in the Lewy bodies of Parkinson's disease patients. Alpha synuclein (α-synuclein) is an unfolded protein in solution but can form oligomers or fibril structures under certain conditions, such as oxidative stress and post-translational modifications. The current state of treatments for Parkinson's disease are limited and only manage the progression of the disease state. Here, we designed a new class of nanoparticles comprised of two antioxidants, ferulic acid and tannic acid. The FAA acid-tannic acid nanoparticles counteracted the fibrillization of α-synuclein independent of the protein acetylation state. The ferulic acid polymer nanoparticle (1cM-PFAA) also displayed a significant inhibition of α-synuclein fibril formation especially when compared to ferulic acid, which indicated the formulation of the antioxidant could also impact α-synuclein self-assembly. Based on these results, we propose that both antioxidant nanoparticles may offer a strategy for reduction of α-synuclein fibrillization and possible prevention of the initial stages of Parkinson's disease.


## INTRODUCTION

Parkinson's disease is a long term, degenerative disorder that affects the motor system of the central nervous system with medical costs estimated at $15.5 billion per year [151, 70]. The pathophysiology of Parkinson's disease results from the loss of

neuromelanin-containing dopaminergic neurons in the substantia nigra pars compacta (SN) and the presence of Lewy bodies [1]. Alpha synuclein plays a critical role in the pathogenesis of Parkinson's disease. Alpha synuclein aggregation starts as soluble protofibrils that can progress into insoluble fibrils composed of β-sheets and amyloid-like filaments [152-155]. These filaments can aggregate and form insoluble fibrillary structures and inclusions, which accumulate into Lewy bodies. The atypical accumulation of α-synuclein aggregates in the neurons, nerve fibers, or glial cells is termed α-synucleinopathy [1, 156].

Human α-synuclein is a 14kDa intrinsically disordered protein consisting of 140 amino acids and contains three distinct regions [157]. The N-terminal region (residues 1-60) consists of multiple amphipathic α-helices and allows for penetration and transportation into membranes of neuronal cells, such as microglia [85, 158]. The central region (residues 61-95) consists of a highly hydrophobic core domain known as the NAC (non-amyloid component) that has a tendency to form oligomers and β-sheet fibrils [87 – 88]. The C-terminal region (residues 96-140) is highly enriched in acidic amino acids and prolines and has been shown to activate microglia [85 – 86, 159].

Point mutations of the SNCA gene, encoding for α-synuclein, have been linked to autosomal dominant forms of Parkinson's disease and can increase the risk of developing sporadic Parkinson's disease [160 – 161]. A variety of α-synuclein amino acid mutations in the N-terminal region include A30P, E46K, H50Q, G51D, and A53T [162 – 164]. Each mutation has been implicated with either early or late stage disease state. The A53T mutation has shown a faster progression in the early stages of Parkinson's disease and has been linked to increases in α-synuclein aggregation and fibril formation [162, 165-166].

The A30P mutation also increases the aggregation rate of α-synuclein and is associated with early stages of Parkinson's disease and characterized by a milder disease state compared to A53T mutation [162]. The E46K mutation can alter the binding of α-synuclein with phospholipids of cell membranes and increase the rate of intracellular α-synuclein aggregation [162, 167]. The H50Q mutation is associated with a later disease stage and patients experience similar pathological features compared to A53T and E46K mutations [168]. The G51D mutation can amplify intracellular α-synuclein aggregation and is linked to early stage Parkinson's disease [161].

The formation of α-synuclein oligomers and fibrils serves as an adverse event for neural cells as the α-synuclein aggregates to promote neural toxicity and apoptosis [74 – 77]. The α-synuclein oligomers and fibrils can also interact with glia cells, such as microglia and astrocytes, to initiate cellular activation and initial stages of Parkinson's disease [78]. Interestingly, there are no current pharmaceutical interventions to modulate α-synuclein aggregation or disrupt fibril formation. Therefore, there exists a need to develop bioactive formulations to attenuate α-synuclein aggregation and fibril dissociation.

Our laboratories have developed a nanotechnology approach to regulate intracellular aggregation of α-synuclein [93]. In this approach, an amphiphilic macromolecule (denoted as 1cM) mimics the charge and hydrophobicity of ligands that bind to microglia scavenger receptors and modulate the uptake of α-synuclein thereby controlling the localized cellular concentration of α-synuclein, and potentially limiting the intracellular aggregation of α-synuclein [93]. In order to stabilize the amphiphile 1cM for optimal efficacy and scavenger receptor binding, 1cM was formulated via flash nanoprecipitation using hydrophobic cores, which resulted in stable nanoparticle

formulations [93, 41]. A series of polymers containing the antioxidant ferulic acid were chosen for the nanoparticle cores to reduce microglial activation and reactive oxygen species, which are also precursor events that can lead to the loss of dopaminergic neurons [93, 169 – 170].

Since our previous work has focused on regulation of intracellular α-synuclein aggregation, our next goal revolved around the impact of nanoparticle components (i.e. shell and core) on the extracellular aggregation of α-synuclein and disruption of fibril formation. This chapter will focus on inhibition of α-synuclein fibrils while future work will unlock the potential of antioxidant nanoparticles to disrupt alpha synuclein fibrils. Previous literature has shown antioxidants classified as both polyphenolics and non-polyphenolics can lower formation of α-synuclein fibrils with approximately a half-maximal effective concentration ($EC_{50}$) in the low micromolar range [98 – 102]. Examples of polyphenolic compounds include curcumin, ferulic acid, rosmarinic acid, and tannic acid [99 – 100]. Examples of non-polyphenolic compounds include amphotericin B, perphenazine, and rifampicin [98]. The choice of antioxidants utilized in the nanoparticle core was driven by two factors: hydrophobicity of the antioxidant in order to ensure successful encapsulation and stable nanoparticle formation, and potential for the antioxidant to either inhibit α-synuclein fibril formation or disrupt α-synuclein fibrils into monomers and lower molecular weight oligomers. Tannic acid and ferulic acid were chosen as nanoparticle cores based on previous activity for both inhibition of α-synuclein fibril formation and disruption of fibrils [99 - 100]. To facilitate the formulation of ferulic acid into a nanoparticle, ferulic acid was chemically conjugated within a poly(anhydride-ester) using an adipic acid linker [123]. Retinoic acid was chosen as a positive control

based on previous literature demonstrating an increase of α-synuclein content in a neuronal cell line after treatment with retinol [105]. In this paper, we demonstrate the formulation of a variety of antioxidants into nanoparticles to determine their impact on generation and dissociation of α-synuclein fibrils. The efficacy of the antioxidant nanoparticle to inhibit or disrupt α-synuclein fibril formation will be challenged in future work by using an α-synuclein mutation A53T, which has shown a higher propensity to form aggregates and fibrils compared to α-synuclein without any mutations. The impact of α-synuclein acetylation on fibril formation of α-synuclein was also explored in this chapter.

## MATERIALS AND METHODS

### *Reagents, chemicals, and raw materials*

All chemicals/materials were purchased from Sigma-Aldrich (Milwaukee, WI) or Fisher Scientific (Pittsburgh, PA) and used as received unless otherwise noted. 18 MΩ·cm resistivity deionized (DI) water was obtained using PicoPure 2 UV Plus (Hydro Service and Supplies - Durham, NC). Non-acetylated α-synuclein was either purchased from rPeptide (Watkinsville, GA) or kindly provided by Dr. Jean Baum's lab. Acetylated α-synuclein was kindly provided by Dr. Jean Baum's lab. A-synuclein A53T mutant was purchased from rPeptide (Watkinsville, GA).

### *Preparation and characterization of nanoparticle formulations*

Nanoparticles were fabricated using the flash nanoprecipitation technique as described previously [41]. Briefly, each shell and core component were dissolved separately in the appropriate solvent and mixed together. Flash nanoprecipitation was performed by mixing the solvent stream with an aqueous stream containing phosphate buffered solution (PBS) at pH 7.4. The nanoparticles were either dialyzed against PBS

using a 6000 MW cutoff ultrafiltration membrane or the solvent was displaced from the solution using vacuum. Nanoparticles were characterized by dynamic light scattering (DLS) using a Malvern-Zetasizer Nano Series DLS detector with a 22 mW He−Ne laser operating at λ 632.8 nm using general purpose resolution mode as previously described [41]. To prepare the sample for zeta potential measurement, each nanoparticle formulation was dialyzed against deionized water using a 3500 Dalton molecular weight cutoff ultrafiltration membrane for approximately 24 hours. Approximately 1mL of sample was added into a zeta potential cell and measured using dynamic light scattering.

*Amphiphilic macromolecule (AM) and antioxidant molecule synthesis*

Macromolecule 1cM was synthesized as previously detailed and characterized using established techniques including $^{1}$H NMR-spectroscopy, gel permeation chromatography, differential scanning calorimetry, and dynamic light scattering [125 - 127]. The critical micelle concentration, size, and charge data has been published in the literature [127]. Anti-oxidant molecules were synthesized and characterized as reported previously in the Uhrich laboratory [128].

*Alpha synuclein fibrillization study*

Fibrillization was carried out using 100 µL of 1 mg/mL monomeric synuclein in a 96 well plate (BD Falcon) with a 5 mm glass bead (Sigma Aldrich) for nucleation and agitated at 300 rpm at 37°C for 7 days on a Southwest Science Multi-Therm plate shaker [171]. Antioxidant nanoparticles at a 1:10 volume dilution in water were added to some of the α-synuclein wells. Plates were sealed using parafilm to minimize evaporation and final volumes were corrected to initial volumes using sterile distilled water. Fibrillization was verified by sampling α-synuclein before and after fibrillization by incubating 2 µM α-

synuclein in PBS with 40 μM Thioflavin-T (Sigma Aldrich) for 10 minutes at room temperature, followed by measuring fluorescence excitation and emission at 450 nm and 485 nm on a Tecan Infinite M200 Pro microplate reader [93]. The same protocol was applied to the α-synuclein and nanoparticle wells for determination of α-synuclein fibrillization. The fluorescence intensity increase normalized to α-synuclein was calculated using the following equation:

$$Fluorescence\ intensity\ increase = \frac{(Sample\ fluorescence - control\ fluorescence)}{(Alpha\ synuclein\ fluorescence - control\ fluorescence)} * 100$$

*Kinetics of Alpha Synuclein Fibrillization*

Samples containing either α-synuclein or α-synuclein and nanoparticles were loaded with 20 μM Thioflavin T (ThT) (Acros Organics, Pittsburgh, PA) into 96 well clear bottomed plates (Corning, Corning, NY) at a concentration of 70 μM and sealed with Axygen sealing tape (Corning, Corning, NY) and shaken at a rate of 600 rpm at 37ºC for at least 200 hours. Samples were taken and measured for each sample type. A POLARstar Omega plate reader (BMG Labtech, Cary, NC) was used to monitor the increase in ThT intensity. This protocol was adapted from literature [172]. The concentration of α-synuclein and nanoparticles utilized in this experiment was described in the previous section entitled Alpha synuclein fibrillization study.

*Atomic Force Microscopy (AFM) Protocol*

AFM images were taken as previously described [173]. Briefly, AFM images were taken on an NX-10 instrument (Park systems, Suwon, South Korea), using non-contact mode tips (PPP-NCHR, force constant 42 N/m; 330 kHz frequency; Nanosensors, Neuchatel, Switzerland). A 1cm x 1cm square of freshly cleaved mica (obtained from Ted

Pella Inc., Redding, CA) had 20 μL of sample deposited on the surface and was allowed to incubate for 5-10 minutes while covered. Then the surface of the sample was washed 3 times with 100 μL of water and the bottom and edges were dried using filter paper. The surface was allowed to air-dry for 1 hour before being imaged. Image processing was conducted using Gwyddion software.

*Statistical Analysis*

Data presented are from at least three independent experiments ($n \geq 3$) and values are represented as mean ± SEM unless otherwise indicated. Statistical analysis was performed considering $p < 0.05$ to be statistically significant. Statistical significance was determined using a one-way ANOVA with Tukey's posthoc test for comparisons between multiple treatment groups.

RESULTS

*Summary of size and zeta potential results for different antioxidant nanoparticles*

All nanoparticles with polymer cores (ie. PS and PFAA) ranged from about 230 – 270 nm with a polydispersity index (PDI) of ≤ 0.2, indicating stable and non-aggregated particles (**Figure 21**). Zeta potential values were uniformly negative for the 1cM-PS and 1cM-PFAA nanoparticles (-26.4 to -27.4 mV), which is another indicator of stable nanoparticles due to the large negative charge distribution (**Figure 21**). The nanoparticles with non-polymer cores (ie. retinoic acid and tannic acid) displayed a higher nanoparticle size between about 450 – 600 nm with a PDI of ≤ 0.3. The PDI was comparable to the nanoparticles with polymer cores, which indicated the nanoparticles should maintain stability. The average size of the nanoparticles with non-polymer cores is higher compared to the polymer core nanoparticles possibly due to differences in hydrophobicity between

polymer and non-polymer cores. FAA acid-tannic acid showed a large variation in size between formulations possibly due to the high aqueous solubility and low hydrophobicity of tannic acid compared to the polymer cores. It might be possible to reduce the nanoparticle size variation by incorporation of tannic acid into a polymer or chemical modification of tannic acid to increase its hydrophobicity. However, for this study, these options were not investigated. The chemical structures of the nanoparticle shells and ferulic acid are depicted in **Figure 24**.

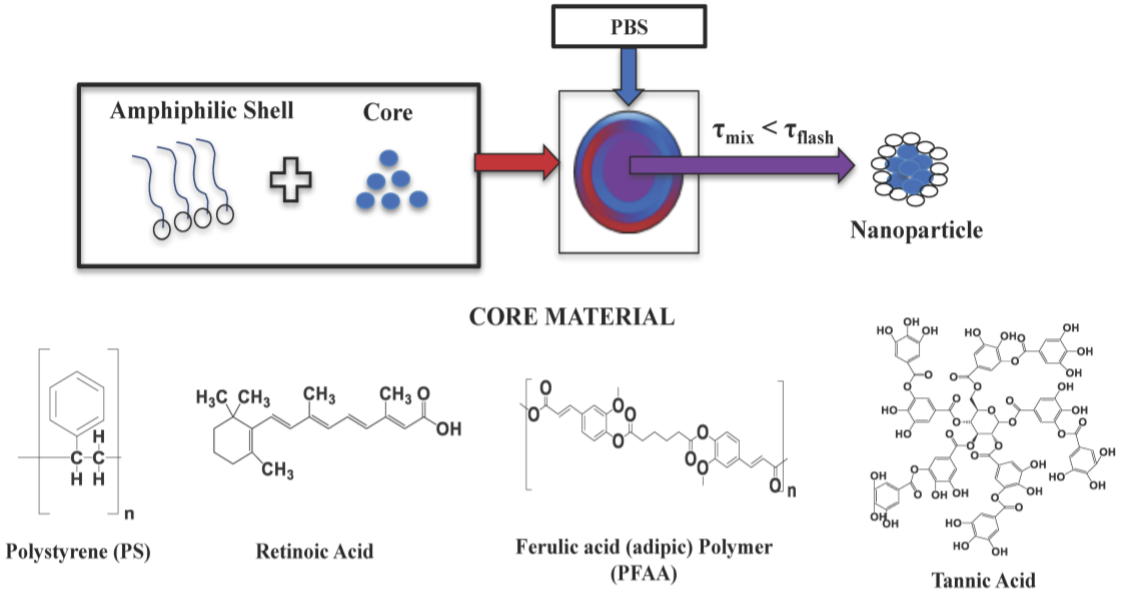


| Shell Material | Core Material | Nanoparticle | $Z_{average}$ (nm) | Polydispersity Index (PDI) | Zeta Potential (mV) |
|---|---|---|---|---|---|
| 1cM (M12P5) | Polystyrene (PS) | | 264 ± 34 | 0.151 ± 0.006 | -26.4 |
| | Retinoic Acid | | 374 ± 32 | 0.341 ± 0.040 | --- |
| | PFAA | | 236 ± 20 | 0.140 ± 0.009 | -27.4 |
| FAA Acid | Tannic Acid | | 586 ± 143 | 0.315 ± 0.023 | --- |

**Figure 21.** ***Nanoparticle Formulation & Results Summary.*** Top: Description of the flash nanoprecipitation process for the formulation of 1cM-PFAA nanoparticles. Middle: Chemical structures of molecules utilized in the nanoparticle core. Bottom: Table with size, PDI, and zeta potential results for each nanoparticle formulation ($n \geq 3$).

*Effect of nanoparticle composition on α-synuclein fibrillization*

1cM-PFAA and FAA acid-tannic acid were statistically significant ($p < 0.05$) for limiting fibril formation of α-synuclein (**Figure 22**). FAA acid-tannic acid displayed a 8% increase in fluorescence intensity in the ThT assay while 1cM-PFAA showed a 32% increase in fluorescence intensity. In addition, both nanoparticles were statistically significant for inhibiting fibril formation compared to 1cM-retinoic acid. The 1cM-retinoic acid nanoparticle showed a 165% increase in fluorescence intensity indicating either the retinoic acid or the combination of 1cM and retinoic acid are substantially increasing the fibril formation of α-synuclein.

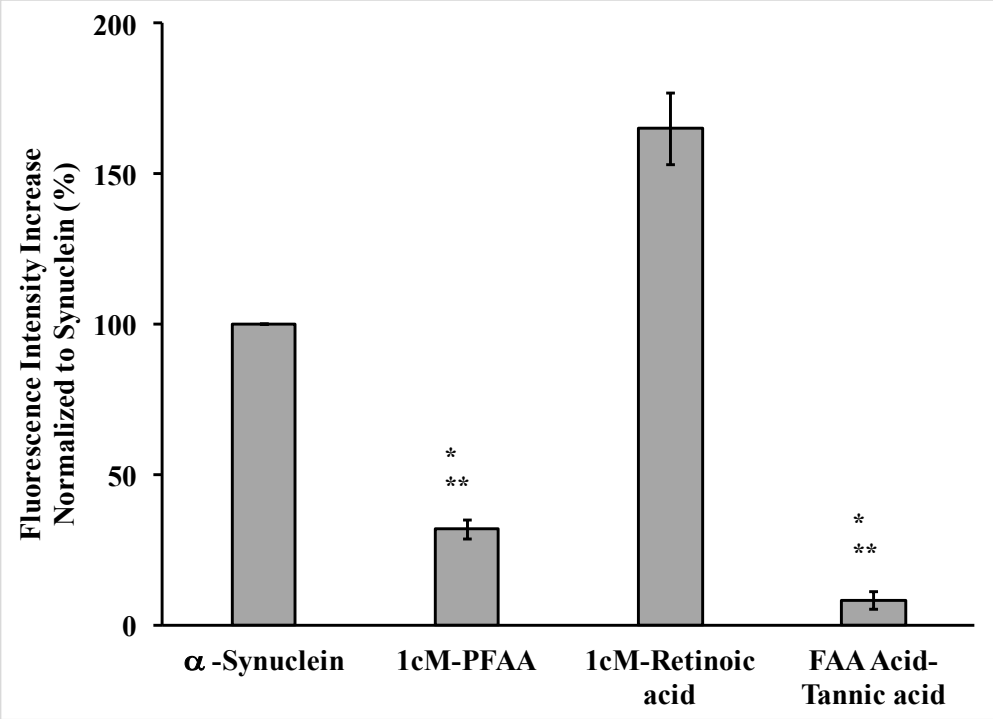


**Figure 22.** ***Effect of Antioxidant Nanoparticles on Non-Acetylated Alpha Synuclein Fibrillization.*** Nanoparticles were incubated with α-synuclein at 37ºC for 7 days and then fluorescence was measured using Tht assay. Fluorescence intensity was normalized against α-synuclein control wells. FAA Acid-Tannic Acid and 1cM-PFAA were the most efficacious

formulations for limiting α-synuclein fibrillization ($n \geq 3$, * $p < 0.01$ compared to 1cM-Retinoic Acid, ** $p < 0.05$ compared to α-synuclein).

Another study was conducted to discern the effect of antioxidant and 1cM on the formation of α-synuclein fibrils. In addition, the effect of acetylation of α-synuclein and kinetic rate of fibril formation for each nanoparticle formulation were also assessed. Tannic acid showed about a 60% reduction in fluorescence intensity compared to 80% for the FAA acid-tannic when incubated with acetylated α-synuclein (**Figure 23**). This result indicates tannic acid is responsible for the majority of regulation of α-synuclein fibril formation and that incorporation of ferulic acid into the nanoparticle shell provided additional inhibitory activity for prevention of fibril formation. Thus, 1cM-PFAA displayed a 70% reduction in fluorescence intensity compared to only 20% for ferulic acid (**Figure 23**). The conjugation of ferulic acid into a polymer combined with encapsulation into a nanoparticle will enhance stability of ferulic acid and could potentially result in a higher activity compared to ferulic acid in solution. The combination of 1cM and retinoic acid resulted in an increase in fibril formation compared to retinoic acid only (**Figure 23**). A control nanoparticle with polystyrene in the core, 1cM-PS, displayed a similar rate of fibril formation compared to the acetylated α-synuclein control (**Figure 23**). This result further confirms the antioxidant in the core of the nanoparticle is responsible for limiting fibril formation.

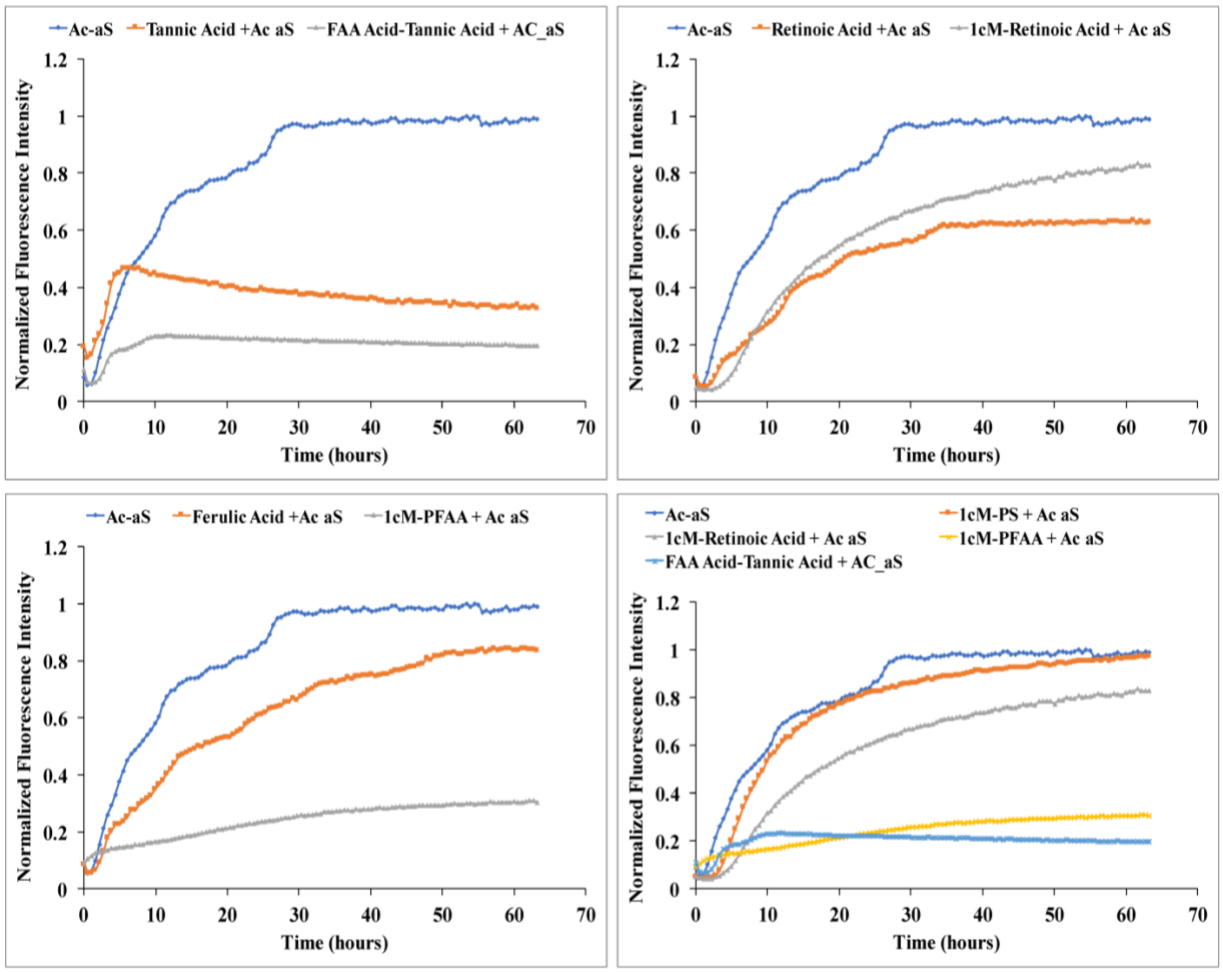


**Figure 23.** ***Effect of Antioxidant Nanoparticles on Kinetics of Acetylated Alpha Synuclein Fibrillization.*** Nanoparticles were incubated with α-synuclein at 37ºC for up to 64 hours and fluorescence was continuously measured using Tht assay. Fluorescence intensity was normalized against α-synuclein control wells. The nanoparticle core was responsible for regulation of α-synuclein fibril formation since 1cM as the shell did not show any impact on fibril formation. FAA Acid-Tannic Acid was the most efficacious formulation for limiting α-synuclein fibrillization due to the combination of tannic acid and ferulic acid (n = 2 except for 1cM-PFAA where n = 1).

FAA acid-tannic acid nanoparticle contained the lowest fluorescence intensity followed by 1cM-PFAA for the inhibition of fibril formation of non-acetylated α-synuclein (**Figure 25**). The fluorescence intensity was similar between tannic acid and FAA acid-tannic acid for the non-acetylated α-synuclein (**Figure 25**). The ability of tannic acid to inhibit fibril formation was slightly more pronounced for the non-acetylated α-synuclein as shown by the lower fluorescence intensity observed (**Figure 25**). The fluorescence intensity trends and kinetic rate of fibril formation was higher for ferulic acid compared to 1cM-PFAA for both acetylated and non-acetylated α-synuclein (**Figure 25**). Retinoic acid and 1cM-retinoic acid displayed similar kinetics of fibril formation for non-acetylated α-synuclein (**Figure 25**). A control nanoparticle with polystyrene in the core, 1cM-PS, displayed a slower rate of fibril formation compared to the acetylated α-synuclein control (**Figure 25**). However, if the study is continued for an additional 3 days, the fluorescence intensity of 1cM-PS is similar to the α-synuclein control (data not shown). The activity of each nanoparticle formulation for limiting fibril formation is similar between acetylated versus non-acetylated α-synuclein, which indicated acetylation does not substantially alter the nanoparticle ability to counteract fibril formation.

## DISCUSSION

The aggregation of α-synuclein is closely linked with the pathogenesis of a variety of neurodegenerative disorders termed α-synucleinopathies, which includes Parkinson's disease. The mechanism of α-synuclein aggregation and fibrillization is extremely complex and dependent on a multitude of factors such as pH, temperature, and association with cell membranes [174]. Therefore, the development of effective strategies to mitigate α-synuclein aggregation and fibrillization and their associated toxicity has been extremely

challenging [175 – 176]. In this study, we advanced the understanding of antioxidants and nanotechnology for unlocking the potential for discovery of therapeutics to reduce α-synuclein fibril formation. We have shown nanoparticles comprised of either tannic acid or ferulic acid attenuated the rate of α-synuclein fibril formation. The FAA acid-tannic acid nanoparticles achieved the maximum activity for limiting α-synuclein fibril formation, which suggests the combination of antioxidants and possibly structure of the antioxidant may be crucial for reducing fibrillization and initiation of Parkinson's disease.

Previous studies have identified that antioxidants containing aromatic groups combined with vicinal hydroxyl groups on a phenyl ring are key features for inhibiting or destabilizing α-synuclein fibrils [177]. Our results indicated tannic acid was more effective for limiting fibril formation compared to ferulic acid, which indicates the increase in vicinal hydroxyl groups on multiple phenyl rings may attribute to the increased efficacy for tannic acid compared to ferulic acid. However, the ferulic acid polymer nanoparticle (1cM-PFAA) displayed a statistically significant ability to reduce α-synuclein fibril formation compared to ferulic acid. This result may suggest the formulation of the antioxidant could also impact α-synuclein self-assembly. In addition, the lower aqueous solubility of ferulic acid might result in unfavorable pharmacokinetics, which can reduce its bioavailability and efficacy [178]. Therefore, the chemical conjugation of ferulic acid into a polymer and its formulation into a nanoparticle can protect ferulic acid from degradation and allow for enhanced bioavailability due to the controlled release of ferulic acid from the nanoparticle.

## CONCLUSION

Alpha synuclein plays a critical role in the pathogenesis of Parkinson's disease. Alpha synuclein aggregates form insoluble fibrillary structures and inclusions, which

accumulate into Lewy bodies and result in the initiation of Parkinson's disease. The current state of treatments for Parkinson's disease are limited and only manage the progression of the disease state. In this study, we advanced the strategy for mitigating α-synuclein fibrillization through the development of dual antioxidant nanoparticles containing ferulic acid and tannic acid. To our knowledge, this study is the first report demonstrating the ability of the FAA acid-tannic acid nanoparticles to inhibit the fibril formation of α-synuclein. Furthermore, the acetylated of α-synuclein accelerated the kinetic rate of fibrillization but did not impact the activity of the FAA acid-tannic acid nanoparticles. In addition, another nanoparticle formulation consisting of a ferulic acid polymer (1cM-PFAA) also showed promise for inhibition of fibril formation. Overall, these antioxidant nanoparticle formulations show promise for attenuating the generation of α-synuclein fibrils, which is a major step forward in the development of novel, antioxidant formulations for treatment of Parkinson's disease.

SUPPLEMENTARY FIGURES

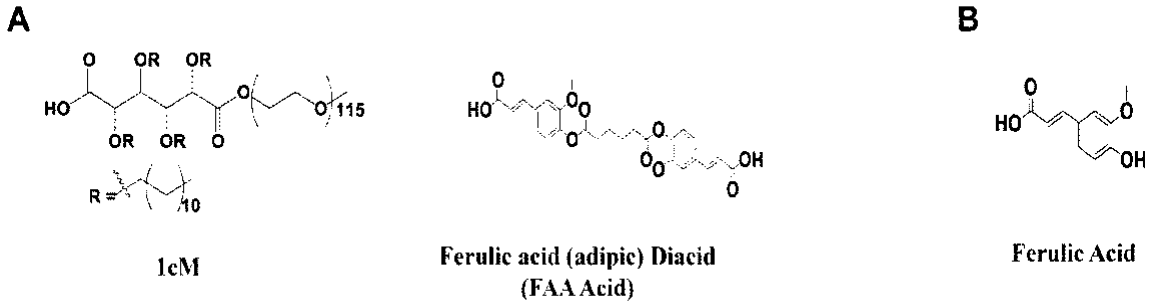


**Figure 24. A)** Chemical structure of the nanoparticle shells, 1cM and FAA acid respectively. **B)** Chemical structure of ferulic acid utilized in this study as a control.

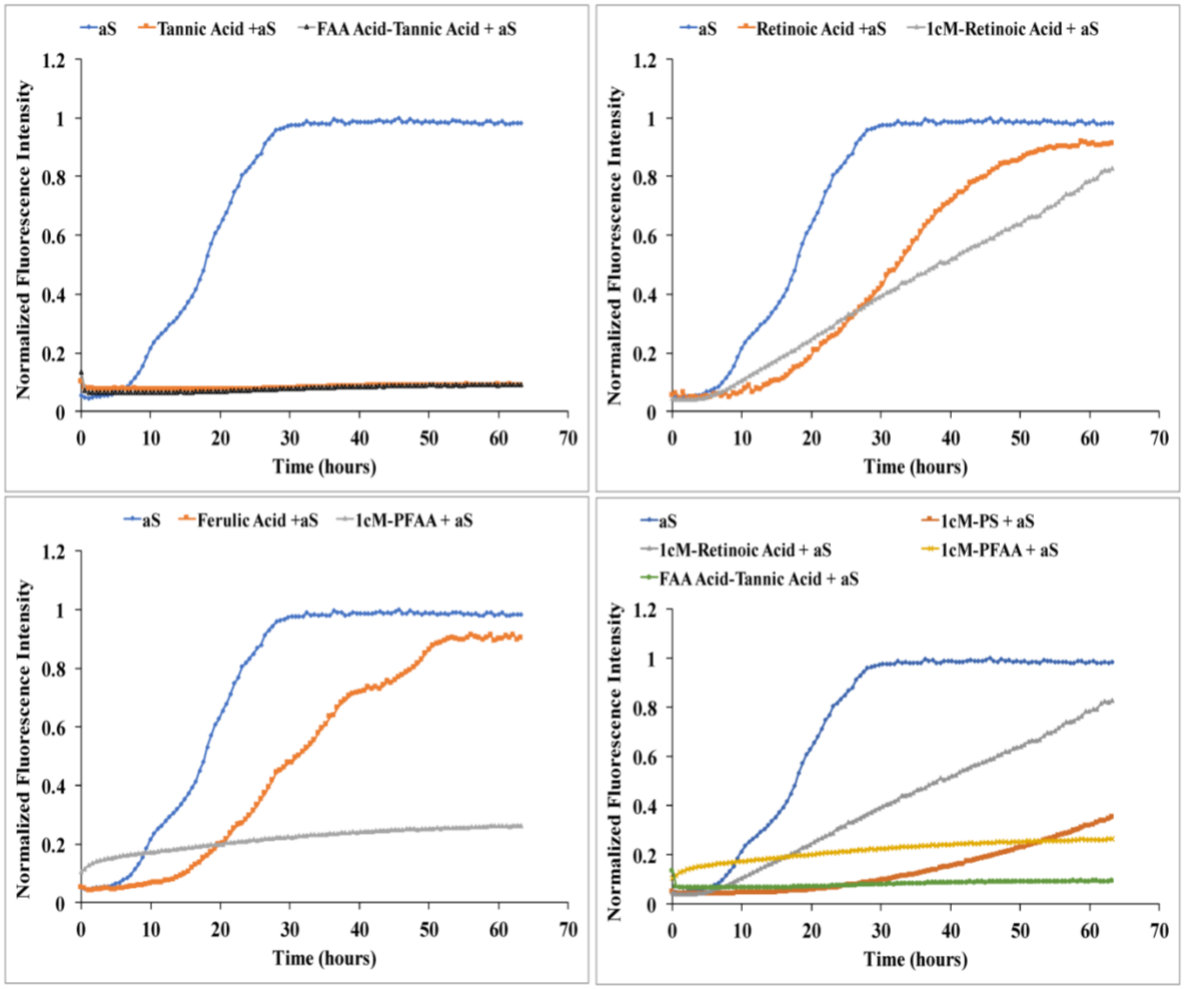


**Figure 25.** ***Effect of Antioxidant Nanoparticles on Kinetics of Non-Acetylated Alpha Synuclein Fibrillization.*** Nanoparticles were incubated with α-synuclein at 37ºC for up to 64 hours and fluorescence was continuously measured using Tht assay. Fluorescence intensity was normalized against α-synuclein control wells. The nanoparticle core was responsible for regulation of α-synuclein fibril formation since 1cM as the shell did not show any impact on fibril formation. The kinetics of α-synuclein fibrillization are slower for non-acetylated compared to acetylated α-synuclein (n = 2). The endpoint fluorescence for each nanoparticle condition is similar between non-acetylated versus acetylated α-synuclein except for 1cM-PS and 1cM-Retinoic acid. The 1cM-PS and 1cM-Retinoic acid formulations need additional time to reach steady state for the formation of non-acetylated α-synuclein fibrils.

# CHAPTER 5 – DISSERTATION SUMMARY AND FUTURE DIRECTIONS

## DISSERTATION SUMMARY

Atherosclerosis and Parkinson's disease are both characterized by the uncontrolled uptake of modified proteins, low density lipoprotein (LDL) and α-synuclein, by macrophages and microglia respectively. The uptake of modified LDL leads to transformation of macrophages into foam cells, which causes plaque build-up in the arterial wall and can progress to a heart attack or stroke dependent on the plaque composition. Alpha synuclein aggregates and fibrils have cytotoxic effects on neurons and microglia and can propagate between interconnected brain regions leading to the initiation of Parkinson's disease. In this work, we have presented two novel paradigms for developing potential treatment options for both diseases, via 1) controlling foam cell formation and inflammatory state of macrophages using scavenger receptor targeted ferulic acid polymer nanoparticles, and 2) significantly decreasing the formation of α-synuclein fibrils by a dual antioxidant nanoparticle formulation comprised of ferulic acid and tannic acid.

In the first part of this work, we investigated the potential for a variety of ferulic acid polymer and diacid nanoparticles for reducing the uncontrolled uptake of oxLDL. We discovered that a nanoparticle comprised of ferulic acid polymer chemically linked by diglycolic acid (PFAG) displayed the largest efficacy for minimizing the uptake of oxLDL by HMDMs. Further investigation showed the 1cM-PFAG nanoparticle was also able to reduce expression of three macrophage scavenger receptors, MSR1, CD36, and LOX1, which enabled the reduction of oxLDL uptake. Since the primary effect of the 1cM-PFAG nanoparticle was the inhibition of oxLDL receptor expression, we hypothesized the 1cM-PFAG nanoparticle could also result in the inhibition of reactive oxygen species production

by HMDMs. All of the nanoparticles composed of either ferulic acid polymers or diacids showed a significant reduction on ROS levels compared to the oxLDL control. Overall, the ferulic acid-based poly(anhydride ester) nanoparticles may offer an integrative strategy for the localized passivation of the early stages of the athero-inflammatory cascade in cardiovascular disease.

In the second part of this work, we investigated the potential of nanoparticles comprised of different antioxidants for attenuating the fibril formation of α-synuclein. We discovered that a nanoparticle comprised of a combination of ferulic acid and tannic acid displayed a significant and maximum efficacy for reduction of α-synuclein fibril formation. Further investigation showed the 1cM shell did not prevent the generation of α-synuclein fibrils, which indicated the antioxidant is key for prevention of fibrillization. The impact of acetylation of α-synuclein increased the kinetic rate of fibril generation but did not impact the efficacy of the ferulic acid and tannic acid nanoparticle for impeding the fibrillization of α-synuclein. Overall, the dual antioxidant nanoparticles present a promising therapeutic avenue for prevention of the initial stages of Parkinson's disease.

## FUTURE DIRECTIONS

### *Continued research for advancement of ferulic acid polymer nanoparticles for mitigation of foam cell formation*

There exists a potential to further understand the ability of the ferulic acid-based poly(anhydride ester) nanoparticles to limit oxLDL uptake and lower the inflammation state of HMDMs. One avenue for future research involves understanding the impact of the ferulic acid polymer nanoparticles to downregulate the expression of additional scavenger receptors as a function of oxLDL concentration (0.5 – 50 μg/mL). Scavenger receptors of interest for limiting oxLDL uptake include scavenger receptor class B type I (SR-B1) and

soluble CXC chemokine ligand sixteen (CXCL16) since both receptors can recognize oxLDL, which renders these receptors attractive targets for future studies. SR-B1 contains similar characteristics as CD36 and is present on both monocytes and macrophages. SR-B1 displayed a high binding affinity for oxLDL ($K_d$ of 4.0 ± 0.5 μg/mL) and showed internalization and degradation of oxLDL that was comparable to other scavenger receptors [179]. CXCL16 is also known as the scavenger receptor for phosphatidylserine and oxLDL (SR-PSOX) [180]. CXCL16 has been identified in both human carotid endarterectomy samples and ApoE mice plaque lesions [181 – 182]. CXCL16 has been shown to bind and internalize oxLDL on both HMDMs and also stimulated THP-1 cells [183].

A second avenue of research could involve an expansion of the anti-inflammatory mechanism of the ferulic acid polymer nanoparticles. The cytokine profiles of HMDMs could be assessed for the different ferulic acid polymer and diacid nanoparticles and compared to the oxLDL control. Cytokines of interest could include tumor necrosis factor-alpha (TNF-α), interleukin-1 beta (IL-1β), IL-6, IL-8, and IL-12 [184]. In addition, reactive oxygen species (ROS) can play critical roles in maintaining the homeostatic functions of macrophages [150]. Since the ferulic acid polymer and diacid nanoparticles displayed inhibition of ROS generation in HMDMs, then the expression of inducible nitric oxide synthase (iNOS) coupled with measuring the nitrate/nitrite levels and nitrous oxide (NO) levels could aid in understanding the mechanism of ROS inhibition. The interactions between NO and ROS levels could be critical for determining macrophage redox and inflammatory responses, especially when linked to oxLDL uptake.

The potential of ferulic acid nanoparticles to prevent oxidation of low density lipoprotein (LDL) could also be studied based on previous literature [147]. A concentration range of ferulic acid nanoparticles could be tested to achieve an $EC_{50}$ value for antioxidant activity for each nanoparticle. The ability of each ferulic acid nanoparticle to reduce the oxidation state of LDL could also be assessed by measuring the thiobarbituric acid reactive substances (TBARS) after incubation with either copper ions or hydrogen peroxide [185].

An *in vivo* study could be conducted to confirm the efficacy of the ferulic acid polymer nanoparticles. Apolipoprotein E-deficient Fibrillin-1 mutant (ApoE-/-Fbn1C1039G+/-) mice could be treated with ferulic acid polymer nanoparticles (1cM-PFAG and 1cM-PFAA) and 1cM-M12 to determine if these nanoparticles have an enhanced efficacy for reducing atherosclerosis compared to 1cM-M12. The ApoE-/-Fbn1C1039G+/- mice model will contain accelerated atherogenesis and spontaneous plaque rupture, which will aid in determining if the ferulic acid nanoparticles would help the mortality rate. In addition, this mouse model will generate high cytokine levels and reactive oxygen species generation. Therefore, levels of cytokines such as TNF-$\alpha$, IL-1$\beta$, and IL-6, along with iNOS expression would be tested to determine if the antioxidant nanoparticles contain an enhanced anti-inflammatory effect *in vivo* compared with 1cM-M12. Additional markers that would be tested include improvement of plaque burden and COX2 levels to determine vascular inflammation. Ultrasound images of the aorta could assess the plaque thickness over the time course of the study to aid in determining the appropriate dose and frequency of dosing for the ferulic acid polymer nanoparticles. The concentrations of total cholesterol (TC), triglycerides (TG), high density lipoprotein

cholesterol (HDL-C) and low density lipoprotein cholesterol (LDL-C) could also be measured along with performing histologic measurements of the aorta to confirm plaque thickness.

Lastly, ferulic acid has exhibited the ability to induce reverse cholesterol transport in macrophages via enhanced expression of ABCA1, ABCG1, and SR-B1 [67, 186 – 187]. Since 1cM can target the scavenger receptors for providing a reduction in oxLDL uptake, then 1cM-PFAG and/or 1cM-PFAA have the potential to control oxLDL uptake and also transport cholesterol out of macrophages and onto HDL particles. Different amphiphilic macromolecules could be utilized as the nanoparticle shell in order to generate nanoparticles with a greater ability for cholesterol efflux from macrophages. This dual nanoparticle design could potentially treat a broad spectrum of atherosclerosis stages for rescuing macrophages from apoptosis and limiting the generation of foam cells.

*Completion of the assessment of antioxidant nanoparticles to regulate α-synuclein fibril formation and dissociation*

The following experiments can be conducted to complete the publication describing the ability of different antioxidant nanoparticle formulations to regulate α-synuclein fibril formation and dissociation.

- Antioxidant nanoparticles incubated with A53T mutant of α-synuclein to challenge the aggregation rate and fibril formation of synuclein
- Generation of α-synuclein fibrils followed by addition of antioxidant nanoparticles to determine if fibrils will dissociate over time. Can also assess the concentration of nanoparticles necessary for dissociation and also challenge the fibril dissociation with the A53T mutant of α-synuclein

- Determine if any aggregates of α-synuclein are generated during the nanoparticle incubation and attempted fibrillization of the protein. If aggregates are generated, then determine their size using a SDS-Page gel or analytical size exclusion chromatography.
- Determine if the α-synuclein maintains an unfolded state when incubated with nanoparticles during the fibrillization experiments by utilization of circular dichroism (CD). In addition, can utilize CD for confirmation of fibril dissociation by showing a reduction in β-sheet confirmation of α-synuclein.

In addition to the proposed experiments above, the interaction of α-synuclein with tannic acid and ferulic acid could potentially be elucidated using an in silico model, NMR studies, or possibly through an experimental design. The three regions of α-synuclein (N-terminal, NAC domain, and C-terminal) could be tested for their ability to generate fibrils in the presence of the 1cM-PFAA and FAA acid-tannic acid nanoparticles and compared to each region of α-synuclein as the controls. This experiment could identify the region of α-synuclein that the nanoparticles are preventing from forming fibrils. Subsequent modeling could be conducted to determine the association of nanoparticles with a particular sequence of amino acids in this region.

*In vitro* cellular studies could be conducted to determine if the ferulic and tannic acid nanoparticles could aid in maintaining an immune homeostasis in the central nervous system. The ferulic and tannic acid nanoparticles could be incubated with various forms of α-synuclein aggregates and the activation state of microglia would be tested. The effect of these nanoparticles in α-synuclein internalization and scavenger receptor expression

could also be determined. Furthermore, the ferulic and tannic acid nanoparticles could be utilized to inhibit extracellular aggregation while the 1cM-PFAA nanoparticle could modulate scavenger receptor expression. Neuron toxicity of the ferulic and tannic acid nanoparticles could be tested using a co-culture with SH-SY5Y neuroblastoma using protocols previous developed by Neal Bennett.

*Development of a human microglia-like cell model to study Parkinson's disease*

Microglia play important roles in neurological diseases, such as Parkinson's disease, and there exists a need to improve our understanding of the function of microglia in neurological diseases. A recent study showed human microglia age differently than murine microglia indicating murine models of neurodegeneration may not be representative of the disease state [188]. The acquisition of primary cells from human fetal or adult central nervous system (CNS) tissue is highly difficult and extremely rare. Therefore, a need exists to develop a human microglia-like cell model to study neurological diseases. Recent literature has exhibited a few attempts to generate human like microglia involving derivation from induced pluripotent stem cells (iPSCs) or human monocytes [189 – 192]. Our protocol for differentiation of human monocytes consisted of using three cytokines, which were granulocyte-macrophage colony-stimulating factor (GM-CSF), IL-34, and nerve growth factor beta (NGF-β). All of these cytokines have been shown previously to be essential for developing and maintaining microglia [193 – 195]. Preliminary results indicated the human like microglia generated displayed a similar morphology to previous published literature (**Figure 26**).

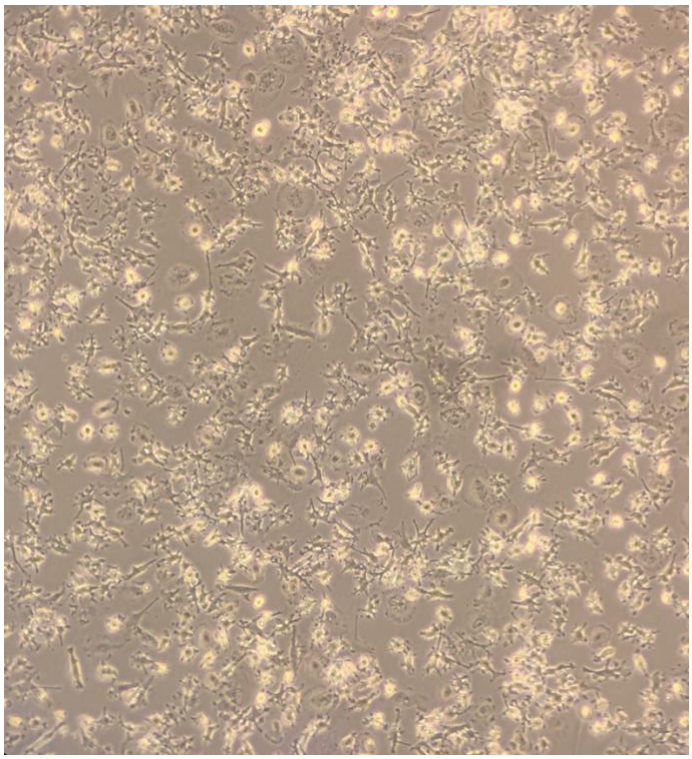

**Figure 26.** ***Image of human like microglia cells during differentiation with cytokines*.** Human monocytes were isolated from donor blood as previously described [130]. Cells were plated in T75 flasks and floating leukocytes were removed after at least 1 hour in the incubator at 37°C, 5% carbon dioxide. The following cytokines were added and the cells were differentiated up to 14 days: IL-34 (25 ng/mL), GM-CSF (~2.5 ng/mL), NGF-β (~8 ng/mL). A microscopic image was taken during differentiation using a 10x objective.

The uptake of α-synuclein and expression of CD36 was assessed for various nanoparticle treatments using the human like microglia cells. The uptake of α-synuclein decreased to about 57% for the 1cM-PFAA nanoparticle compared to the α-synuclein control (**Figure 27A**), which was similar to previous results using rat microglia cells. The expression of CD36 also decreased for the 1cM-PFAA nanoparticle, which conforms with previous data linking expression of CD36 to α-synuclein uptake using rat microglia (**Figure 27B**). The FAA acid-Tannic acid exhibited a smaller reduction in α-synuclein uptake to about 74% (**Figure 27A**) but did not display any change in Cd36 expression (**Figure 27B**). The 1cM-PS nanoparticle did not display any reduction in α-synuclein uptake or CD36 expression (**Figures 27A & B**), which did not correlate with previous results using rat microglia. Therefore, additional work to confirm the successful differentiation of monocytes into human like microglia could include the investigation of the expression of surface receptors that are common in microglia but not in macrophages.

**A) Alpha Synuclein Uptake by Human Like Microglia Cells**

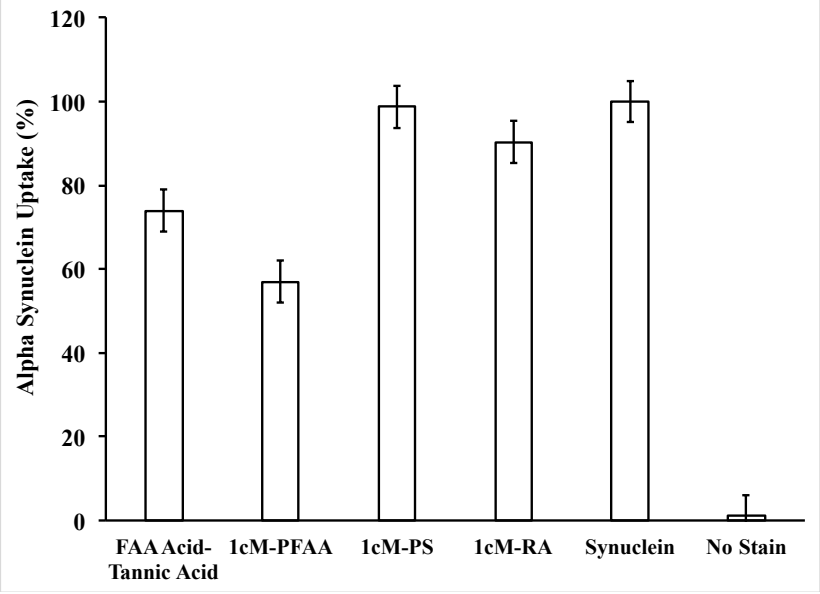

**B) CD36 Expression by Human Like Microglia Cells**

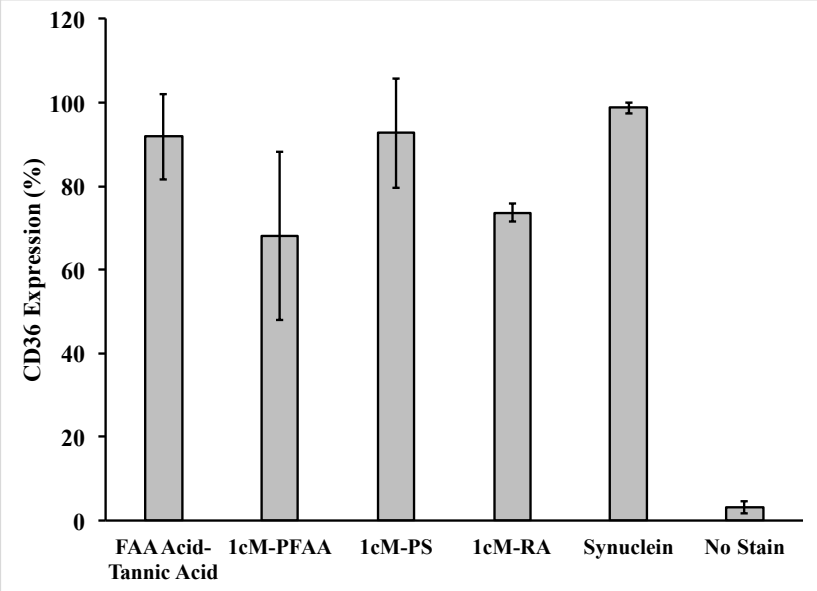


**Figure 27.** ***Effect of antioxidant nanoparticles on α-synuclein uptake and CD36 expression using human like microglia cells*.** Treatments using nanoparticles and α-synuclein were executed as previously described [93]. **A)** 1cM-PFAA showed the lowest uptake of α-synuclein at about 57% (n = 3). **B)** 1cM-PFAA also exhibited the lowest expression of CD36 at about 68% (n = 3). Statistical analysis did not show any statistically significant treatments compared to the α-synuclein control. However, it is possible additional replicates need to be performed in order to capture the statistical significance.

PUBLICATIONS

1. **R.A. Chmielowski**, N. Zhao, X. Yang, Y. Cao, N. Francis, J. Baum, K.E. Uhrich, L.B. Joseph, P.V. Moghe. Novel Therapeutics for Altering Parkinson's Disease: Antioxidant Nanoparticles Regulate Alpha Synuclein Fibril Generation and Dissociation. Journal to be determined. Article to be submitted 1Q2018.
2. **R.A. Chmielowski**, D.S. Abdelhamid, J.J Faig, L.K. Petersen, C.R. Gardner, K.E. Uhrich, L.B. Joseph, P.V. Moghe. Athero-inflammatory nanotherapeutics: Ferulic acid-based poly(anhydride-ester) nanoparticles attenuate foam cell formation by regulating macrophage lipogenesis and reactive oxygen species generation. Acta Biomaterialia. 2017, 57, 85-94.
3. N.K. Bennett, **R. Chmielowski**, D.S. Abdelhamid, J.J. Faig, N. Francis, J. Baum, Z.P. Pang, K.E. Uhrich, P.V. Moghe. Polymer brain-nanotherapeutics for multipronged inhibition of microglial α-synuclein aggregation, activation, and neurotoxicity. Biomaterials. 2016, 111, 179-189.
4. A. Moretti, Q. Li, **R. Chmielowski**, P. Moghe, L. Joseph, K. Uhrich. Lithocholic acid-based amphiphilic macromolecules: Macrophage-targeted nanotherapeutics reduce inflammation in atherosclerosis. Article to be submitted 4Q2017.

## CHAPTER 6 – REFERENCES


1. A. Recasens, B. Dehay. Alpha-synuclein spreading in Parkinson's disease. Front Neuroanat. 2014, 8:159.
2. W.S. Kim, K. Kagedal, G.M. Halliday. Alpha-synuclein biology in Lewy body diseases. Alzheimers Res. Ther. 2014, 6(5): 73.
3. J.L. Fleg, D.E. Forman, K. Berra, V. Bittner, J.A. Blumenthal, M.A. Chen, S. Cheng, D.W. Kitzman, M.S. Maurer, M.W. Rich, W. Shen, M.A. Williams, S.J. Zieman. Secondary prevention of atherosclerotic cardiovascular disease in older adults: A scientific statement from the American Heart Association. Circulation. 2013, 128(22): 2422-2446.
4. P. Libby. Inflammation in Atherosclerosis. Arterioscler., Thromb., Vasc. Biol. 2012, 32(9): 2045-2051.
5. M. Wildgruber, H. Lee, A. Chudnovskiy, T. Yoon, M. Etzrodt, M.J. Pittet, M. Nahrendorf, K. Croce, P. Libby, R. Weissleder, F.K. Swirski. Monocyte subset dynamics in human atherosclerosis, in: Recent Advances in Nanotechnology, 1st ed., Apple Academic Press, 2011.
6. K.J. Moore, I. Tabas. Macrophages in the pathogenesis of atherosclerosis. Cell. 2011, 145(3): 341-355.
7. Y.I. Miller, S. Choi, P. Wiesner, L. Fang, R. Harkewicz, K. Hartvigsen, A. Boullier, A. Gonen, C.J. Diehl, X. Que, E. Montano, P.X. Shaw, S. Tsimikas, C.J. Binder, J.L. Witztum. Oxidation-specific epitopes are danger-associated molecular patterns recognized by pattern recognition receptors of innate immunity. Circ. Res. 2011, 108(2): 235-248.
8. A. Gisteraa, G.K. Hansson. The immunology of atherosclerosis. Nature Reviews Nephrology. 2017, 13(6), 368-380.
9. J. Kzhyshkowska, C. Neyen, S. Gordon. Role of macrophage scavenger receptors in atherosclerosis. Immunobiology. 2012, 217(5): 492-502.
10. K.J. Moore, M.W. Freeman. Scavenger receptors in atherosclerosis: beyond lipid uptake. Arterioscler., Thromb., Vasc. Biol., 2006, 26(8): 1702-1711.
11. J.L. Goldstein, Y.K. Ho, S.K. Basu, M.S. Brown. Binding site on macrophages that mediates uptake and degradation of acetylated low density lipoprotein, producing massive cholesterol deposition. Proc. Natl. Acad. Sci. U.S.A. 1979, 76(1): 333–337.
12. J. Kzhyshkowska, C. Neyen, S. Gordon. Role of macrophage scavenger receptors in atherosclerosis. Immunobiology. 2012, 217(5): 492-502.
13. S.L. Acton, P.E. Scherer, H.F. Lodish, M. Krieger. Expression cloning of SR-BI, a CD36-related class B scavenger receptor. J. Biol. Chem. 1994, 269(33): 21003–21009.

14. G. Endemann, L.W. Stanton, K.S. Madden, C.M. Bryant, R.T. White, A.A. Protter. CD36 is a receptor for oxidized low density lipoprotein. J. Biol. Chem. 1993, 268(16): 11811–11816.
15. T. Kodama, M. Freeman, L. Rohrer, J. Zabrecky, P. Matsudaira, M. Krieger. Type I macrophage scavenger receptor contains alpha-helical and collagen-like coiled coils. Nature. 1990, 343(6258): 531–535.
16. M. Krieger. The other side of scavenger receptors: pattern recognition for host defense. Curr. Opin. Lipidol. 1997, 8(5): 275–280.
17. I.A. Zani, S.L. Stephen, N.A. Mughal, D. Russell, S. Homer-Vanniasinkam, S.B. Wheatcroft, S. Ponnambalam. Scavenger receptor structure and function in health and disease. Cells. 2015, 4(2): 178-201.
18. S.O. Rahaman, D.J. Lennon, M. Febbraio, E.A. Podrez, S.L. Hazen, R.L. Silverstein. A CD36-dependent signaling cascade is necessary for macrophage foam cell formation. Cell Metab. 2006, 4(3): 211–221.
19. S. Agrawal, M. Febbraio, E. Podrez, M.K. Cathcart, G.R. Stark, G.M. Chisolm. Signal transducer and activator of transcription 1 is required for optimal foam cell formation and atherosclerotic lesion development. Circulation. 2007, 115(23): 2939–2947.
20. V.V. Kunjathoor, M. Febbraio, E.A. Podrez, K.J. Moore, L. Andersson, S. Koehn, J.S. Rhee, R. Silverstein, H.F. Hoff, M.W. Freeman. Scavenger receptors class A-I/II and CD36 are the principal receptors responsible for the uptake of modified low density lipoprotein leading to lipid loading in macrophages. J. Biol. Chem. 2002, 277(51): 49982–49988.
21. N.M. Plourde, S. Kortagere, W. Welsh, P.V. Moghe. Structure–activity relations of nanolipoblockers with the atherogenic domain of human macrophage scavenger receptor A. Biomacromolecules. 2009, 10(6): 1381–1391.
22. L.K. Petersen, A.W. York, D.R. Lewis, S. Ahuja, K.E. Uhrich, R.K. Prud'homme, P.V. Moghe, Amphiphilic nanoparticles repress macrophage atherogenesis: novel core/shell designs for scavenger receptor targeting and downregulation, Mol. Pharmaceutics. 2014, 11(8): 2815-2824.
23. F. McTaggart, P. Jones. Effects of statins on high-density lipoproteins: a potential contribution to cardiovascular benefit. Cardiovasc. Drugs Ther. 2008, 22(4): 321-338.
24. H.C. Bucher, L.E. Griffith, G.H. Guyatt. Systematic review on the risk and benefit of different cholesterol-lowering interventions. Arterioscler. Thromb. Vasc. Biol. 1999, 19(2): 187-195.
25. E.S. Istvan, J. Deisenhofer. Structural mechanism for statin inhibition of HMG-CoA reductase. Science. 2001, 292(5519): 1160-1164.
26. A.M. Gotto Jr. Antioxidants, statins, and atherosclerosis. J. Am. Coll. Cardiol. 2003, 41(7): 1205-1210.

27. R. Klingenberg, G.K. Hansson. Treating inflammation in atherosclerotic cardiovascular disease: emerging therapies. European Heart Journal. 2009, 30(23): 2838-2844.
28. Y.A. Sheikine, G.K. Hansson. Chemokines as potential therapeutic targets in atherosclerosis. Current Drug Targets. 2006, 7(1): 13-27.
29. Y. Levy, S. Blum, A.P. Levy. Antioxidants in the prevention of atherosclerosis: the importance of proper patient selection. Clinical Nutrition. 2009, 28(5): 581-582.
30. S.R. Steinhubl. Why have antioxidants failed in clinical trials? American Journal of Cardiology. 2008, 101(10A): 14D-19D.
31. Anon. Learning lessons from Pfizer's $800 million failure. Nat. Rev. Drug Discovery. 2011, 10(3): 163-164.
32. K. Huynh. Atherosclerosis PCSK9 inhibition reduces cardiovascular events in high risk patients. Nature Reviews Cardiology. 2017, 14(5): 251.
33. M. Shapiro, S. Fazio. PCSK9 and atherosclerosis – lipids and beyond. Journal of atherosclerosis and thrombosis. 2017, 24(5): 462-472.
34. D.S. Kazi, A.E. Moran, P.G. Coxon, J. Penko, D.A. Ollendorf, S.D. Pearson, J.A. Tice, D. Guzman, K. Bibbins-Domingo. Cost-effectiveness of PCSK9 inhibitor therapy in patients with heterozygous familial hypercholesterolemia or atherosclerotic cardiovascular disease. Journal of the American Medical Association. 2016, 316(7): 743-753.
35. N. Luciani, F. Gazeau, C. Wilhelm. Reactivity of the monocyte/macrophage system to superparamagnetic anionic nanoparticles. J. Mater. Chem. 2009, 19(35): 6373-6380.
36. E. Chnari, J.S. Nikitczuk, J. Wang, K.E. Uhrich, P.V. Moghe. Engineered polymeric nanoparticles for receptor-targeted blockage of oxidized low density lipoprotein uptake and atherogenesis in macrophages. Biomacromolecules. 2006, 7(6): 1796-1805.
37. E. Chnari, H.B. Lari, L. Tian, K.E. Uhrich, P.V. Moghe. Nanoscale anionic macromolecules for selective retention of low-density lipoproteins. Biomaterials. 2005, 26(17): 3749-3758.
38. D.R. Lewis, V. Kholodovych, M.D. Tomasini, D. Abdelhamid, L.K. Petersen, W.J. Welsh, K.E. Uhrich, P.V. Moghe. In silico design of anti-atherogenic biomaterials. Biomaterials. 2013, 34(32): 7950-7959.
39. D.E. Poree, K. Zablocki, A. Faig, P.V. Moghe, K.E. Uhrich. Nanoscale amphiphilic macromolecules with variable lipophilicity and stereochemistry modulate inhibition of oxidized low-density lipoprotein uptake. Biomacromolecules. 2013, 14(8): 2463-2469.
40. E. Chnari, J.S. Nikitczuk, K.E. Uhrich, P.V. Moghe. Nanoscale anionic macromolecules can inhibit cellular uptake of differentially oxidized LDL. Biomacromolecules. 2006, 7(2): 597-603.

41. A.W. York, K.R. Zablocki, D.R. Lewis, L. Gu, K.E. Uhrich, R.K. Prud'homme, P.V. Moghe. Kinetically assembled nanoparticles of bioactive macromolecules exhibit enhanced stability and cell-targeted biological efficacy. Adv. Mater. (Weinheim, Ger.). 2012, 24(6): 733-739.
42. D.R. Lewis, K. Kamisoglu, A.W. York, P.V. Moghe. Polymer-based therapeutics: nanoassemblies and nanoparticles for management of atherosclerosis. Wiley Interdiscip. Rev.: Nanomed. Nanobiotechnol. 2011, 3(4): 400-420.
43. N.M. Plourde, S. Kortagere, W. Welsh, P.V. Moghe. Structure-activity relations of nanolipoblockers with the atherogenic domain of human macrophage scavenger receptor A. Biomacromolecules. 2009, 10(6): 1381-1391.
44. S.M. Sparks, N. Iverson, N. Plourde, P.V. Moghe, K.E. Uhrich. Nanoscale amphiphilic macromolecules: multifunctional polymers for management of cardiovascular disease. 238th ACS National Meeting, Washington, DC, August 16th – 20th 2009, PMSE-313.
45. M.D. Tomasini, K. Zablocki, L.K. Petersen, P.V. Moghe, M.S. Tomassone. Coarse grained molecular dynamics of engineered macromolecules for the inhibition of oxidized low-density lipoprotein uptake by macrophage scavenger receptors. Biomacromolecules. 2013, 14(8): 2499-2509.
46. A.W. York, K.R. Zablocki, D.R. Lewis, L. Gu, K.E. Uhrich, R.K. Prud'homme, P.V. Moghe. Formulation and in vitro evaluation of serum stable bioactive polymeric nanoparticles for managing atherosclerosis. 242nd ACS National Meeting, Denver, CO, August 28th – September 1st 2011, COLL-353.
47. N. Iverson, N. Plourde, E. Chnari, G.B. Nackman, P.V. Moghe. Convergence of nanotechnology and cardiovascular medicine: progress and emerging prospects. BioDrugs. 2008, 22(1): 1-10.
48. B.K. Johnson, R.K. Prud'homme. Flash nanoprecipitation of organic actives and block copolymers using a confined impinging jets mixer. Aust. J. Chem. 2003, 56(10): 1021-1024.
49. M.E. Gindy, S. Ji, T.R. Hoye, A.Z. Panagiotopoulos, R.K. Prud'homme. Preparation of poly(ethylene glycol) protected nanoparticles with variable bioconjugate ligand density. Biomacromolecules. 2008, 9(10): 2705-2711.
50. R.K. Prud'homme, M.H. Alonso, M. Gindy, S. Budijuno, B. Ungan. Drug delivery and imaging using nanoparticles produced by block-copolymer directed flash nanoprecipitation. Polym. Prepr. (Am. Chem. Soc., Div. Polym. Chem.). 2008, 49(2): 1043.
51. J.A. Leopold. Antioxidants and coronary artery disease: from pathophysiology to preventive therapy. Coronary Artery Disease. 2015, 26(2): 176-183.
52. S. Parthasarathy, A. Raghavamenon, M.O. Garelnabi, N. Santanam. Oxidized low-density lipoprotein. Methods Mol. Biol. 2010, 610(Free radicals and antioxidant protocols (2nd edition)), 403-417.

53. S. Parthasarathy, L.G. Fong, M.T. Quinn, D. Steinberg. Oxidative modification of LDL: Comparison between cell-mediated and copper-mediated modification. Eur. Heart J. 1990, 11 (Suppl. E): 83-87.
54. R. Salvayre, A. Negre-Salvayre, C. Camare. Oxidative theory of atherosclerosis and antioxidants. Biochimie. 2016, 125: 281-296.
55. M. Meydani. Vitamin E and atherosclerosis: beyond prevention of LDL oxidation. Journal of Nutrition. 2001, 131(2): 366S-368S.
56. A.C. Carr, M.R. McCall, B. Frei. Oxidation of LDL by myeloperoxidase and reactive nitrogen species. Reaction pathways and antioxidant protection. Arteriosclerosis, Thrombosis, and Vascular Biology. 2000, 20(7): 1716-1723.
57. M.J. Stampfer, C.H. Hennekens, J.E. Manson, G.A. Colditz, B. Rosner, W.C. Willett. Vitamin E consumption and the risk of coronary disease in women. New Engl. J. Med. 1993, 328(20): 1444-1449.
58. L.H. Kushi, A.R. Folsom, R.J. Prineas, P.J. Mink, Y. Wu, R.M. Bostick. Dietary antioxidant vitamins and death from coronary heart disease in postmenopausal women. New Engl. J. Med. 1996, 334(18): 1156-1162.
59. J.M. Rapola, J. Virtamo, J.K. Haukka, O.P. Heinonen, D. Albanes, P.R. Taylor, J.K. Huttunen. Effect of vitamin E and beta carotene on the incidence of angina pectoris. A randomized, double-blind, controlled trial. JAMA. 1996, 275(9): 693–698.
60. J. Virtamo, J.M. Rapola, S. Ripatti, O.P. Heinonen, P.R. Taylor, D. Albanes, J.K. Huttunen. Effect of vitamin E and beta carotene on the incidence of primary nonfatal myocardial infarction and fatal coronary heart disease. Arch. Int. Med. 1998, 158(6): 668–675.
61. V.W. Bowry, K.U. Ingold, R. Stocker. Vitamin E in human low-density lipoprotein: when and how this antioxidant becomes a pro-oxidant. Biochemical Journal. 1992, 288(2): 341-344.
62. E. Hood, E. Simone, P. Wattamwar, T. Dziubla, V. Muzykantov. Nanocarriers for vascular delivery of antioxidants. Nanomedicine. 2011, 6(7): 1257-1272.
63. M. Srinivasan, A.R. Sudheer, V.P. Menon. Ferulic acid: therapeutic potential through its antioxidant property. J. Clin. Biochem. Nutr. 40 (2007) 92.
64. N. Yanai, S. Shiotani, S. Hagiwara, H. Nabetani, M. Nakajima. Antioxidant combination inhibits reactive oxygen species mediated damage. Bioscience, Biotechnology, and Biochemistry. 2008, 72(12): 3100-3106.
65. E. Graf. Antioxidant potential of ferulic acid, Free Radical Biol. Med. 1992, 13(4): 435-448.
66. C. Xie, J. Kang, J.-R. Chen, S. Nagarajan, T.M. Badger, X. Wu. Phenolic acids are in vivo atheroprotective compounds appearing in the serum of rats after blueberry consumption. J. Agric. Food Chem. 2011, 59(18): 10381-10387.

67. F.-X. Chen, L.-K. Wang. Effect of ferulic acid on cholesterol efflux in macrophage foam cell formation and potential mechanism. Zhongguo Zhongyao Zazhi. 2015, 40(3): 533-537.
68. J.F. Oram, R.M. Lawn. ABCA1: the gatekeeper for eliminating excess tissue cholesterol. Journal of Lipid Research. 2001, 42(8): 1173-1179.
69. D.R. Michael, T.G. Ashlin, M.L. Buckley, D.P. Ramji. Liver X receptors, atherosclerosis, and inflammation. Current Atherosclerosis Reports. 2012, 14(3): 284-293.
70. S.L. Kowal, T.M. Dall, R. Chakrabarti, M.V. Storm, A. Jain. The current and projected economic burden of Parkinson's disease in the United States. Mov. Disord. 2013, 28(3): 311-318.
71. C.L. Gooch, E. Pracht, A.R. Borenstein. The burden of neurological disease in the United States: a summary report and call to action. Annals of Neurology. 2017, 81(4): 479-484.
72. A. Recchia, D. Rota, P. Debetto, D. Peroni, D. Guidolin, A. Negro, S.D. Skaper, P. Giusti. Generation of a α-synuclein-based rat model of Parkinson's disease. Neurobiology of Disease. 2008, 30(1): 8-18.
73. V.M. Lee, J.Q. Trojanowski. Mechanisms of Parkinson's disease linked to pathological alpha-synuclein: new targets for drug discovery. Neuron. 2006, 52(1): 33-38.
74. B.I. Giasson, J.E. Duda, S.M. Quinn, B. Zhang, J.Q. Trojanowski, V.M. Lee. Neuronal alpha-synucleinopathy with severe movement disorder in mice expressing A53T human alpha-synuclein. Neuron. 2002, 34(4): 521–533.
75. P.J. Kahle. α-Synucleinopathy models and human neuropathology: similarities and differences. Acta Neuropathol. 2008, 115(1): 87–95.
76. L. Pieri, K. Madiona, L. Bousset, R. Melki. Fibrillar α-synuclein and huntingtin exon 1 assemblies are toxic to the cells. Biophysical Journal. 2012, 102(12): 2894–2905.
77. B. Winner, R. Jappelli, S.K. Maji, P.A. Desplats, L. Boyer, S. Aigner, C. Hetzer, T. Loher, M. Vilar, S. Campioni, et al. In vivo demonstration that alpha-synuclein oligomers are toxic. Proc Natl Acad Sci U S A. 2011, 108(10): 4194–4199.
78. B. Di Marco Vieira, R.A. Radford, R.S. Chung, G.J. Guillemin, D.L. Pountney. Neuroinflammation in multiple system atrophy: response to and cause of α-synuclein aggregation. Front. Cell. Neurosci. 2015, 9: 437.
79. P. Ugalde-Muniz, J. Perez-H, A. Chavarria. Is chronic systemic inflammation a determinant factor in developing Parkinson's disease, in: Challenges in Parkinson's Disease, InTechOpen, 2016.
80. S.R. Subramaniam, H.J. Federoff. Targeting microglial activation states as a therapeutic avenue in Parkinson's disease. Frontiers in Aging Neuroscience. 2017, 9: 176.

81. R.B. Rock, G. Gekker, S. Hu, W.S. Sheng, M. Cheeran, J.R. Lokensgard, P.K. Peterson. Role of microglia in central nervous system infections. Clin. Microbiol. Rev. 2004, 17(4): 942–64.
82. M.L. Block, L. Zecca, J-S. Hong. Microglia-mediated neurotoxicity: uncovering the molecular mechanisms. Nat. Rev. Neurosci. 2007, 8(1): 57–69.
83. M. Block, J. Hong. Chronic microglial activation and progressive dopaminergic neurotoxicity. Biochem. Soc. Trans. 2007, 35(5): 1127–1132.
84. A. Gerhard, N. Pavese, G. Hotton, F. Turkheimer, M. Es, A. Hammers, K. Eggert, W. Oertel, R.B. Banati, D.J. Brooks. In vivo imaging of microglial activation with [11C](R)-PK11195 PET in idiopathic Parkinson's disease. Neurobiol. Dis. 2006, 21(2): 404–412.
85. S. Lee, S.M. Park, K.J. Ahn, K.C. Chung, S.R. Paik, J. Kim. Identification of the amino acid sequence motif of α-synuclein responsible for macrophage activation. Biochemical and Biophysical Research Communications. 2009, 381(1): 39-43.
86. L. Fellner, R. Irschick, K. Schanda, M. Reindl, L. Klimaschewski, W. Poewe, G.K. Wenning, N. Stefanova. Toll-like receptor 4 is required for α-synuclein dependent activation of microglia and astroglia. Glia. 2013, 61(3): 349-360.
87. C. Lavedan. The synuclein family. Genome Res. 1998, 8(9): 871-880.
88. B.I. Giasson, I.V. Murray, J.Q. Trojanowski, V.M. Lee. A hydrophobic stretch of 12 amino acid residues in the middle of alpha-synuclein is essential for filament assembly. J. Biol. Chem. 2001, 276(4): 2380-2386.
89. A. Klegeris, S. Pelech, B.I. Giasson, J. Maguire, H. Zhang, E.G. McGeer, P.L. McGeer. Alpha synuclein activates stress signaling protein kinases in THP-1 cells and microglia. Neurobiol. Aging. 2008, 29(5): 739-752.
90. X. Su, K.A. Maguire-Zeiss, R. Giuliano, L. Prifti, K. Venkatesh, H.J. Federoff. Synuclein activates microglia in a model of Parkinson's disease. Neurobiol. Aging. 2008, 29(11): 1690-1701.
91. C. Kim, D.H. Ho, J.E. Suk, S. You, S. Michael, J. Kang, S.J. Lee, E. Masliah, D. Hwang, H.-J. Lee, et al. Neuron-released oligomeric α-synuclein is an endogenous agonist of TLR2 for paracrine activation of microglia. Nat. Commun. 2013, 4: 1562.
92. D. Doens, P.L. Fernandez. Microglia receptors and their implications in the response to amyloid β for Alzheimer's disease pathogenesis. Journal of Neuroinflammation. 2014, 48(11): 1-14.
93. N.K. Bennett, R. Chmielowski, D.S. Abdelhamid, J.J. Faig, N. Francis, J. Baum, Z.P. Pang, K.E. Uhrich, P.V. Moghe. Polymer brain-nanotherapeutics for multipronged inhibition of microglial α-synuclein aggregation, activation, and neurotoxicity. Biomaterials. 2016, 111, 179-189.

94. MNT Editorial Team. What are the treatment options for Parkinson's disease? https://www.medicalnewstoday.com/info/parkinsons-disease/treatment-for-parkinsons-disease.php. Last updated January 5, 2016.
95. R. Barbour, K. Kling, J.P. Anderson, K. Banducci, T. Cole, L. Diep, M. Fox, J.M. Goldstein, F. Soriano, P. Seubert, T.J. Chilcote. Red blood cells are the major source of alpha-synuclein in blood. Neurodegener. Dis. 2008, 5(2): 55-59.
96. X. Wang, S. Yu, F. Li, T. Feng. Detection of α-synuclein oligomers in red blood cells as a potential biomarker of Parkinson's disease. Neuroscience Letters. 2015, 599: 115-119.
97. D. Sulzer, R.N. Alcalay, F. Garretti, L. Cote, E. Kanter, J. Agin-Liebes, C. Liong, C. McMurtrey, W.H. Hildebrand, X. Mao, et al. T cells from patients with Parkinson's disease recognize α-synuclein peptides. Nature. 2017, 546(7660): 656-661.
98. J-C. Rochet, F. Liu. Inhibition of α-synuclein aggregation by antioxidants and chaperones in Parkinson's disease, in: Protein Folding and Misfolding: Neurodegenerative Diseases, Springer Netherlands, 2009.
99. M. Masuda, N. Suzuki, S. Taniguchi, T. Oikawa, T. Nonaka, T. Iwatsubo, S. Hisanaga, M. Goedert, M. Hasegawa. Small molecule inhibitors of alpha-synuclein filament assembly. Biochemistry. 2006, 45(19): 6085-6094.
100. K. Ono, M. Yamada. Antioxidant compounds have potent anti-fibrillogenic and fibril-destabilizing effects for alpha-synuclein fibrils in vitro. J. Neurochem. 2006, 97(1): 105-115.
101. D.E. Ehrnhoefer, J. Bieschke, A. Boeddrich, M. Herbst, L. Masino, R. Lurz, S. Engemann, A. Pastore, E.E. Wanker. EGCG redirects amyloidogenic polypeptides into unstructured, off-pathway oligomers. Nat. Struct. Mol. Biol. 2008, 15(6): 558-566.
102. N. Pandey, J. Strider, W.C. Nolan, S.X. Yan, J.E. Galvin. Curcumin inhibits aggregation of alpha-synuclein. Acta Neuropathol. 2008, 115(4): 479-489.
103. S-H. Cha, S-J. Heo, Y-J. Jeon, S.M. Park. Dieckol, an edible seaweed polyphenol, retards rotenone-induced neurotoxicity and α-synuclein aggregation in human dopaminergic neuronal cells. RSC Advances. 2016, 6(111): 110040-110046.
104. N. Sharma, B. Nehru. Curcumin affords neuroprotection and inhibits α-synuclein aggregation in lipopolysaccharide-induced Parkinson's disease model. Inflammopharmacology. 2017, 1-12.
105. A. Kunzler, E.A. Kolling, J.D. Da-Silva Jr., J. Gasparotto, M.A. de Bittencourt Pasqual, J.C. Fonseca Moreira, D.P. Gelain. Retinol (Vitamin A) increases α-synuclein, β-amyloid peptide, tau phosphorylation and RAGE content in human SH-SY5Y neuronal cell line. Neurochem Res. 2017, 42(10): 2788-2797.

106. M. Aviram. Interaction of oxidized low density lipoprotein with macrophages in atherosclerosis and the antiatherogenicity of antioxidants. Eur. J. Clin. Chem. Clin. Biochem. 1996, 34(8): 599-608.
107. K.J. Moore, F.J. Sheedy, E.A. Fisher. Macrophages in atherosclerosis: a dynamic balance. Nat Rev Immunol. 2013, 13(10): 709-721.
108. P.R. Moreno, E. Falk, I.F. Palacios, J.B. Newell, V. Fuster, J.T. Fallon. Macrophage infiltration in acute coronary syndromes. Implications for plaque rupture. Circulation. 1994, 90(2): 775-778.
109. A. Faig, L.K. Petersen, P.V. Moghe, K.E. Uhrich. Impact of Hydrophobic Chain Composition on Amphiphilic Macromolecule Antiatherogenic Bioactivity. Biomacromolecules. 2014, 15(9): 3328-3337.
110. D. Abdelhamid, P.V. Moghe, K.E. Uhrich. Design and synthesis of novel amphiphilic macromolecules for cardiovascular applications. 246th ACS National Meeting & Exposition, Indianapolis, IN, USA, September 8-12, 2013, POLY-189.
111. D.R. Lewis, L.K. Petersen, A.W. York, K.R. Zablocki, L.B. Joseph, V. Kholodovych, R.K. Prud'homme, K.E. Uhrich, P.V. Moghe. Sugar-based amphiphilic nanoparticles arrest atherosclerosis in vivo. Proc. Natl. Acad. Sci. U. S. A. 2015, 112(9): 2693-2698.
112. D.R. Lewis, P.V. Moghe, L.K. Petersen, A.W. York, S.Ahuja, H. Chae, L.B. Joseph, S. Rahimi, P.B. Haser, K.E. Uhrich. Nanotherapeutics for inhibition of atherogenesis and modulation of inflammation in atherosclerotic plaques. Cardiovasc Res. 2016, 109(2): 283-293.
113. C. Auger, J. Rouanet, R. Vanderlinde, A. Bornet, K. Decorde, N. Lequeux, J. Cristol, P. Teissedre. Polyphenols-enriched Chardonnay white wine and sparkling Pinot Noir red wine identically prevent early atherosclerosis in hamsters. J. Agric. Food Chem. 2005, 53(25): 9823-9829.
114. L.H. Opie. New developments in cardiovascular drugs: vitamin E and antioxidants - an informal and personal viewpoint. Cardiovasc. Drugs Ther. 1997, 11(6): 719-721.
115. G.H.R. Rao, S. Parthasarathy. Antioxidants, atherosclerosis and thrombosis. Prostaglandins, Leukotrienes Essent. Fatty Acids. 1996, 54(3): 155-166.
116. D.R. Illingworth. The potential role of antioxidants in the prevention of atherosclerosis. J. Nutr. Sci. Vitaminol. 1993, 39(Suppl.): S43-S47.
117. A. Munteanu, J.M. Zingg, A. Azzi. Anti-atherosclerotic effects of vitamin E - myth or reality? J. Cell. Mol. Med. 2004, 8(1): 59-76.
118. J.C. Tardif. Antioxidants: the good, the bad and the ugly. Can. J. Cardiol. 2006, 22 Suppl B: 61B-65B.
119. A.L. Catapano, F.M. Maggi, E. Tragni. Low density lipoprotein oxidation, antioxidants, and atherosclerosis. Curr Opin Cardiol. 2000, 15(5): 355-363.

120. R. Stocker. The ambivalence of vitamin E in atherogenesis. Trends Biochem. Sci. 1999, 24(6): 219-223.
121. E. Hood, E. Simone, P. Wattamwar, T. Dziubla, V. Muzykantov. Nanocarriers for vascular delivery of antioxidants. Nanomedicine (London, U. K.). 2011, 6(7): 1257-1272.
122. Y.-Z. Hou, J. Yang, G.-R. Zhao, Y.-J. Yuan. Ferulic acid inhibits vascular smooth muscle cell proliferation induced by angiotensin II. Eur. J. Pharmacol. 2004, 499(1-2): 85-90.
123. M.A. Ouimet, J.J. Faig, W. Yu, K.E. Uhrich. Ferulic Acid-Based Polymers with Glycol Functionality as a Versatile Platform for Topical Applications. Biomacromolecules. 2015, 16(9): 2911-2919.
124. J.V. Jokerst, T. Lobovkina, R.N. Zare, S.S. Gambhir. Nanoparticle PEGylation for imaging and therapy. Nanomedicine (London, U. K.). 2011, 6(4): 715-728.
125. J. Djordjevic, L.S. del Rosario, J. Wang, K.E. Uhrich. Amphiphilic scorpion-like macromolecules as micellar nanocarriers. J. Bioact. Compat. Polym. 2008, 23(6): 532-551.
126. N.M. Iverson, S.M. Sparks, B. Demirdirek, K.E. Uhrich, P.V. Moghe. Controllable inhibition of cellular uptake of oxidized low-density lipoprotein: structure-function relationships for nanoscale amphiphilic polymers. Acta Biomater. 2010, 6(8): 3081-3091.
127. L. Tian, L. Yam, N. Zhou, H. Tat, K.E. Uhrich. Amphiphilic Scorpion-like Macromolecules: Design, Synthesis, and Characterization. Macromolecules. 2004, 37(2): 538-543.
128. M.A. Ouimet. Design, synthesis, and fabrication of biodegradable, bioactive-based polymers for controlled release applications. Rutgers University Thesis. 2013.
129. J.W. Chan, D.R. Lewis, L.K. Petersen, P.V. Moghe, K.E. Uhrich. Amphiphilic macromolecule nanoassemblies suppress smooth muscle cell proliferation and platelet adhesion. Biomaterials. 2016, 84: 219-229.
130. K. Menck, D. Behme, M. Pantke, N. Reiling, C. Binder, T. Pukrop, F. Klemm. Isolation of human monocytes by double gradient centrifugation and their differentiation to macrophages in teflon-coated cell culture bags. J. Visualized Exp. 91 (2014) e51554/1-e51554/10.
131. R. Scherer, H.T. Godoy. Antioxidant activity index (AAI) by the 2,2-diphenyl-1-picrylhydrazyl method. Food Chem. 2008, 112(3): 654-658.
132. N.D. Stebbins, J.J. Faig, W. Yu, R. Guliyev, K.E. Uhrich. Polyactives: controlled and sustained bioactive release via hydrolytic degradation. Biomater. Sci. 2015, 3(8): 1171-1187.

133. L.F. Dalmolin, N.M. Khalil, R.M. Mainardes. Delivery of vanillin by poly(lactic-acid) nanoparticles: Development, characterization and in vitro evaluation of antioxidant activity. Mater. Sci. Eng., C. 2016, 62: 1-8.
134. S. Kim, H. Park, Y. Song, D. Hong, O. Kim, E. Jo, G. Khang, D. Lee. Reduction of oxidative stress by p-hydroxybenzyl alcohol-containing biodegradable polyoxalate nanoparticulate antioxidant. Biomaterials. 2011, 32(11): 3021-3029.
135. Anon. Excipient Development for Pharmaceutical, Biotechnology, and Drug Delivery Systems. Ashok Katdare and Mahesh V. Chaubal. Pharm. Dev. Technol. 2007, 12(1): 109-110.
136. T. Seimon, I. Tabas. Mechanisms and consequences of macrophage apoptosis in atherosclerosis. J. Lipid Res. 2009, Suppl.: S382-S387.
137. K.M. Botham K.M, C.P.D. Wheeler-Jones. Postprandial lipoproteins and the molecular regulation of vascular homeostasis. Progress in Lipid Research. 2013, 52(4): 446-464.
138. J.E. Feig, S. Parathath, J.X. Rong, S.L. Mick, Y. Vengrenyuk, L. Grauer, S.G. Young, E.A. Fisher. Reversal of hyperlipidemia with a genetic switch favorably affects the content and inflammatory state of macrophages in atherosclerotic plaques. Circulation. 2011, 123(9): 989-998.
139. J.E. Feig, J.X. Rong, R. Shamir, M. Sanson, Y. Vengrenyuk, J. Liu, K. Rayner, K. Moore, M. Garabedian, E.A. Fisher. HDL promotes rapid atherosclerosis regression in mice and alters inflammatory properties of plaque monocyte-derived cells. Proc. Natl. Acad. Sci. 2011, 108(17): 7166-7171.
140. X.D. Zhu, Y. Zhuang, J.J. Ben, L.L Qian, H.P. Huang, H. Bai, J.H. Sha, Z.G. He, Q. Chen. Caveolae-dependent endocytosis is required for class A macrophage scavenger receptor-mediated apoptosis in macrophages. J. Biol. Chem. 2011, 286(10): 8231-8239.
141. E.S. Wintergerst, J. Jelk, C. Rahner, R. Asmis. Apoptosis induced by oxidized low density lipoprotein in human monocyte-derived macrophages involves CD36 and activation of caspase-3. Eur. J. Biochem. 2000, 267(19): 6050-6059.
142. N. Kume, T. Kita. Lectin-like oxidized low-density lipoprotein receptor-1 (LOX-1) in atherogenesis. Trends Cardiovasc Med. 2001, 11(1): 22-25.
143. H. Kataoka, N. Kume, S. Miyamoto, M. Minami, M. Morimoto, K. Hayashida, N. Hashimoto, T. Kita. Oxidized LDL modulates Bax/Bcl-2 through the lectinlike oxLDL receptor-1 in vascular smooth muscle cells. Arterioscler. Thromb. Vasc. Biol. 2001, 21(6): 955-960.
144. C.R. Stewart, L.M. Stuart, K. Wilkinson, J.M. van Gils, A. Hallie, K.J. Rayner, L. Boyer, R. Zhong, W.A. Frazier, A. Lacy-Hulbert, J. El Khoury, D.T. Golenbock, K.J. Moore. CD36 ligands promote sterile inflammation through assembly of a Toll-like receptor 4 and 6 heterodimer. Nat. Immunol. 2010, 11(2): 155-161.

145. J. Husemann, A. Obstfeld, M. Febbraio, T. Kodama, S.C. Silverstein. CD11b/CD18 mediates production of reactive oxygen species by mouse and human macrophages adherent to matrixes containing oxidized LDL. Arterioscler. Thromb. Vasc. Biol. 2001, 21(8): 1301-1305.
146. D.R. Greaves, S. Gordon. Thematic review series: the immune system and atherogenesis. Recent insights into the biology of macrophage scavenger receptors. J. Lipid Res. 2005, 46(1): 11-20.
147. L.C. Bourne, C.A. Rice-Evans. The effect of the phenolic antioxidant ferulic acid on the oxidation of low density lipoprotein depends on the pro-oxidant used. Free Radic Res. 1997, 27(3): 337-344.
148. S.J. Lee, C.H.T. Quach, K.-H. Jung, J.-Y. Paik, J.H. Lee, J.W. Park, K.-H. Lee. Oxidized low-density lipoprotein stimulates macrophage 18F-FDG uptake via hypoxia-inducible factor-1Î± activation through Nox2-dependent reactive oxygen species generation. J. Nucl. Med. 2014, 55(10): 1699-1705.
149. Y.S. Bae, J.H. Lee, S.H. Choi, S. Kim, F. Almazan, J.L. Witztum, Y.I. Miller. Macrophages generate reactive oxygen species in response to minimally oxidized low-density lipoprotein. Circ. Res. 2009, 104(2): 210-218.
150. H.-Y. Tan, N. Wang, S. Li, M. Hong, X. Wang, Y. Feng. The reactive oxygen species in macrophage polarization: reflecting its dual role in progression and treatment of human diseases. Oxid Med Cell Longev. 2016, 2016: 2795090.
151. NINDS. Parkinson's Disease Information Page. https://www.ninds.nih.gov/Disorders/All-Disorders/Parkinsons-Disease-Information-Page. June 30, 2016.
152. K.A. Conway, J.C. Rochet, R.M. Bieganski, P.T. Lansbury Jr. Kinetic stabilization of the alpha-synuclein protofibril by a dopamine-alpha-synuclein adduct. Science. 2001, 294(5545): 1346-1349.
153. H.J. Lee, S.J. Lee. Characterization of cytoplasmic alpha-synuclein aggregates. Fibril formation is tightly linked to the inclusion-forming process in cells. J. Biol. Chem. 2002, 277(50): 48976-48983.
154. O.M. El-Agnaf, R. Jakes, M.D. Curran, A. Wallace. Effects of the mutations Ala30 to Pro and Ala53 to Thr on the physical and morphological properties of alpha-synuclein protein implicated in Parkinson's disease. FEBS Lett. 1998, 440(1-2): 67-70.
155. M. Hashimoto, L.J. Hsu, Y. Xia, A. Takeda, A. Sisk, M. Sundsmo, E. Masliah. Oxidative stress induces amyloid-like aggregate formation of NACP/alpha-synuclein in vitro. Neuroreport. 1999, 10(4): 717-721.
156. H. McCann, C.H. Stevens, H. Cartwright, G.M. Halliday. α-synucleinopathy phenotypes. Parkinsonism and Related Disorders. 2014, 20(1): S62-S67.
157. M. Shahaduzzaman, K. Nash, C. Hudson, M. Sharif, B. Grimmig, X. Lin, G. Bai, H. Liu, K.E. Ugen, C. Cao, P.C. Bickford. Anti-human α-synuclein N-terminal

peptide antibody protects against dopaminergic cell death and ameliorates behavioral deficits in an AAV-α-synuclein rat model of Parkinson's disease. PLoS One. 2015, 10(2): e0116841/1-e0116841/16.

158. P.J. McLean, H. Kawamata, S. Ribich, B.T. Hyman. Membrane association and protein conformation of alpha-synuclein in intact neurons. Effect of Parkinson's disease-linked mutations. J Biol Chem. 2000, 275(12): 8812–8816.
159. T.D. Kim, S.R. Paik, C.H. Yang. Structural and functional implications of C-terminal regions of alpha-synuclein. Biochemistry. 2002, 41(46): 13782-13790.
160. E.K. Tan, V.R. Chandran, S. Fook-Chong, H. Shen, K. Yew, M.L. Teoh, Y. Yuen, Y. Zhao. Alpha-synuclein mRNA expression in sporadic Parkinson's disease. Mov Disord. 2005, 20(5): 620-623.
161. D.F. Lazaro, E.F. Rodrigues, R. Langohr, H. Shahpasandzadeh, T. Ribeiro, P. Guerreiro, E. Gerhardt, K. Krohnert, J. Klucken, M.D. Pereira, B. Popova, N. Kruse, B. Mollenhauer, S.O. Rizzoli, G.H. Braus, K.M. Danzer, T.F. Outeiro. Systematic comparison of the effects of alpha-synuclein mutations on its oligomerization and aggregation. PLOS Genetics. 2014, Nov 13;10(11):e1004741. doi: 10.1371/journal.pgen.1004741. eCollection 2014 Nov.
162. A. Oczkowska, W. Kozubski, M. Lianeri, J. Dorszewska. Mutations in PRKN and SNCA genes important for the progress of Parkinson's disease. Curr. Genomics. 2013, 14(8): 502-517.
163. S. Lesage, M. Anheim, F. Letournel, L. Bousset, A. Honore, N. Rozas, L. Pieri, K. Madiona, A. Duerr, R. Melki, et al. G51D alpha-synuclein mutation causes a novel parkinsonian-pyramidal syndrome. Ann. Neurol. 2013, 73(4): 459–471.
164. C. Proukakis, C.G. Dudzik, T. Brier, D.S. MacKay, J.M. Cooper, G.L. Millhauser, H. Houlden, A.H. Schapira. A novel alpha-synuclein missense mutation in Parkinson disease. Neurology. 2013, 80(11): 1062–1064.
165. C.B. Lücking, A. Brice. Alpha-synuclein and Parkinson's disease. Cell. Mol. Life Sci. 2000, 57(13-14): 1894-1908.
166. L. Narhi, S.J. Wood, S. Steavenson, Y. Jiang, G.M. Wu, D. Anafi, S.A. Kaufman, F. Martin, K. Sitney, P. Denis, J.C. Louis, J. Wypych, A.L. Biere, M. Citron. Both familial Parkinson's disease mutations accelerate alpha-synuclein aggregation. J. Biol. Chem. 1999, 274(14): 9843-9846.
167. N. Pandey, R.E. Schmidt, J.E. Galvin. The alpha-synuclein mutation E46K promotes aggregation in cultured cells. Exp Neurol. 2006, 197(2): 515-520.
168. O. Khalaf, B. Fauvet, A. Oueslati, I. Dikiy, A.L. Mahul-Mellier, F.S. Ruggeri, M.K. Mbefo, F. Vercruysse, G. Dietler, S.-J. Lee, et al. The H50Q mutation enhances alpha-synuclein aggregation, secretion and toxicity. J. Biol. Chem. 2014, 289(32): 21856–21876.
169. V. Sanchez-Guajardo, C.J. Barnum, M.G. Tansey, M. Romero-Ramos. Neuroimmunological processes in Parkinson's disease and their relation to alpha

synuclein: microglia as the referee between neuronal processes and peripheral immunity. ASN Neuro. 2013, 5(2): 113 - 139.

170. M.L. Block, J.S. Hong. Microglia and inflammation-mediated neurodegeneration: multiple triggers with a common mechanism. Prog. Neurobiol. 2005, 76(2): 77 - 98.
171. L. Giehm, D.E. Otzen. Strategies to increase the reproducibility of protein fibrillization in plate reader assays. Anal. Biochem. 2010, 400(2): 270 - 281.
172. R. Khurana, C. Coleman, C. Ionescu-Zanetti, S.A. Carter, V. Krishna, R.K. Grover, R. Roy, S. Singh. Mechanism of thioflavin T binding to amyloid fibrils. J. Struct. Biol. 2005, 151(3): 229-238.
173. G.M. Moriarty, M.P. Olson, T.B. Atieh, M.K. Janowska, S.D. Khare, J. Baum. A pH dependent switch promotes β-synuclein fibril formation via glutamate residues. Journal of Biological Chemistry. 2017, 292(39):16368-16379.
174. A.K. Buell, C. Galvagnion, R. Gaspar, E. Sparr, M. Vendruscolo, T.P.J. Knowles, S. Linse, C.M. Dobson. Solution conditions determine the relative importance of nucleation and growth processes in α-synuclein aggregation. Proc. Natl. Acad. Sci. USA, 2014, 111(21): 7671-7676.
175. G. Toth, S.J. Gardai, W. Zago, C.W. Bertoncini, N. Cremades, S.L. Roy, M.A. Tambe, J-C. Rochet, C. Galvagnion, G. Skibinski, S. Finkbeiner, M. Bova, K. Regnstrom, S-S. Chiou, J. Johnston, K. Callaway, J.P. Anderson, M.F. Jobling, A.K. Buell, T.A. Yednock, T.P.J. Knowles, M. Vendruscolo, J. Chirstodoulou, C.M. Dobson, D. Schenk, L. McConlogue. Targeting the intrinsically disordered structural ensemble of α-synuclein by small molecules as a potential therapeutic strategy for Parkinson's Disease. PLoS One. 2014, 9(2): e87133.
176. V.M.Y. Lee, J.Q. Trojanowski. Mechanisms of Parkinson's disease linked to pathological alpha-synuclein: New targets for drug discovery. Neuron, 2006, 52(1): 33-38.
177. M. Caruana, T. Hogen, J. Levin, A. Hillmer, A. Giese, N. Vassallo. Inhibition and disaggregation of α-synuclein oligomers by natural polyphenolic compounds. FEBS Letters. 2011, 585(8): 1113-1120.
178. J.M. Nadal, M. de Graca Toldeo, Y.M. Pupo, J.P. de Paula, P.V. Farago, S.M.W. Zanin. A stability indicating HPLC-DAD method for determination of ferulic acid into microparticles: development, validation, forced degradation, and encapsulation efficiency. Journal of Analytical Methods in Chemistry. 2015, 1-11.
179. K. Gillotte-Taylor, A. Boullier, J.L. Witztum, D. Steinberg, O. Quehenberger. Scavenger receptor calss B type I as a receptor for oxidized low density lipoprotein. J. Lipid Res. 2001, 42(9): 1474-1482.
180. A.M. Aslanian, I.F. Charo. Targeted disruption of the scavenger receptor and chemokine CXCL16 accelerates atherosclerosis. Circulation. 2006, 114(6): 583-590.

181. M. Minami, N. Kume, T. Shimaoka, H. Kataoka, K. Hayashida, Y. Akiyama, I. Nagata, K. Ando, M. Nobuyoshi, M. Hanyuu, M. Komeda, S. Yonehara, T. Kita. Expression of SR-PSOX, a novel cell-surface scavenger receptor for phosphatidylserine and oxidized LDL in human atherosclerotic lesions. Arterioscler. Thromb. Vasc. Biol. 2001, 21(11): 1796-1800.
182. D.M. Wuttge, X. Zhou, Y. Sheikine, D. Wagsater, V. Stemme, U. Hedin, S. Stemme, G.K. Hansson, A. Sirsjo. CXCL16/SR-PSOX is an interferon-γ-regulated chemokine and scavenger receptor expressed in atherosclerotic lesions. Arterioscler. Thromb. Vasc. Biol. 2004, 24(4): 750-755.
183. T. Shimaoka, N. Kume, M. Minami, K. Hayashida, H. Kataoka, T. Kita, S. Yonehara. Molecular cloning of a novel scavenger receptor for oxidized low density lipoprotein, SR-PSOX, on macrophages. J. Biol. Chem. 2000, 275(52): 40663-40666.
184. G.A. Duque, A. Descoteaux. Macrophage cytokines: involvement in immunity and infectious diseases. Front. Immunol. 2014, 5, 491.
185. A.E. Scoccia, M.S. Molinuevo, A.D. McCarthy, A.M. Cortizo. A simple method to assess the oxidative susceptibility of low density lipoproteins. BMC Clin. Pathol. 2001, 1(1): 1.
186. H. Uto-Kondo, M. Ayaori, M. Ogura, K. Nakaya, M. Ito, A. Suzuki, S. Takiguchi, E. Yakushiji, Y. Terao, H. Ozasa, T. Hisada, M. Sasaki, F. Ohsuzu, K. Ikewaki. Coffee consumption enhances high-density lipoprotein-mediated cholesterol efflux in macrophages. Circ. Res. 2010, 106(4): 779-787.
187. M.F. Burke, A.V. Khera, D.J. Rader. Polyphenols and cholesterol efflux: Is coffee the next red wine? Circ. Res. 2010, 106(4): 627-629.
188. T.F. Galatro, I.R. Holtman, A.M. Lerario, I.D. Vainchtein, N. Brouwer, P.R. Sola, M.M. Veras, T.F. Pereira, R.E.P. Leite, T. Moller, P.D. Wes, M.C. Sogayar, J.D. Laman, W. den Dunnen, C.A. Pasqualucci, S.M. Oba-Shinjo, E.W.G.M. Boddeke, S.K.N. Marie, B.J.L. Eggen. Transcriptomic analysis of purified human cortical microglia revelas age-associated changes. Nature Neuroscience. 2017, 20(8): 1162-1171.
189. E.M. Abud, R.N. Ramirez, E.S. Martinez, L.M. Healy, C.H.H. Nguyen, S.A. Newman, A.V. Yeromin, V.M. Scarfone, S.E. Marsh, C. Fimbres, C.A. Caraway, G.M. Fote, A.M. Madany, A. Agrawal, R. Kayed, K.H. Gylys, M.D. Cahalan, B.J. Cummings, J.P. Antel, A. Mortazavi, M.J. Carson, W.W. Poon, M. Blurton-Jones. iPSC-derived human microglia-like cells to study neurological diseases. Neuron. 2017, 94(2): 278-293.
190. M. Ohgidani, T.A. Kato, D. Setoyama, N. Sagata, R. Hashimoto, K. Shigenobu, T. Yoshida, K. Hayakawa, N. Shimokawa, D. Miura, H. Utsumi, S. Kanba. Direct induction of ramified microglia-like cells from human monocytes: Dynamic microglial dysfunction in Nasu-Hakola disease. Scientific Reports. 2014, 4: 4957.

191. C. Leone, G. Le Pavec, W. Meme, F. Porcheray, B. Samah, D. Dormont, G. Gras. Characterization of human monocyte-derived microglia-like cells. Glia. 2006, 54(3): 183-192.
192. S. Etemad, R.M. Zamin, M.J. Ruitenberg, L. Filgueira. A novel *in vitro* human microglia model: characterization of human monocyte-derived microglia. Journal of Neuroscience Methods. 2012, 209(1): 79-89.
193. Y. Wang, K.J. Szretter, W. Vermi, S. Gilfillan, C. Rossini, M. Cella, A.D. Barrow, M.S. Diamond, M. Colonna. IL-34 is a tissue-restricted ligand of CSF1R required for the development of Langerhans cells and microglia. Nat. Immunol. 2012, 13(8): 753-760.
194. F. Aloisi, R. De Simone, S. Columba-Cabezas, G. Penna, L. Adorini. Functional maturation of adult mouse resting microglia into an APC is promoted by granulocyte-macrophage colony-stimulating factor and interaction with Th1 cells. J. Immunol. 2000, 164(4): 1705-1712.
195. J. Zhang, C. Geula, C. Lu, H. Koziel, L.M. Hatcher, F.J. Roisen. Neurotrophins regulate proliferation and survival of two microglia cell lines in vitro. Exp. Neurol. 2003, 183(2): 469-481.